ıllege of

Oceanic and Atmospheric Sciences

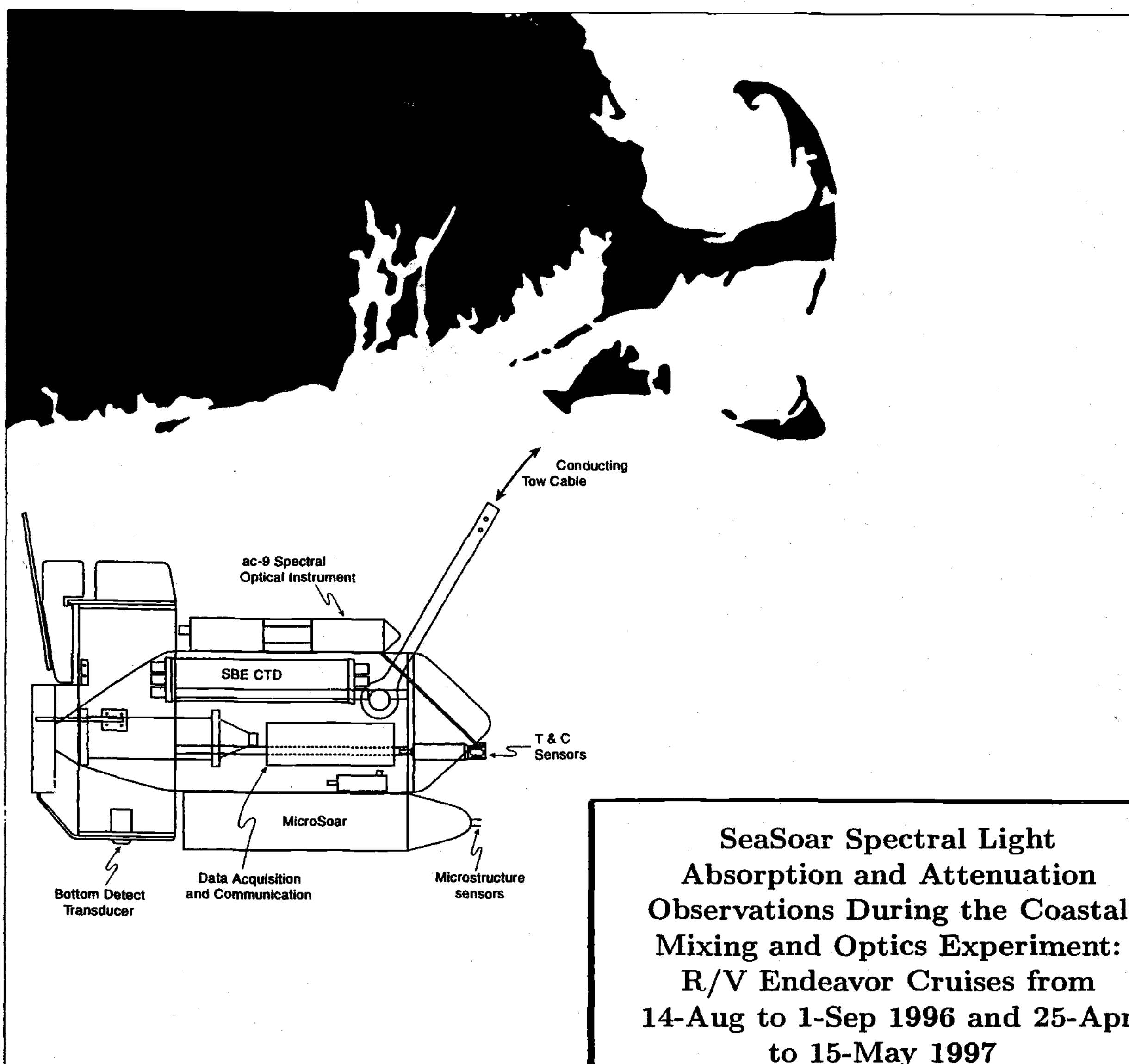

Oregon State University

SeaSoar Spectral Light Absorption and Attenuation Observations During the Coastal Mixing and Optics Experiment: R/V Endeavor Cruises from 14-Aug to 1-Sep 1996 and 25-Apr to 15-May 1997

by

J. Simeon, J. A. Barth, D. J. Bogucki,
A. Erofeev, R. O'Malley and
S. D. Pierce

College of Oceanic & Atmospheric
Sciences
Oregon State University
Corvallis, OR 97331–5503

Data Report 179
Reference 00-3
June 2000

SeaSoar Spectral Light Absorption and Attenuation Observations During the Coastal Mixing and Optics Experiment: R/V Endeavor Cruises from 14-Aug to 1-Sep 1996 and 25-Apr to 15-May 1997

J. Simeon
J. A. Barth
D. J. Bogucki
A. Erofeev
R. O'Malley
S. D. Pierce

College of Oceanic and Atmospheric Sciences
Oregon State University
Corvallis, OR 97331-5503

Data Report 179
Reference 00-3
June 2000

http://diana.oce.orst.edu/cmoweb/ac9/main.html

This data report includes documentation of the Coastal Mixing and Optics (CMO) Experiment inherent optical property surveys on the continental shelf and slope in the Mid-Atlantic Bight south of Cape Cod, Massachusettes, USA. The surveys were conducted aboard the *R/V Endeavor* during two physical oceanography cruises: E9608 (14 August to 1 September 1996) and E9704 (25 April to 15 May 1997). The objective of the CMO Experiment was to rapidly survey a region in the Mid-Atlantic Bight (centered around 40.5°N, 70.5°W) to obtain three-dimensional, high-resolution measurements which would allow further elucidation of the lengthscales, distributions and relationships between hydrographic and optical properties. This report describes the installation and deployment of the optical instrumentation as well as the data acquisition, data processing and editing of the inherent optical property data. Vertical sections and maps of the inherent optical properties obtained from the surveys are also presented.

Contents

1 **Introduction** 4

2 **Installation and Deployment** 8

3 **Data Processing and Editing** 11

3.1 Factory Calibration 11

3.2 Merging of ac-9 data with navigational and hydrographic data 12

3.3 Time lag correction 12

3.4 Temperature and Salinity Correction 16

3.5 Post Calibration Correction 16

3.6 Scattering Correction 20

3.7 Editing 23

4 **Data Presentation** 30

4.1 Spectra 30

4.2 Maps 30

4.3 Sections 30

5 **Acknowledgements** 31

6 **References** 32

7 **Section Times and Cruise Tracks** 34

7.1 E9608 34

7.2 E9704 42

8 **Spectra** 50

9 **E9608 Bigbox Maps** 54

10 **E9608 Smallbox Maps** 92

11 E9608 Bigbox Sections **112**

12 E9608 Smallbox Sections **130**

13 E9608 Butterfly Sections **150**

14 E9704 Bigbox Maps **164**

15 E9704 Smallbox Maps **190**

16 E9704 Bigbox Sections **210**

17 E9704 Smallbox Sections **226**

1 Introduction

This report includes information on the deployment, data aquisition, data processing and recorded measurements of the inherent optical properties during two physical oceanography cruises: E9608 (14 August to 1 September 1996) and E9704 (25 April to 15 May 1997). These two physical oceanography cruises were conducted by the co-PIs Jack Barth and Mike Kosro as part of the ONR-sponsored Coastal Mixing and Optics (CMO) Accelerated Research Initiative. The objective was to rapidly survey a region around 40.5°N, 70.5°W where a set of moorings and a stationary vessel conducting profiling operations were located. The first cruise (14 August to 1 September 1996) took place during a period of strong summer stratification; the second cruise was conducted in the spring (25 April to 15 May 1997) as water over the shelf restratified after mixing by winter storms.

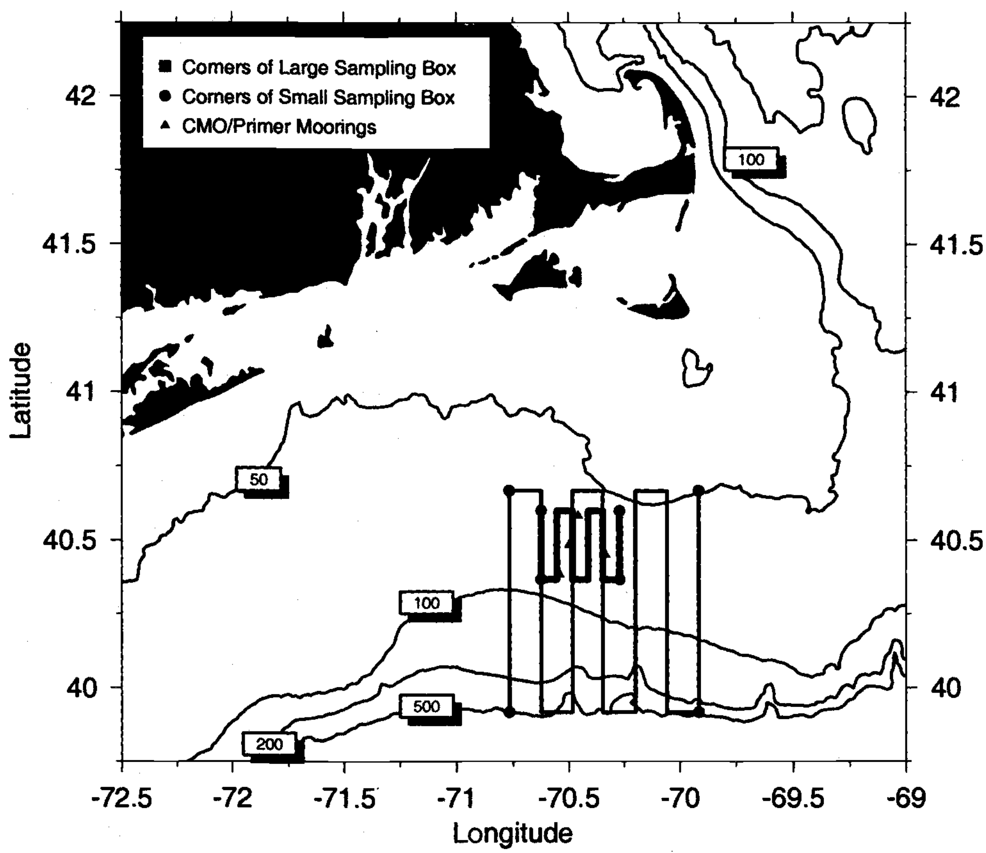

Figure 1: Map of the Coastal Mixing and Optics study region in the Middle Atlantic Bight south of Cape Cod, Massachusetts. Bottom topography in meters.

Maps of hydrographic properties, velocity (from a shipboard acoustic Doppler current profiler) and inherent optical properties were obtained over the continental shelf and slope. The water column was sampled by towing the undulating vehicle SeaSoar from the surface to within 5-7 m of the bottom. The SeaSoar tows were concentrated in three patterns: 1) a small box roughly 25 by 30 km centered on 40.5°N, 70.5°W (in 70 m of water on the mid-shelf) and with north-south lines separated by about 6 km; 2) a big box roughly 70 by 80 km which included the small box region but extended out over the continental slope and with north-south lines separated by about 12 km; and 3) a butterfly roughly 28 by 30 km centered on 40.5°N, 70.5°W. Each of these boxes was sampled repeatedly during the cruise (Figure 1). Surface temperature and salinity, and meteorological measurements were made continuously during E9608 (Figure 2) and E9704 (Figure 3).

Further details of SeaSoar operation, SeaSoar CTD processing data processing and conventional CTD data as well as cruise narratives for the two cruises can be found in O'Malley *et al.* (1998). Details of the acoustic Doppler current profiler (ADCP) operation and data processing can be found in Pierce *et al.* (1998). A summary version of this report has been previously published in *Deep-Sea Res.*, (Barth and Bogucki, 2000). All data reports are available at *http://diana.oce.orst.edu/cmoweb.*

Measurements of the inherent optical properties (IOPs) are obtained using a nine-wavelength spectral absorption and attenuation meter (WET Labs, ac-9). For readers unfamiliar with the design and engineering of an ac-9, a summary description of this field deployable spectrophotometer is as follows. The ac-9 unit is composed of two cylindrical pressure cases with dual connecting, specially designed tubes through which sampled water can flow. The shorter of the two pressure cases houses the light source, filter wheel and transmitter optics. The longer pressure case houses the receiver optics as well as the control and data aquisition electronics. Dual DC incandescent light sources from the shorter pressure case are collimated, passed through bandpass filters seated on a single rotating wheel, then transmitted through the flow tubes (25 cm pathlength). Light which has been neither absorbed (photon annihilation) nor scattered (photon redirection), through the flow tube pathlength is refocused, then sensed by detectors located in the longer pressure case. For this survey, the ac-9 was configured with the following visible spectrum wavelengths (nm): 412, 440, 510, 532, 560, 650, 676 and 715. The ac-9 power and communications are mediated by the bulkhead connector at the end of the long housing. The ac-9 operates with 10-18 volts, requires nine watts of power and sends data at about 400 bytes s^{-1} over a RS-485 serial channel. A power and data communications package is necessary for the real-time transfer of data from the deployed instrument to the shipboard computers. Details of data post processing are discussed later in this report. Further recommended reading is the *ac-9 User's Guide*, WET Labs (1995).

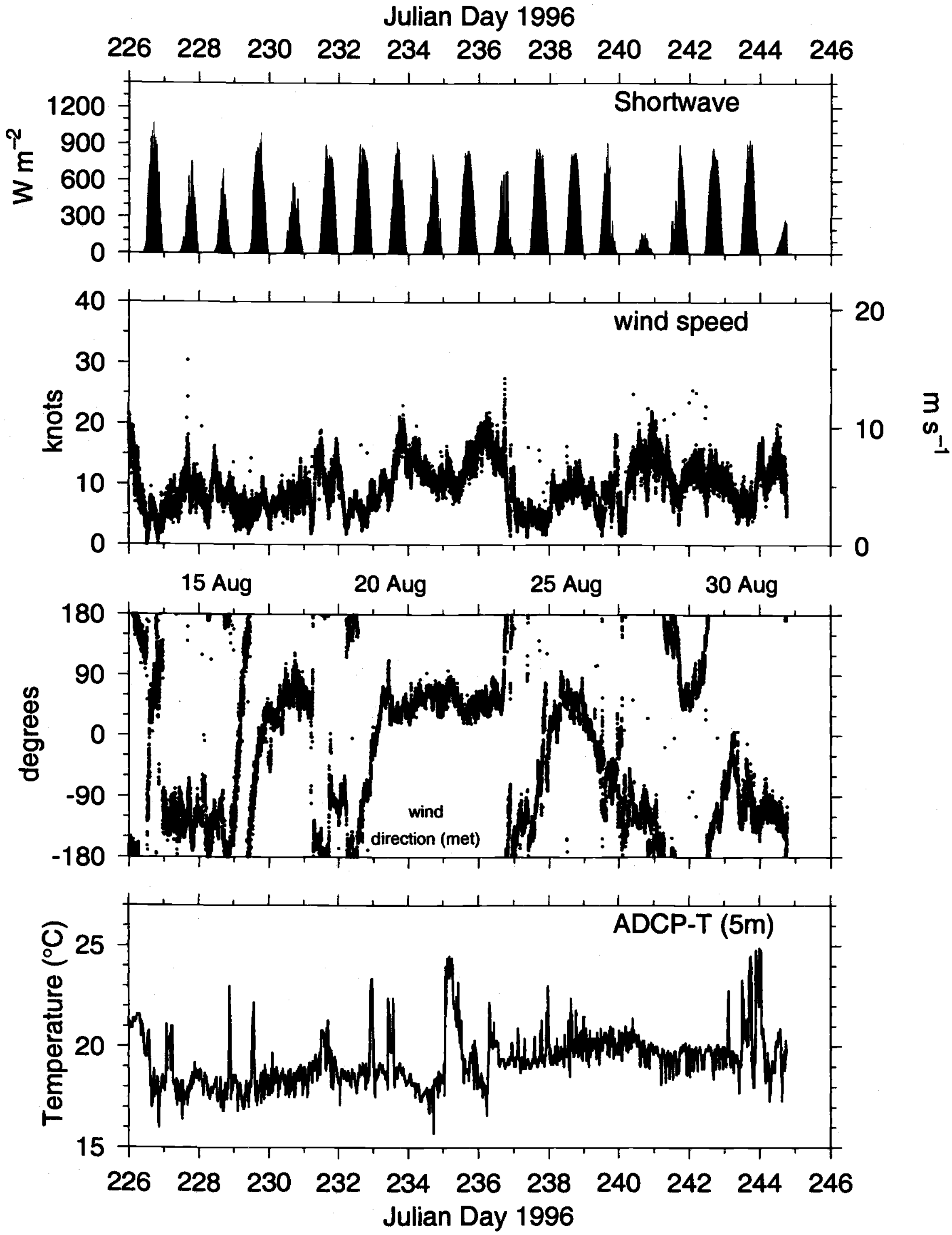

Figure 2: Irradiance, wind speed and wind direction from the R/V Endeavor's meteorological instruments, and 5-m water temperature from the ADCP transducer well during E9608.

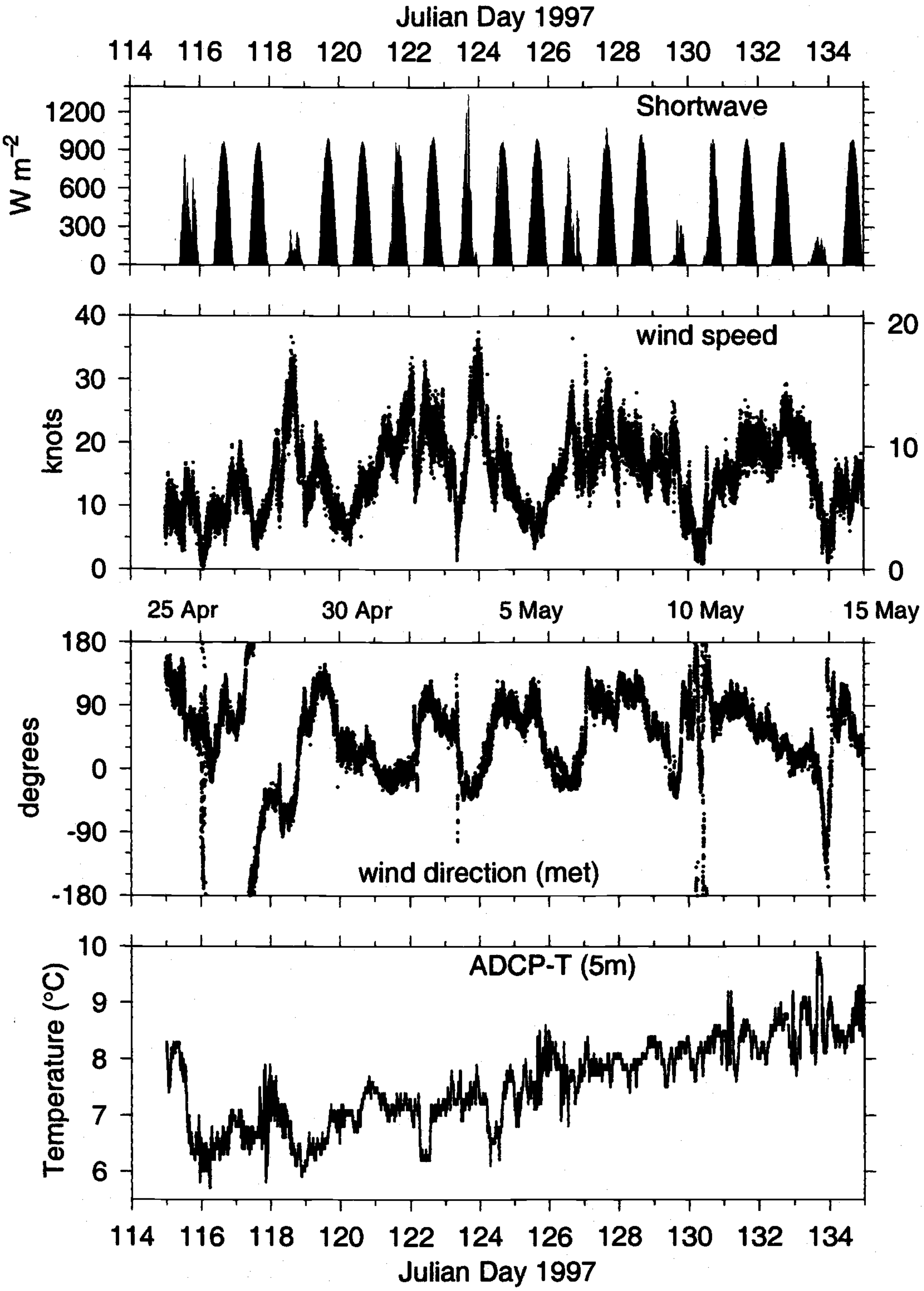

Figure 3: Irradiance, wind speed and wind direction from the R/V Endeavor's meteorological instruments, and 5-m water temperature from the ADCP transducer well during E9704.

2 Installation and Deployment

The SeaSoar was equipped with a Seabird 911+ conductivity-temperature-depth (CTD) instrument, a nine-wavelength light absorption and attenuation meter (WETLabs ac-9) and a new microstructure instrument, MicroSoar (*Erofeev et al.*, 1998; *Dillon et al.*, 2000), which measured conductivity and temperature using robust, fast-response probes. The Seabird (SBE) 911+ CTD, with its pressure case, was mounted inside the vehicle with the dual temperature/conductivity (T/C) sensors mounted pointing forward through SeaSoar's nose (Figure 4a). Dual SBE pumps mounted inside the vehicle ensured a steady flow past the T/C sensors. A nine-wavelength light absorption and attenuation instrument, ac-9 (WETLabs, Inc., Philomath, Oregon), was mounted on top of SeaSoar in a rigid saddle and with a streamlined nose cone to minimize drag (Figure 4b). The placement of the ac-9 on top of SeaSoar caused no adverse effects on the vehicle's performance. The rigid saddle was designed to avoid placing torque on the light paths through the ac-9's flow tubes (WETLabs, 1995; Moore and Bruce, 1996). The SBE pump for the ac-9 was mounted downstream in the flow which entered at an inlet just above the CTD T/C sensors in the nose of SeaSoar (Figure 4a). Water for the ac-9 was pumped from the inlet/outlet to ensure comparable hydrographic and optical measurements. The sampled water entered through a 1/2"-ID hose, then flowed serially through the absorption ("a") flow tube and the attenuation ("c") flow tube before passing through the pump and exiting through the outlet in a 1/2"-ID hose. The outlet was located symmetrically, with respect to the flow around SeaSoar, from the inlet to minimize any dynamic pressure gradient. The position of the outlet near the inlet does not reintroduce previously sampled water as a result of the dynamic flight of the vehicle through the water column. The SBE 5T 3000-rpm centrifugal pump is capable of an unrestricted flow rate of 150 mL s^{-1}. The true pumping rate during deployment was approximately 50 mL s^{-1}.

Power and data transfer requirements of the ac-9 were supplied by a power and data communications package, specifically, a WET Labs Modular Ocean Data and Power System (MODAPS). For the first half of the E9608 cruise, a prototype MODAPS+ unit was used, after which, a conventional MODAPS was used for the remainder of the E9608 cruise and the entire E9704 cruise. Data received from the instrument is stored on shipboard PCs or UNIX workstations. The serial data stream is also input to a real-time monitor and display software package which allows the user to monitor the instrument's performance (*Barth and Bogucki*, 2000). This is critical for the successful operation of an ac-9 aboard SeaSoar for the immediate detection of malfunction of the ac-9 plumbing system or flow tube clogging. The real-time displays of absorption and attenuation spectra, time series (single channels or algebraic combinations of channels), or color raster plots of parameters as a function of time and depth, would also allow targeted sampling concentrated on bio-optical features.

An additional optical instrument, a prototype single-channel fluorometer (FlashPak, WETLabs, Inc.) flown at the request of CMO investigator Dr. Paula Coble (University of South Florida), was mounted alongside the ac-9 on top of SeaSoar. The FlashPak was placed downstream of the ac-9 in the pumped optics water supply, and was powered by and returned data via the SBE CTD. Results from Dr. Coble's fluorometer are not reported here.

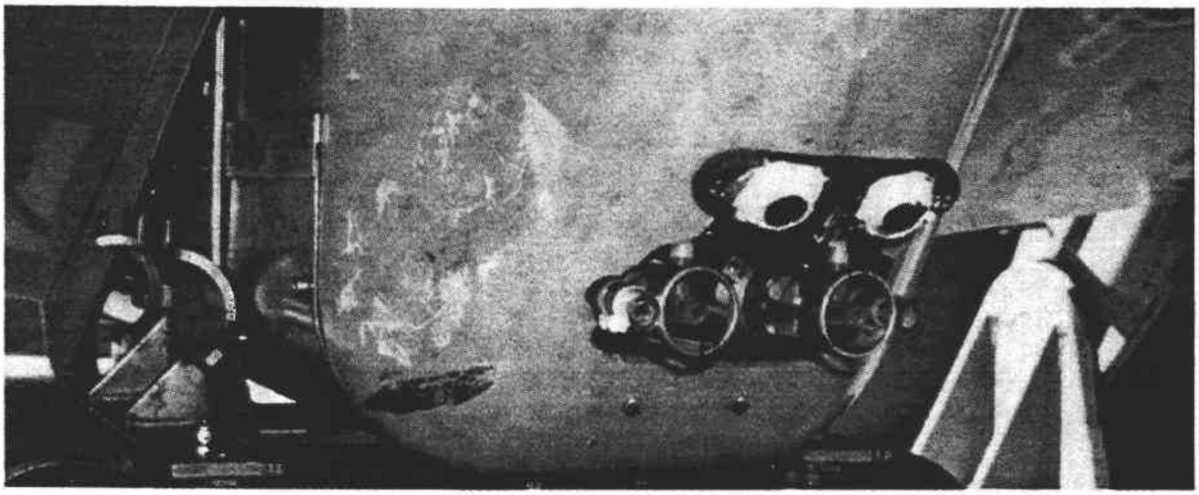

Figure 4: Inlet and outlet for the ac-9 water supply located in SeaSoar's nose adjacent to the dual Sea-Bird temperature-conductivity sensors (above). Closeup of the spectral absorption and attenuation meter (WET Labs ac-9) mounted on top of SeaSoar showing pump and hose configuration (below).

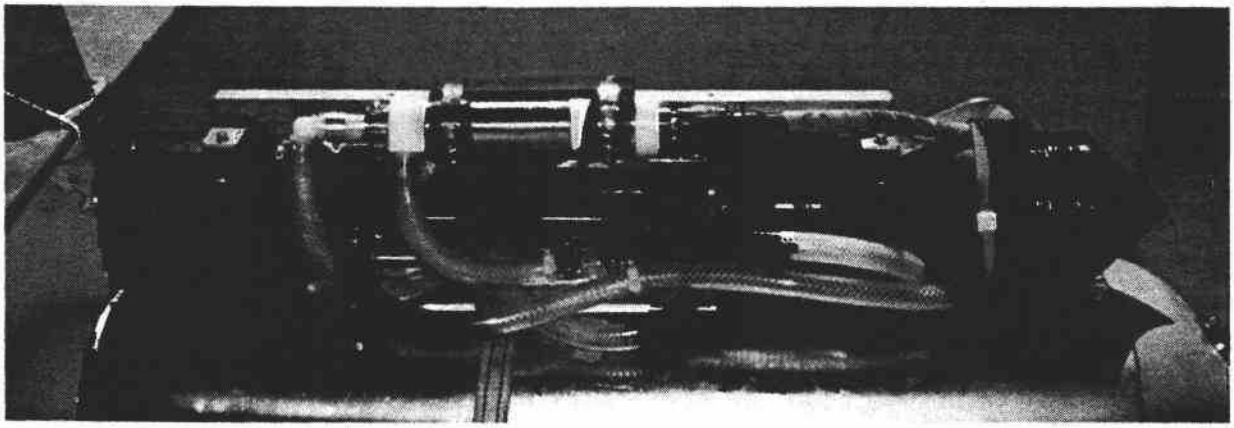

An important consideration for processing and analyzing data from SeaSoar is its flight pattern through the water column. The vehicle samples from the surface to within five to ten meters of the bottom. The ship's echosounder supplied the SeaSoar control software with water depth in order to avoid bottom collisions while the vehicle was towed at six to eight knots (3.1 to 4.1 m s^{-1}) behind a research vessel. During the CMO experiment conducted over the continental shelf, the time to complete an ascending and descending cycle varied between 1.5 and 4.0 minutes for shallow (55 m) and deep (105 m) profiles, respectively. The vehicle's vertical speed varied with depth and differed between the ascending and descending profiles. Vertical speeds ranged from 0 to 3 m s^{-1}, with an average value of 1 m s^{-1} (*Barth and Bogucki*, 2000). The SeaSoar's typical vertical speed is in excess of the typical descent and ascent rates used while profiling from a stationary research vessel. The variable flow past the vehicle has the potential to influence the pumped flow rates through dynamic pressure gradients, but, as demonstrated by Barth *et al.* (1996) this effect is small. The vehicle's vertical velocity influences the ac-9's vertical resolution given its 6-Hz sampling rate and is critical for calculating depth offsets from time lags induced by water samples passing through the plumbing and optical flow tubes (see following section).

Throughout the 11 days of towing SeaSoar during the 1996 CMO Experiment, the vehicle was recovered only a few times to correct problems with the optical instrumentation. Partial clouding of the optical paths in one or the other flow tube occurred several times during the E9608 cruise due to inefficient clearance of gelatinous plankton from the flow tubes. Data from these periods were recoverable using a technique described in the next section. During the E9704 cruise, on 30 April, an electrical short caused the loss of a MODAPS communications channel. This required an alteration in the power and data communications system configuration for the remainder of the E9704 cruise. The SBE data telemetry was run in parallel with the RS-485 MODAPS communications. This configuration permitted the potential for crosstalk between the CTD (run by SBE data telemetry) and the ac-9 and MicroSoar (both run by the MODAPS data telemetry). The use of the SBE data telemetry with the RS-485 MODAPS communications resulted in a reduction of acquired ac-9 data which has made the time lag correction and merging of the CTD files with IOP files, at times, unfeasible.

3 Data Processing and Editing

The attainment of accurate IOP measurements from a towed platform requires a multi-step post-processing procedure: 1) factory calibration; 2) merging of ac-9 data with navigational and hydrographic data; 3) time lag correction; 4) temperature and salinity correction; 5) post-calibration correction; and 6) scattering correction. Then, the processed data is edited to eliminate data spikes, incomplete spectra, values associated with excessive variances, values associated with GPS errors and, if possible, to adjust values to eliminate offsets due to a clouding substance.

The filenaming convention for the summer and spring cruise data files is as follows: eYYP#L#(##); where e = *R/V Endeavor*, YY = year (e.g. 96, 97), P# = pattern number (e.g. smallbox (s), bigbox (b), butterfly (f)) and L#(##) = line number (e.g. 5, ns). So that the filename "e97s5l6" reads, cruise E9704, Smallbox 5, Line 6 or "e96f2lns" reads, cruise E9608, Butterfly 2, Line north to south. An extension is added to indicate different types of files. The possible extensions are: .dat, .acvar, .ac.cut and .ac.junk. The first extension, .dat, indicates an edited file which has undergone data quality checks and is considered the final product. The second extension, .acvar, indicates a data file that contains the calculated variance in the processed, unedited data. The third extension, .ac.cut, indicates a data file that contains processed data with some editing, but prior to a clog adjustment (see Table 1). The fourth extension, .ac.junk, indicates a file that contains data which have been removed from the processed, unedited data file. The columns in files with extensions, .dat, are ordered

1) Julian Date
2) latitude
3) longitude
4) pressure
5) temperature
6) salinity
7) sigma-t
8-16) absorption (412 440 488 510 532 560 650 676 715)
17-25) attenuation (412 440 488 510 532 560 650 676 715)
26) flags
27) bottom topography .

3.1 Factory Calibration

A factory calibration of ac-9 (S/N 152) was performed at WET Labs prior to the E9608 cruise, on 8 May 1996. Subsequent factory calibrations were again performed before and after the E9704 cruise on 23 October 1996 and 26 August 1997, respectively. The factory calibration is necessary for the removal of pure water offsets from the acquired, raw IOP measurements. The ac-9, like any spectrophotometer, requires a reference substance with which to compare measured values. In this case, the ac-9 is factory calibrated to measure the absorption and attenuation coefficients, respectively symbolized as a and c, at nine wavelengths, relative to pure water at 25°C. This allows the detection of optical signals of suspended dissolved and particulate materials removed from pure water. During the factory pure water calibration, a calibration file containing the pure water value readings is created. This calibration file is utilized by the factory-provided ac-9 software (1995) to correct the clean water offsets in the raw measurements. Further details can be found in the WET Labs *ac-9 User's Guide.*

3.2 Merging of ac-9 data with navigational and hydrographic data

The 6-Hz ac-9 data stream, averaged to 1-second values, is merged with the ship's GPS navigational record as well as with the SeaSoar hydrographic data stream. The ac-9 data stream, though recorded concurrently in real-time with the GPS and hydrographic data, must be processed to account for delays in the transmission of data packets, flow delays due to residence time in the plumbing and random errors due to sometimes poor transmission. The main purpose of the data processing is to remove these effects. First, the ac-9 data stream is synchronized with the rest of the SeaSoar data by matching the two independent pressure traces. This is accomplished given the depth and internal time of the ac-9 as well as the depth and real world time from the CTD and GPS, respectively. Superimposing the two pressure traces then provides a time and location stamp for the ac-9 data stream. This process has led to the discovery that the ac-9 acquisition system clock drifts on average 1 s over 1000 s and that the drift varies considerably with time (*Barth and Bogucki*, 2000).

3.3 Time lag correction

The rapid movement of SeaSoar through the water column (3.1-4.1 m s^{-1} in the horizontal, 0-3 m s^{-1} in the vertical) contrasts with the slower (0.5 m s^{-1}) conventional method of vertical profiling. The dynamic movement of the SeaSoar and the plumbing for the ac-9 introduces a temporal lag in the data streams between the recorded pressure and IOP of a particular sampled volume. This results in a pressure offset between the IOP measurements from the SeaSoar's descent versus measurements from the SeaSoar's ascent, as well as the true depth. These plumbing related, space variable, time variable and other unknown delays introduced during the SeaSoar acquistion go far beyond the constant and known delays associated with the vertical profiling mode of ac-9 data acquisition. To correct the temporal offsets in the data streams, an optimal time lag is determined by varying the applied lag to minimize the difference between the descending and ascending traces. This technique relies on the existence of vertical variations in optical properties over the water column, a common situation in the coastal ocean, where subsurface optical features exist (e.g. phytoplankton layers, resuspended bottom sediments; see Figure 5).

Further, it is assumed that optical features are horizontally uniform over the distance of the SeaSoar's ascent and descent. The assumption is justified given that strong summer stratification produces temporally consistent phytoplankton and sediment vertical distributions (Houghton and Marra, 1983; Zaneveld *et al.*, 1997; Roesler *et al.*, 1997). During the CMO experiment, conducted over the continental shelf, this distance at the top and bottom of the profile varied between 300 and 800 m for shallow (55 m) and deep (105 m) profiles,

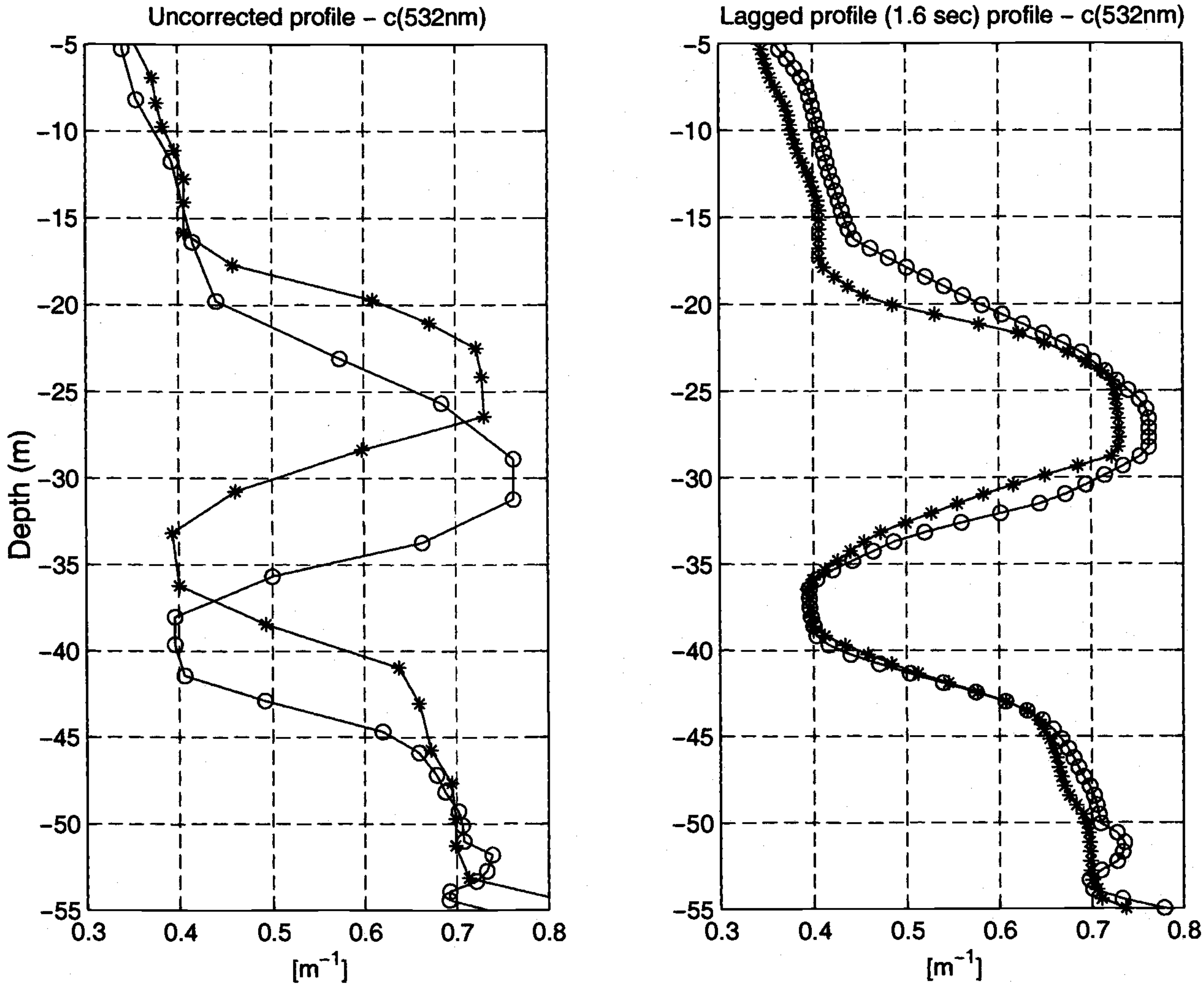

Figure 5: The $c(532)$ as a function of depth from adjacent ascending (asterisks) and descending (circles) profiles for (a) uncorrected 1-Hz data and (b) lag corrected linearly interpolated data.

respectively. Given the sawtooth shape of the SeaSoar flight path, at other depths the horizontal separation is reduced (e.g. by a factor of two at mid-depth so that measurments are separated by 150-400 m depending on the profiling depth).

To find the optimal time lag, the 1-s ac-9 measurements are first linearly interpolated to a finer spatial grid with 200 points in the vertical so a typical profile has a grid spacing of 100m/200 = 0.5 m. To translate between time lags and depth offsets, the vertical velocity, w, of the vehicle is computed from time differencing the CTD pressure record then filtering with a five-point running mean. For a vertical velocity of 1 m s^{-1} the five point filter is about 2 s wide. Next, the time lag in the relation $z_{true} = z_{measured} - w{*}\text{lag}$ is varied to minimize (in the least squares sense) the difference between the measured and optical signal on the ascending and descending traces. The optimum lag is calculated for each channel, since all 18 channels are not measured simultaneously. By example, the method applied to a 2600 s transect determined 26 lag values for each channel. The average delay over the nine absorption and nine attenuation channels as a function of ascending/descending pair number is shown in Figure 6. The mean delay over all 26 pairs for c is approximately 1.35 s and -0.15 s for a. The negative value exists due to the ac-9 acquisition software delay, because pressure is recorded at the end of each data packet, and the "physical" delay due to a finite rate of fluid flow through the ac-9's plumbing system. The difference between the observed a and c delays gives a total time delay of 1.5 s. Given the length and inner diameter of the tubing, we estimate that the fluid flow speed through the ac-9's plumbing was fairly constant at approximately 50 mL s^{-1}. This flow rate agrees with the reported flow rate (46 mL s^{-1}) for a SBE 5T operating at 3000 rpm for flow through a SBE conductivity cell. The variance of the difference between the a and c lags (open circles in Fig. 6) is smaller than the variance for either the a or c lags alone, which indicates the analysis yields a good estimate of the physical delay.

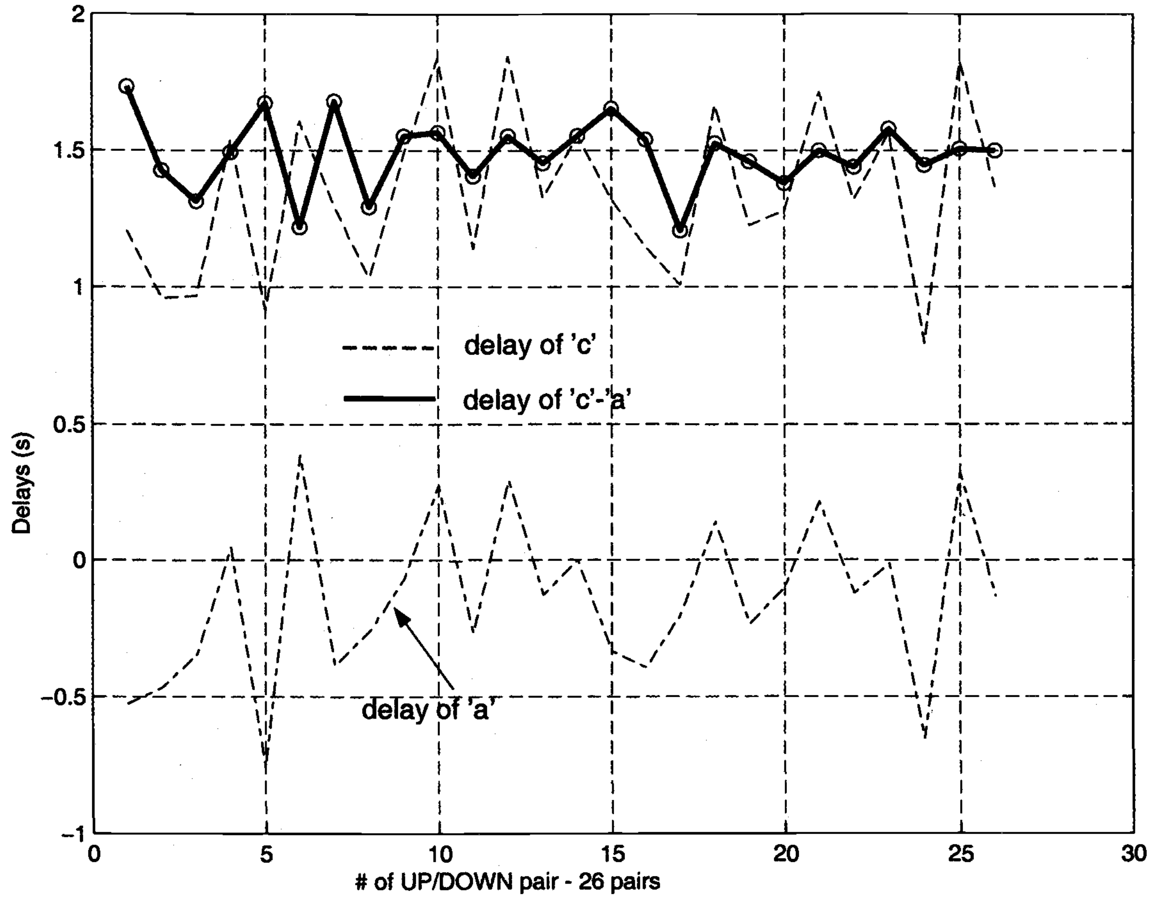

Figure 6: Time delays from lagged correlation of adjacent ascending and descending optical profiles as funciton of ascending-descending profile pairs along the SeaSoar track.

For each a and c channel, the optimum time lag is then multiplied by the depth-dependent veritical velocity to obtain the true depth of the optical measurements. An example of a vertical profile of c(532 nm) before and after removing the delay is shown in Figure 5. To find the relative "error" of the ac-9 measurements the differences between the ascending and descending absorption measurements at 532 nm normalized by the descending values as a function of depth for the entire 2600-s transect are plotted (Figure 7a). These differences could be due to both the processing technique, e.g. inability to get a good least-squares fit between ascending and descending profiles, and natural horizontal variability between profiles. The differences in vertical speed of the SeaSoar vehicle between the ascending and descending profiles are also plotted (Fig. 7b). The relative "error" is less than 10% for all a and c channels and there is no visible dependence of the "error" on vertical speed, lending confidence to the processing algorithm. The lag-corrected a and c profiles at the nine wavelengths serve as input to the next stage of processing.

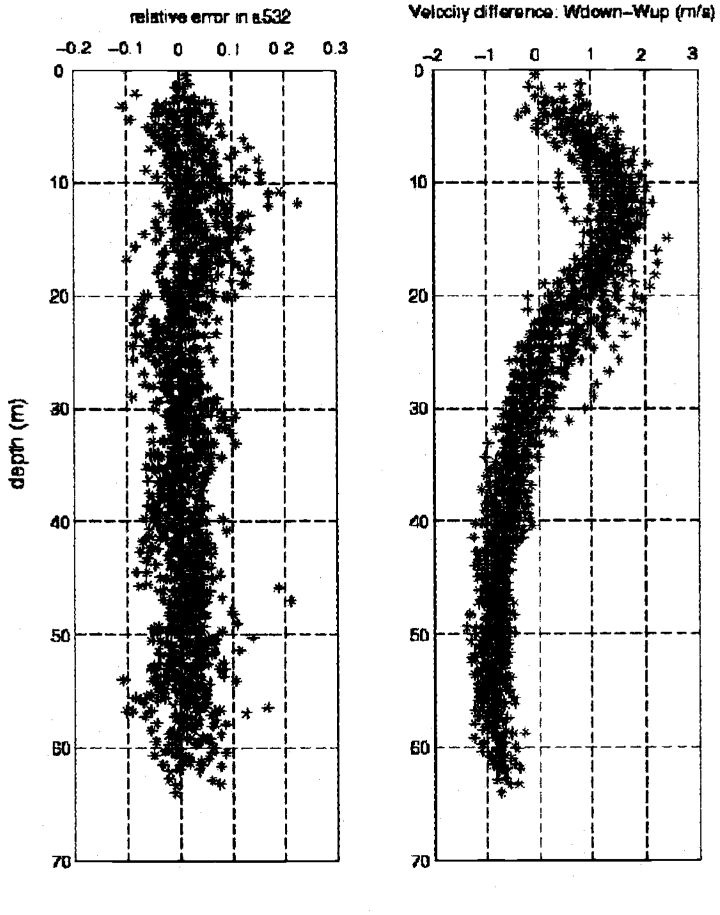

Figure 7: Relative "error" in absorption at 532 nm $((a_{ascend} - a_{descend})/a_{descend})$ and vertical velocity difference as a function of depth.

3.4 Temperature and Salinity Correction

The absorption spectrum of water is temperature and salinity dependent (Pegau *et al.*, 1997). The effect of temperature on the pure water absorption spectrum is much greater than that of salinity. The contrast between the 25°C pure water reference and the *in situ* instrument and water sample temperatures, which can be 10°C or less, causes a notable absorption decrease in the far red channel, 715 nm. For this region, the salinity dependence of the pure water absorption spectrum are small enough to apply a constant salinity correction (Moore and Bruce, 1996). The ac-9 does not measure the temperature of the ambient water, therefore lag-corrected temperatures measured by the CTD were applied to perform the temperature correction.

Temperature and salinity corrected absorption as a function of wavelength, $a_{TS}(\lambda)$, is calculated as

$$a_{TS}(\lambda) = a_m(\lambda) - [R1*(T_m - T_{ref}) + R2_a*(S_{const})]$$

Temperature and salinity corrected attenuation as a function of wavelength, $c_{TS}(\lambda)$, which is also the "true" attenuation coefficient, is calculated as

$$c_{TS}(\lambda) = c_m(\lambda) - [R1*(T_m - T_{ref}) + R2_c*(S_{const})]$$

Here, the subscript, m, indicates the *in situ* measured parameter. The subscript, ref, indicates the reference sample and the R coefficients are empirically derived correction coefficients (Pegau *et al.*, 1997; Moore and Bruce, 1996). Table 1 lists the correction coefficients used to process the CMO optical data.

Table 1. Temperature and Salinity Correction Coefficients

λ nm	$R1$ [m^{-1} (^oC)$^{-1}$]	$R2_a$ [m^{-1} psu^{-1}]	$R2_c$ [m^{-1} psu^{-1}]
412	0.0000	0.00018	0.00007
440	0.0000	0.00008	-0.00007
488	0.0000	0.00008	-0.00007
510	0.0002	0.00009	-0.00007
532	0.0001	0.00004	-0.00008
560	0.0001	0.00008	-0.00008
650	0.0001	0.00011	-0.00005
676	0.0001	0.00008	-0.00007
715	0.0029	-0.00008	-0.00032

3.5 Post Calibration Correction

During a cruise, frequent clean water calibrations and cleanings of the ac-9 are recommended for the most accurate IOP measurements. The use of a calibration reference record is valid so long as the instrument configuration, temperature, optics, etc. as well as the ambient temperature, temperature of the sampled volume and ambient air quality are identical. Therefore, updates of the reference record is recommended after physically moving the instrument. Frequent clean water calibrations and cleaning of the ac-9 were impractical during the cruise given the sampling method of multi-day towing of the SeaSoar. The ac-9 optics were thoroughly cleaned between each SeaSoar tow of which there were 15(10) during E9608(E9704). To mitigate any errors in the IOP measurements due to use of an outdated reference record, processed and edited SeaSoar IOP data were compared to spatially (horizontal and vertical) and temporally similar stationary, vertical IOP profiles collected by the Oregon State University optical oceanography group's vertical profiler, Slow-Drop, aboard *R/V Seward Johnson* (August-September 1996) and aboard the *R/V Knorr* (April 1997). Table 3 lists data files used to determine post-calibration offsets. The E9704 cruise post-calibration calculation was limited by the availability of comparable Slow-Drop data (existing Slow-Drop IOP data for the majority of the cruise are filtered measurements, therefore incompatible with the SeaSoar unfiltered ac-9 data).

Table 3. Coincident SeaSoar and Slow-Drop Measurements

R/V Endeavor Filename	*R/V Johnson* Filename	Start Time	Stop Time	Latitude,^{o}N	Longitude,^{o}W	Depth range (meters
e96b1lC		17-Aug-96 19:24	17-Aug-96 20:11	40.17 to 40.64	70.48	40-60
	c9681807	18-Aug-96 07:00		40.17	70.50	40-60
	c9681808	18-Aug-96 08:46		39.99	70.50	40-60
e96f2lwe		27-Aug-96 11:12	27-Aug-96 14:15	40.41 to 40.52	70.28 to 70.65	20-30
	c9682701	27-Aug-96 12:18		40.50	70.49	20-30
	c9682702	27-Aug-96 12:31		40.50	70.49	20-30
	c9682703	27-Aug-96 12:41		40.50	70.49	20-30
	c9682704	27-Aug-96 12:54		40.50	70.49	20-30
	c9682705	27-Aug-96 13:05		40.50	70.49	20-30
	c9682706	27-Aug-96 13:15		40.50	70.49	20-30
e96f2ns		27-Aug-96 17:31	27-Aug-96 20:00	40.37 to 40.63	70.43 to 70.53	1-20
	c9682712	27-Aug-96 17:34		40.49	70.49	1-20
	c9682713	27-Aug-96 17:45		40.50	70.49	1-20
	c9682714	27-Aug-96 18:57		40.50	70.47	1-20
	c9682715	27-Aug-96 19:07		40.50	70.47	1-20
	c9682716	27-Aug-96 19:20		40.50	70.47	1-20
	c9682717	27-Aug-96 19:29		40.50	70.47	1-20
	c9682718	27-Aug-96 19:38		40.50	70.47	1-20
	c9682719	27-Aug-96 19:48		40.50	70.47	1-20
e96b3lF		01-Sep-96 00:21	01-Sep-96 04:46	39.75 to 40.33	70.06	60-100
	c9690508	05-Sep-96 18:14		40.00	70.50	60-100
	c9690509	05-Sep-96 12:57		40.00	70.50	60-100
	c9690601	06-Sep-96 13:07		39.85	70.50	60-100
	c9690602	06-Sep-96 13:18		39.85	70.50	60-100
	c9690603	06-Sep-96 13:18		39.85	70.50	60-100
R/V Endeavor Filename	*R/V Knorr* Filename	Start Time	Stop Time	Latitude,^{o}N	Longitude,^{o}W	Depth range (meters
e97s3l3		29-Apr-97 11:21	29-Apr-97 13:27	40.3 to 40.6	70.5	15-40
	C9742901	29-Apr-97 12:52		40.5	70.49	15-40
	C9742902	29-Apr-97 13:02		40.5	70.49	15-40
	C9742903	29-Apr-97 13:10		40.5	70.49	15-40
	C9742904	29-Apr-97 13:17		40.5	70.49	15-40
	C9742905	29-Apr-97 13:28		40.5	70.49	15-40
	C9742906	29-Apr-97 13:34		40.5	70.49	15-40

To obtain the post-calibration offsets, SeaSoar and Slow Drop profiles were first averaged into 1 meter depth bins. Less than five SeaSoar profiles were used to construct the average SeaSoar vertical profile. The Slow-Drop files listed in Table 3 indicate the data used to obtain an averaged Slow-Drop profile. The temporal and spatial window of SeaSoar optical data used for the post-calibration was necessarily restrictive to achieve SeaSoar profiles comparable to the stationary, vertical profiles. SeaSoar data extracted to calculate the average SeaSoar profiles were at the nearest possible location (1 km or less) and within an hour of the stationary, vertical profiles. In two cases, the comparison of "clear" deep (> 100 m) water measurements were also used to determine the offset in SeaSoar data from Slow-Drop's data. The deep water profiles were not subjected to a restrictive time window. Since differences between the above specified SeaSoar and Slow-Drop profiles were still observed due to spatial heterogeneity, the post-calibration offsets were calculated using only portions of the vertical profiles where the average of the differences ($10 < N < 40$) between SeaSoar and Slow-Drop profiles exhibited low standard deviations. The depth intervals chosen for inclusion in the calculation of the post-calibration offset are documented in the last column of Table 3.

A final, wavelength-dependent offset is obtained from the comparison of the temperature and salinity corrected Slow-Drop and SeaSoar IOP measurements (Table 4). The results of the comparison between the Slow Drop and SeaSoar profiles show that the offsets in $a(\lambda)$ generally decrease as a function of wavelength during both cruises (see Table 4). Offsets in a at each wavelength exhibited a fairly consistent range of deviation over time (Figure 9). The E9608 data offsets in $c(\lambda)$ are generally spectrally flat with a spectrally constant deviation (see Table 4). The calculated offsets in c (Figure 8) contrasts the offsets in a (Figure 9) with a much larger deviation over time.

Table 4. Mean post-calibration offsets for T,S corrected a and c

wavelength	E9608 offset	E9608 std dev	E9704 offset	E9704 std dev
$a(412)$	0.0703	0.0996	0.1019	0.0014
$a(440)$	0.0513	0.1018	0.0788	0.0014
$a(488)$	0.0460	0.1022	0.0580	0.0012
$a(510)$	0.0451	0.1020	0.0648	0.0009
$a(532)$	0.0458	0.1018	0.0496	0.0008
$a(560)$	0.0402	0.1023	0.0494	0.0009
$a(650)$	0.0358	0.1026	0.0384	0.0006
$a(676)$	0.0403	0.1025	0.0674	0.0012
$a(715)$	0.0227	0.1040	0.0286	0.0005
$c(412)$	0.0182	0.1086	0.0203	0.0065
$c(440)$	0.0210	0.1082	0.0176	0.0081
$c(488)$	0.0224	0.1084	0.0223	0.0087
$c(510)$	0.0292	0.1077	0.0241	0.0088
$c(532)$	0.0372	0.1070	0.0060	0.0081
$c(560)$	0.0258	0.1080	0.0135	0.0080
$c(650)$	0.0275	0.1072	0.0285	0.0111
$c(676)$	0.0305	0.1070	0.0233	0.0109
$c(715)$	0.0005	0.1123	0.0078	0.0116

The ensemble mean of the post-calibration offsets shown in Figures 8 and 9 were used to calculate mean, wavelength-dependent, post-calibration offsets shown in Table 4. The ensemble mean offsets are then subtracted from the temperature and salinity corrected E9608 and E9704 spectra. The comparisons of post-calibrated SeaSoar and Slow-Drop attenuation (Figure 10a and 11a) and absorption (Figure 10b and 11b) spectra show that the subtraction of a mean post-calibration offset from temperature and salinity corrected data retrieves the Slow-Drop temperature and salinity corrected spectra. Correlation coefficients calculated for comparable E9608 and E9704 post-calibrated SeaSoar and temperature and salinity corrected Slow-Drop data are $r \approx 0.8$ and $r \approx 0.95$ (Figures 12-15).

The validity of the application of the E9608 and E9704 post-calibration corrections were assessed using selected data subsamples that temporally spanned the length of the cruise periods. After examining the sub-sampled data for effects of the post-calibration on the magnitude and shape of the a and c spectra, it was determined that the post-calibration offsets for the E9608 optical data were satisfactory, but the post-calibration offsets for the E9704 optical data led to poor results. Therefore, the post-calibration was performed only on the E9608 data set. The E9704 post-calibration offsets are presented here to allow individual investigators to gauge the magnitude of the errors in the E9704 optical data that are due to poor calibration and/or instrument noise or drift. The scattering correction follows to complete the ac-9 IOP data processing.

3.6 Scattering Correction

The ac-9's reflective flow tube, used to obtain absorption measurements, imperfectly captures all the scattered light travelling towards the detector. Thus, the absorption coefficients, as measured by the detector, is an overestimate of the true absorption. It is, therefore,

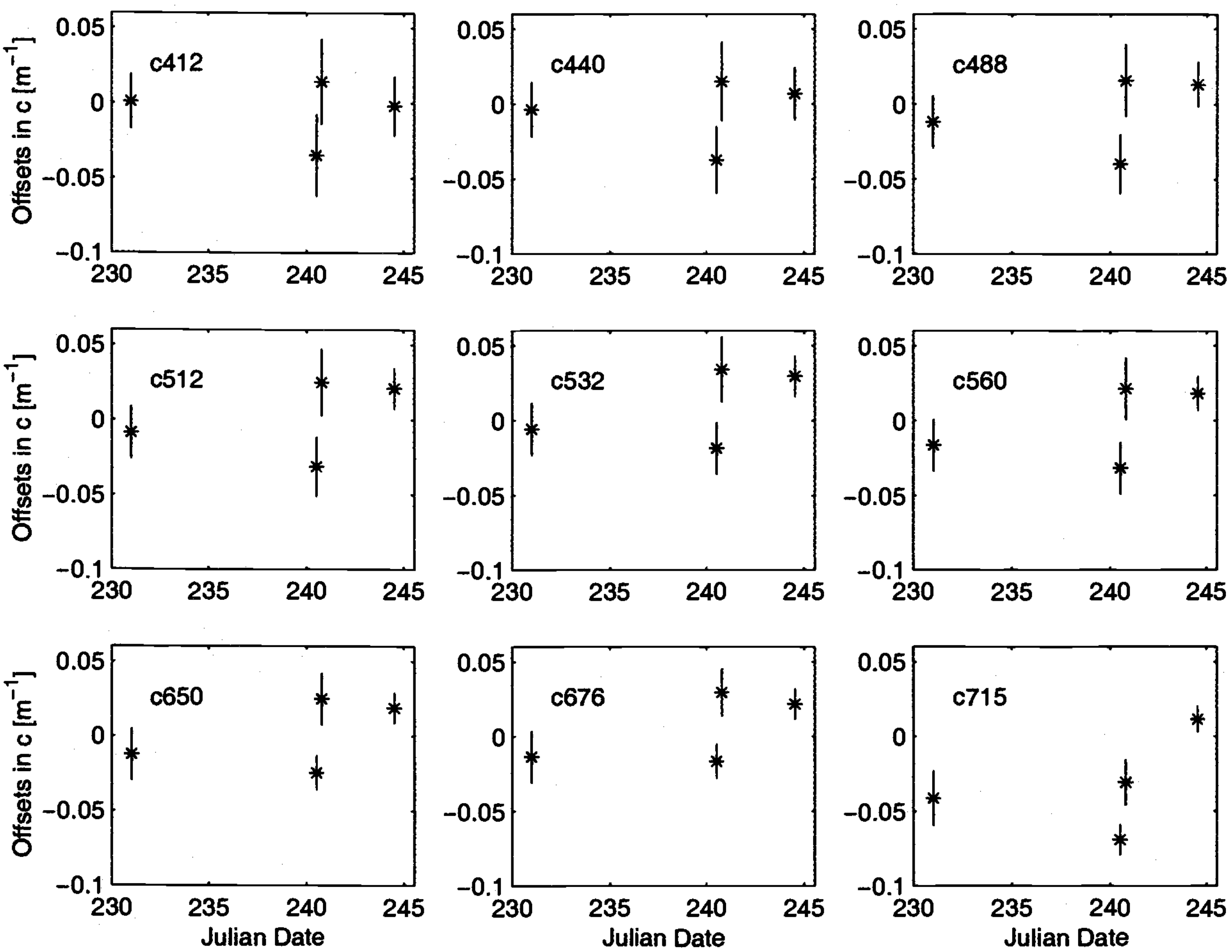

Figure 8: Post-calibration offsets in attenuation spectra as a function of time. Profiles taken from spatially and temporally comparable SeaSoar (<5 profiles) and Slow-Drop (<8 profiles) measurements are each averaged into 1-m bins then offsets are calculated from the differences in the smoothed profiles. Offsets are calculated from regions of the vertical profile exhibiting the smallest standard deviation.

necessary to apply a scattering correction scheme to the ac-9's time-lag, temperature and salinity corrected data. The SeaSoar ac-9 data are scattering corrected according to Roesler and Zaneveld, (1994).

The Roesler and Zaneveld scattering correction method is performed by first calculating a first order scattering spectrum, $b'(\lambda)$,

$$b'(\lambda) = c_{TS}(\lambda) - a_{TS}(\lambda)$$

The scattering correction method assumes that there is no absorption at 715 nm and that any value associated with $a_{TS}(715)$ is due to scattering, but at all other wavelengths, some fraction of the detected absorption signal is due to scattering. Therefore, the shape of the first order scattering spectrum, $b'(\lambda)$ weighted by the reference wavelength, $a(715)$, is used to

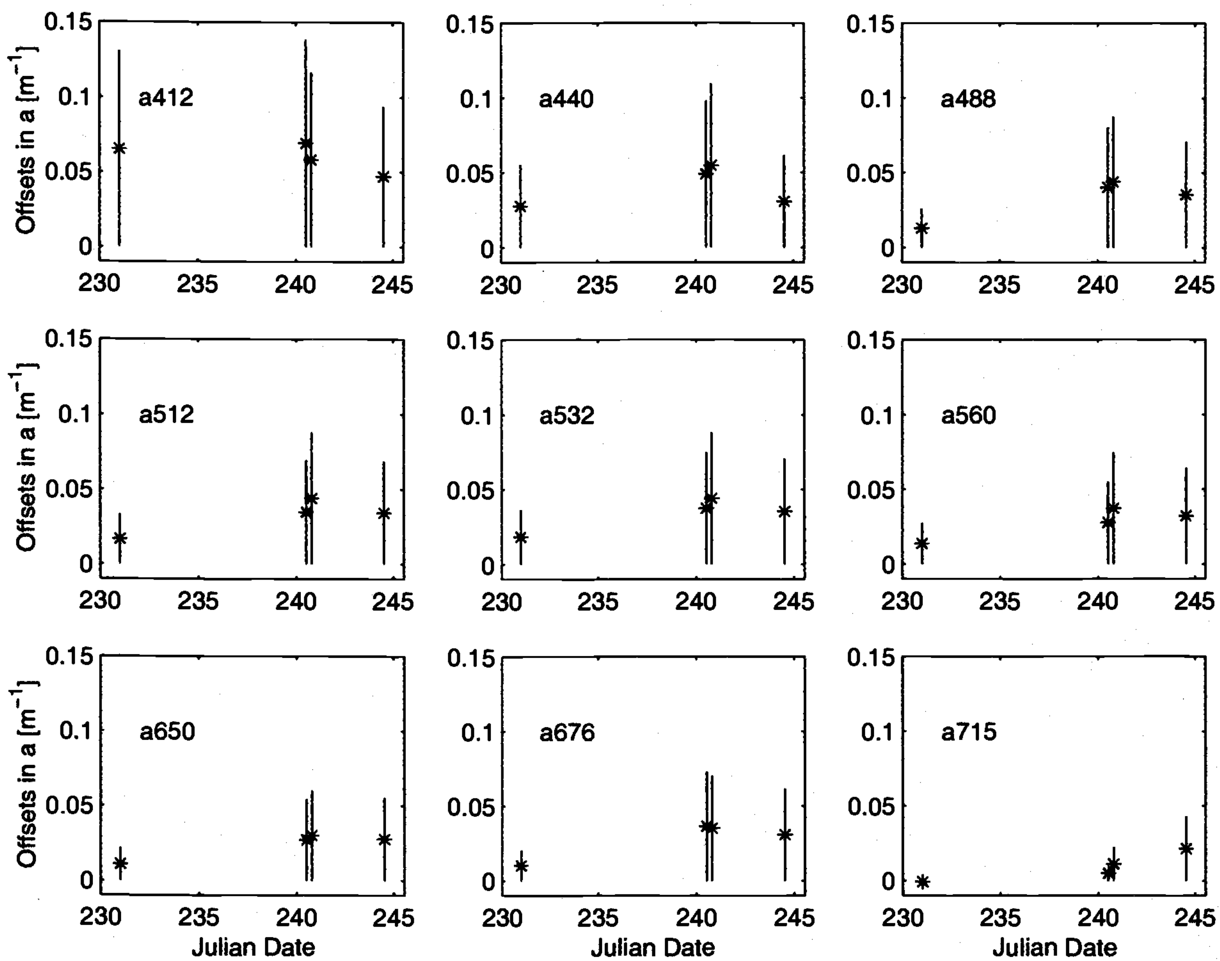

Figure 9: Post-calibration offsets in absorption spectra as a function of time. Identical criteria for the calculation of the post-calibration offsets in $c(\lambda)$ were also applied towards the calculation of the post-calibration offsets in $a(\lambda)$.

remove scattering errors in the detected absorption measurement. The temperature, salinity and scattering corrected absorption coefficients, which are the "true" absorption coefficients, are then:

$$a(\lambda) = a_{TS}(\lambda) - b'(\lambda)*[a_{TS}(715)/\ b'(715)]$$

The true scattering coefficients can then be determined from the temperature and salinity corrected attenuation and the temperature, salinity and scattering corrected absorption:

$$b(\lambda) = c_{TS}(\lambda) - a(\lambda)$$

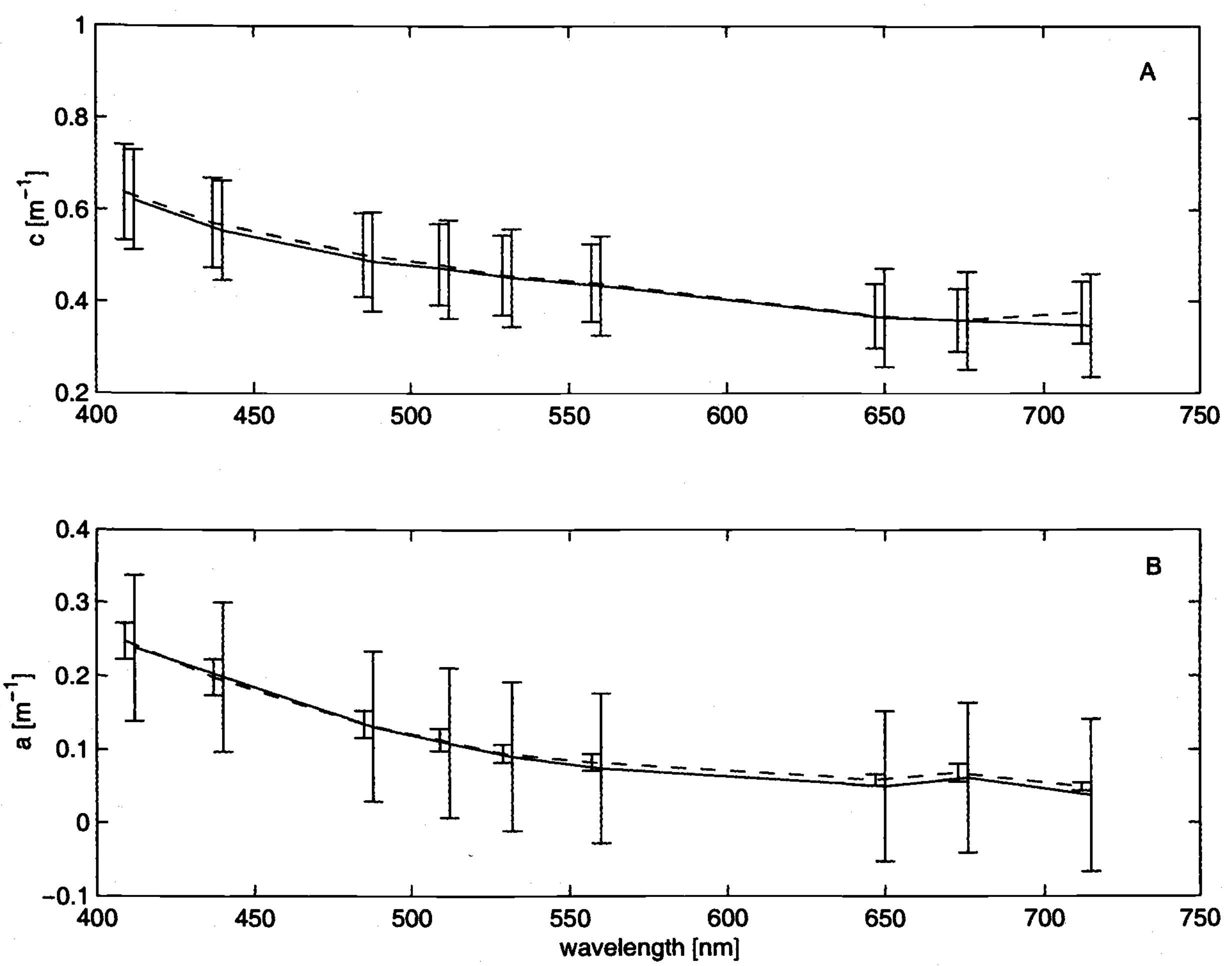

Figure 10: Comparison of 1-m bin averaged post-calibrated SeaSoar (solid) and temperature and salinity corrected Slow-Drop (dashed) spectra for E9608 butterfly 2 line N-S at 20 m. The Slow-Drop spectrum is shifted 3 nm to the left to make the standard deviations distinguishable.

The application of the scattering correction to the temperature and salinity corrected, post-calibrated SeaSoar data is illustrated in the following section.

3.7 Editing

The IOP data files, after processing, are edited to eliminate spectra containing data spikes and data with erroneous GPS values. An adjustment for only the E9608 data collected during optical path clouding of the a or c flow tubes is also performed when necessary.

The elimination of data spikes is accomplished by requiring the data to satisfy the following criteria: 1) a and c must be non-negative and less than some large, rare value (e.g. 10 m^{-1}); 2) data must not exhibit a variance that exceeds a pre-determined variance value. The variance in the data was calculated using a 5-point running mean. The cut-off variance value for E9608 data was 0.002 and 0.04 m^{-2} for a and c, respectively, and for E9704, 0.0015

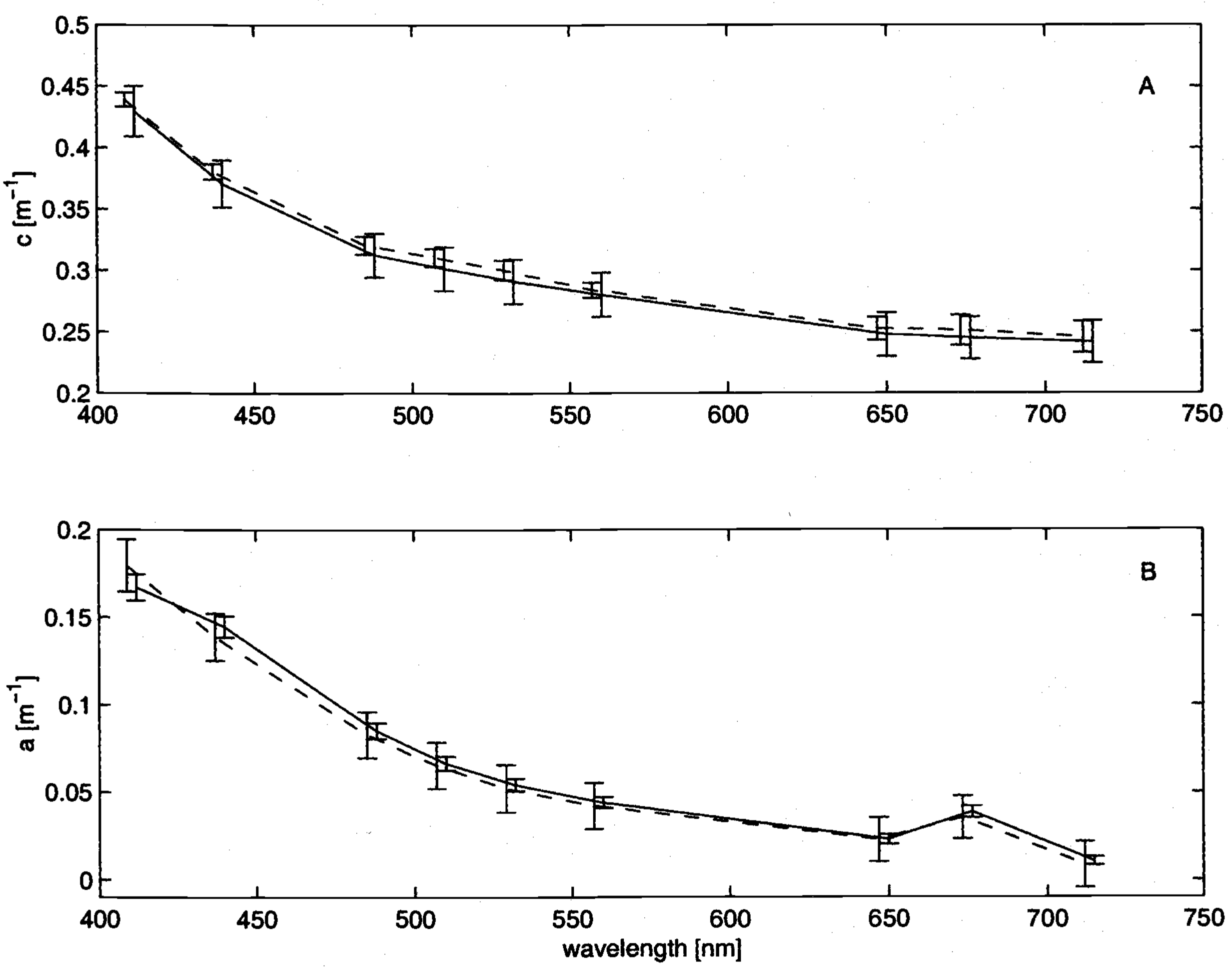

Figure 11: Comparison of post-calibrated SeaSoar (solid) and temperature and salinity corrected Slow-Drop (dashed) spectra for E9704 smallbox 3 line 3 at 20 m. The Slow-Drop spectrum is shifted 3 nm to the left to make the standard deviations distinguishable.

and 0.01 m^{-2} for a and c, respectively. The cut-off variance values chosen were of three orders of magnitude or greater than the average variance exhibited by the data, which translates to a and c values an order of magnitude larger than the mean value. Incorrect recordings of GPS values were found in several data files. These data, constituting less than 1% of the total data file, were eliminated.

On several occassions during the E9608 cruise, either or both the a and/or c flow tube(s) inefficiently cleared opaque materials (e.g. gelatinous zooplankton) from the optical paths. The resultant measured IOP exhibited a jump or discontinuity, which was an approximately constant offset in the magnitude. For these cases, adjustments to the data were performed in order to salvage qualitative data of the IOP distributions. The offset adjustment was partially unsuccessful in the preservation of spectral shapes, while the absolute magnitudes of the optical parameters were not retrievable with a high degree of confidence. The offset adjustment enabled "clouded" IOP data to be comparable to data on either side of the

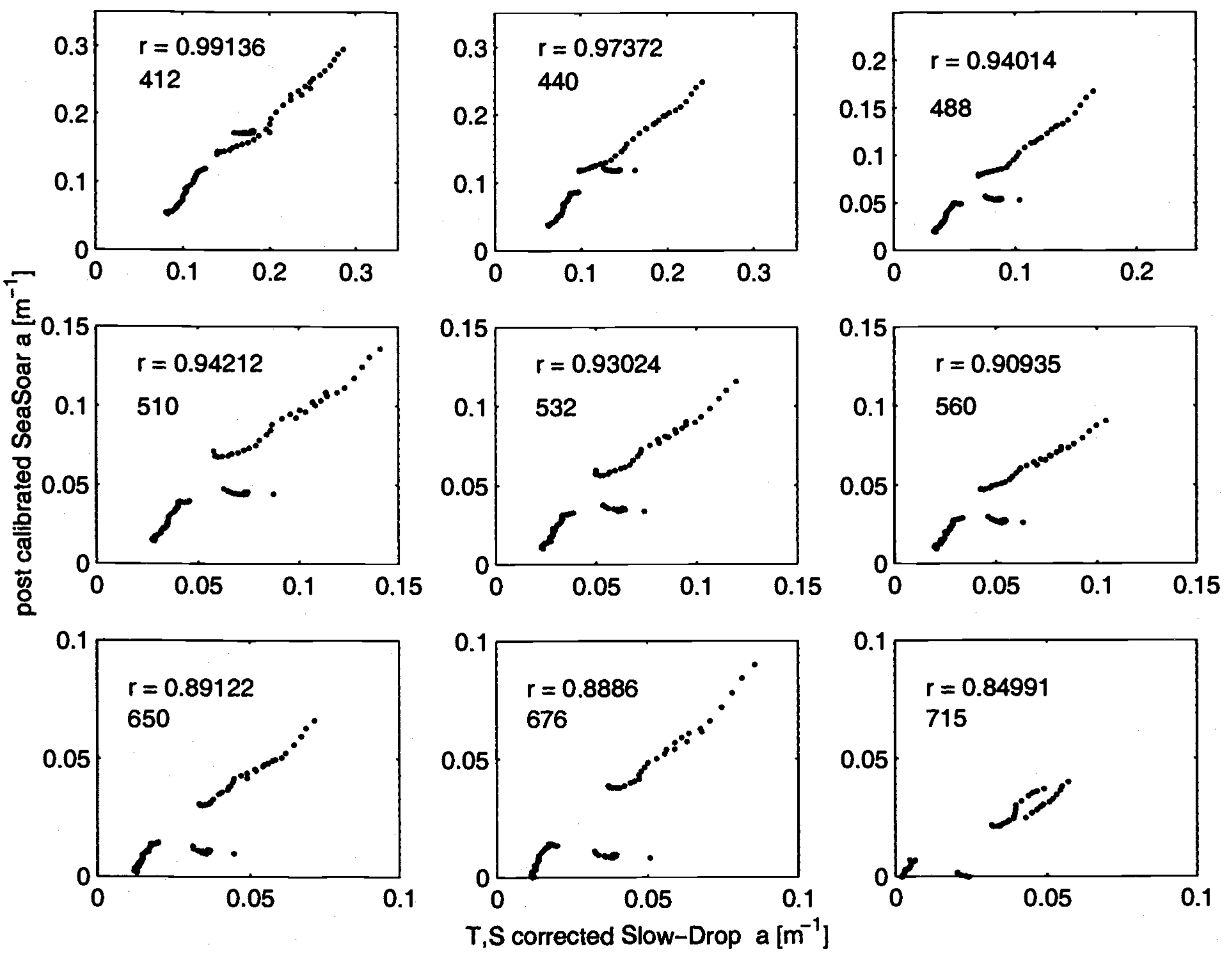

Figure 12: Plots of E9608 post-calibrated SeaSoar absorption coefficients (m^{-1}) regressed against Slow-Drop attenuation coefficients (m^{-1}). Text in each panel states the calculated correlation coefficient and wavelength. post-calibration of deep "clear" water values was the least precise.

corrected period. The data adjustment was performed by first identifying the start and stop time of the clog during the E9608 cruise (Table 2). Each section(line) of a cross-shelf box survey was averaged and plotted as a function of bottom bathymetry[1]. The IOP cross-shelf sections of the box pattern were then averaged together to obtain an ensemble mean a and/or c as a function of bottom depth (or equivalently, cross-shelf distance) for each box. The calculated ensemble mean as a function of bottom depth is used to determine the magnitude of the offset for each "clouded" data point (offset = "clouded" data value − ensemble mean value). Since this offset is approximately constant, a mean offset was calculated from all the individually calculated offsets. The removal of the mean offset is expected to correct the optical measurements corrupted by a clouding substance. Data which could not be adjusted

[1]Bottom bathymetry was obtained from an awk subroutine written by S. Pierce that utilizes latitude and longitude coordinates as input to produce bottom depth corresponding to unpublished USGS bottom bathymetry archives compiled by Rich Signell in 1996.

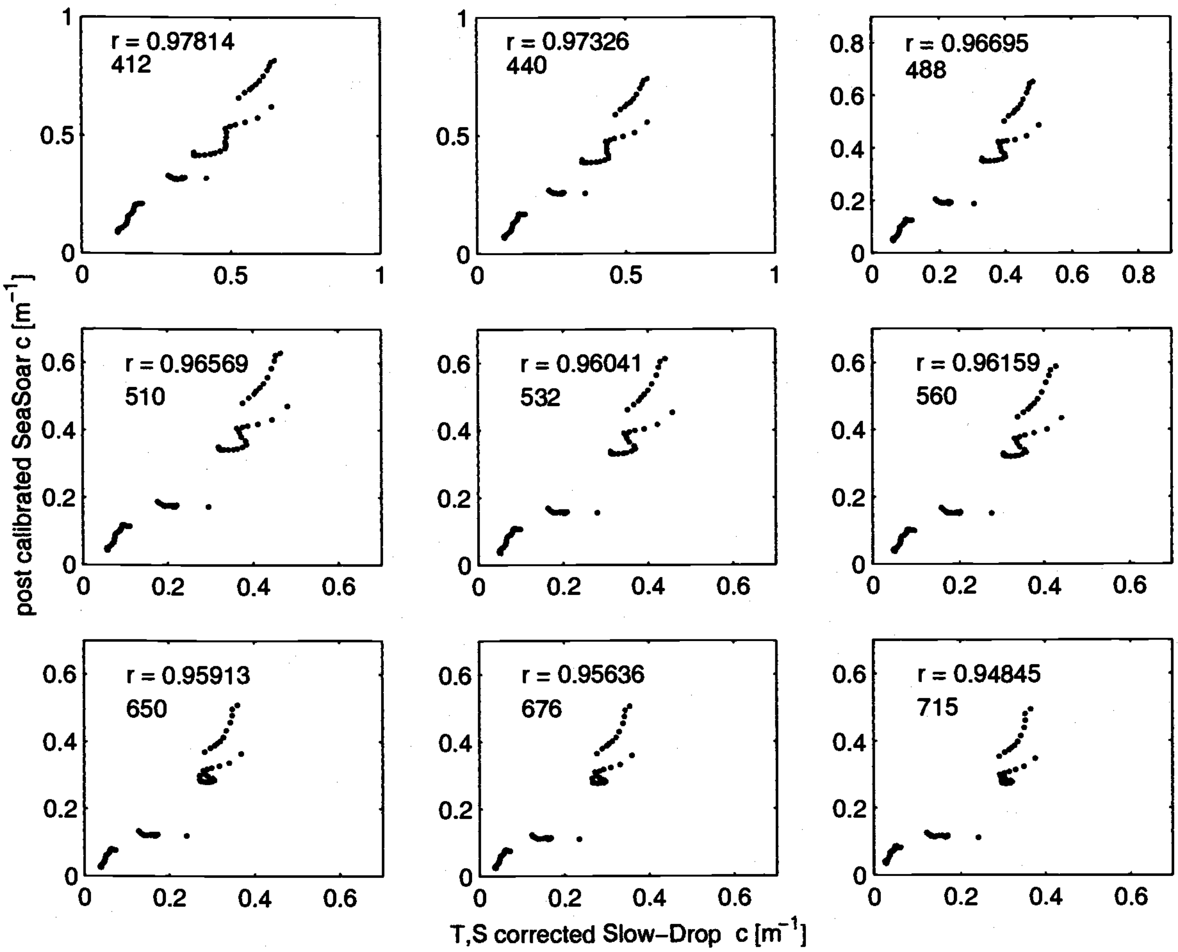

Figure 13: Plots of E9608 post-calibrated SeaSoar attenuation coefficients (m^{-1}) regressed against Slow-Drop attenuation coefficients (m^{-1}). Text in each panel states the calculated correlation coefficient and wavelength. post-calibration of deep "clear" water values was the least precise.

were completely eliminated from the final version of the data file. While data which have undergone this adjustment is not absolutely correct, this correction preserves important spatial information of optical properties. Table 2 summarizes the start and stop times of the "clouding" events, the duration of the "clouding" event and the percentage of the data which was salvaged by the adjustment method previously described. The "clouded" data constitute approximately 12% of the entire E9608 cruise data set.

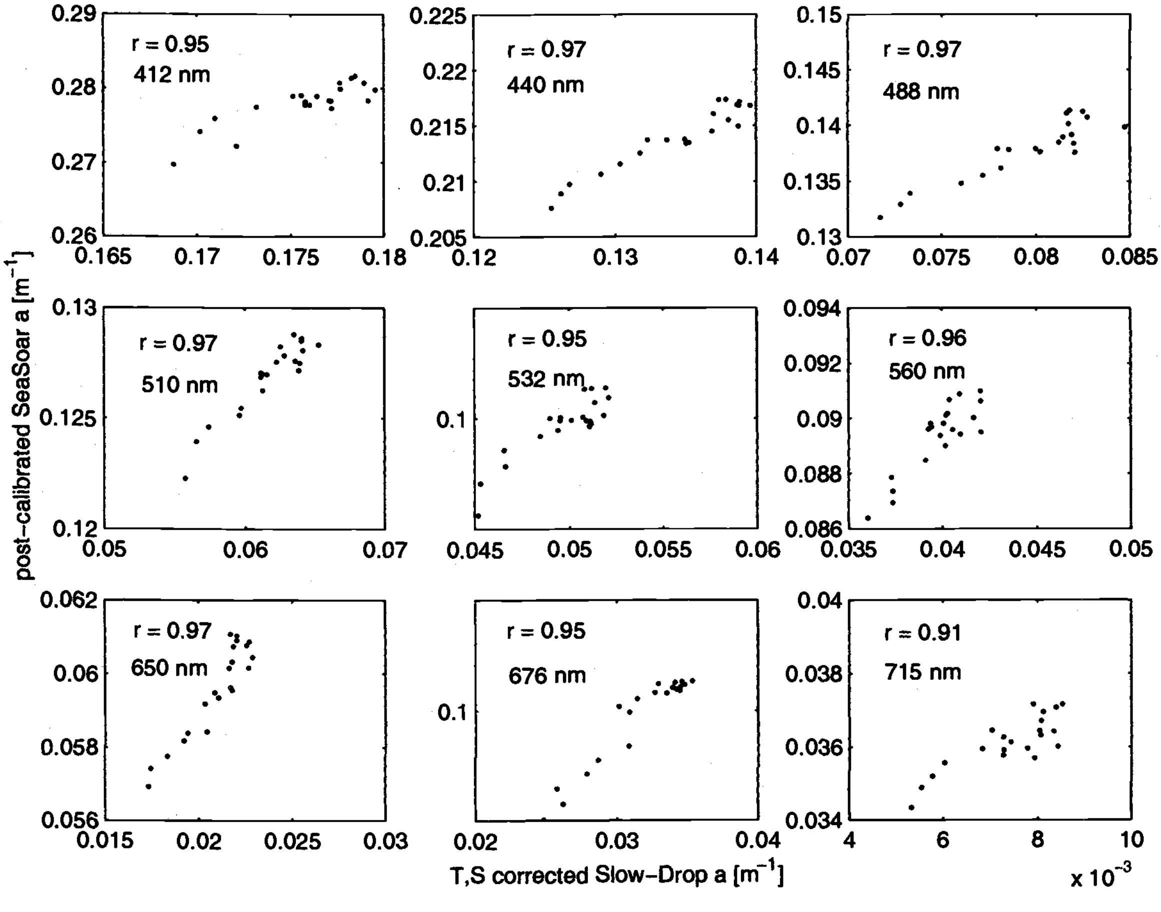

Figure 14: Plots of E9704 post-calibrated SeaSoar attenuation coefficients (m^{-1}) regressed against Slow-Drop absorption coefficients (m^{-1}). Text in each panel states the calculated correlation coefficient and wavelength.

Table 2. E9608 ac-9 clouding events

Section	Start Time	Section	Stop Time	Duration (HH:MM)	Percent recovered
bigbox 2, line B	21-Aug-96 00:14:24	bigbox 2, line C1	21-Aug-96 09:59:02	9:45	100
smallbox 5 to smallbox 6	26-Aug-96 01:29:08	smallbox 6, line 6	26-Aug-96 04:22:13	3:07	91
smallbox 7, line 4	29-Aug-96 09:49:49	smallbox 7, line 3	29-Aug-96 13:25:06	3:17	92
smallbox 8, line 6	29-Aug-96 21:55:26	smallbox 8, line 4-5	30-Aug-96 01:56:21	4:01	15
smallbox 8, line 3	30-Aug-96 06:59:20	smallbox 8, line 1	30-Aug-96 10:32:53	4:27	83
bigbox 3, line C0	31-Aug-96 05:52:36	bigbox 3, line C0	31-Aug-96 07:55:39	2:03	0

Flags are included in each data file to indicate editing performed on the data, as well as the percentage of data which has been discarded from the processed file. The flags are located

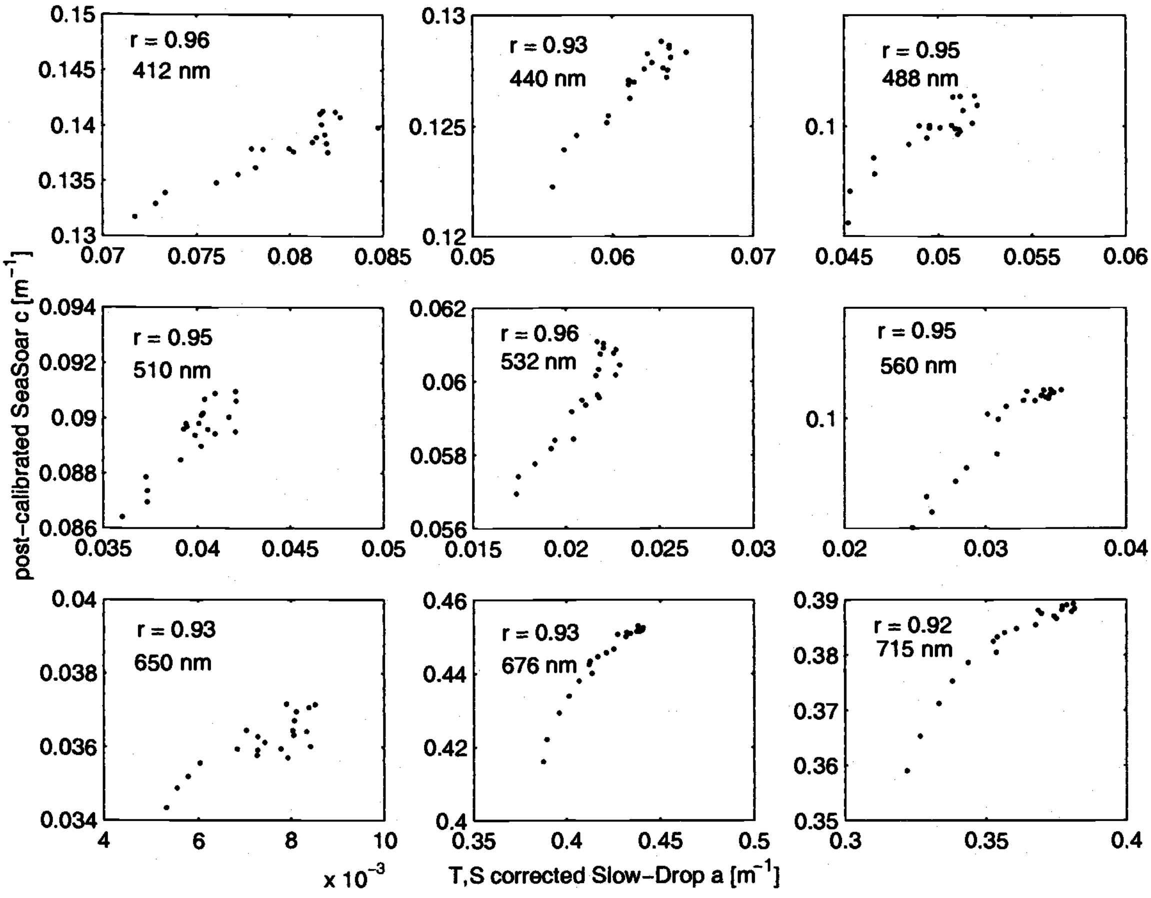

Figure 15: Plots of E9704 post-calibrated SeaSoar attenuation coefficients (m^{-1}) regressed against Slow-Drop attenuation coefficients (m^{-1}). Text in each panel states the calculated correlation coefficient and wavelength.

in the first three rows of the 26th column of the data file: the editing flags are encoded on the first row (see next paragraph), the second flag indicates the presence of a missing value flag within the data record (i.e. a non-zero value indicates that the missing value, 1.0e+22, was used to substitute for discarded values), and the third flag indicates the percentage of the 1-s binned, unedited data that was removed during the editing process.

The editing flag consists of 9 numeric characters and are either "0" or "1". The first and ninth values are "1" and serve as place holders. A non-zero second character indicates incomplete spectra were found in the raw file and removed. A non-zero third character indicates negative IOP values were removed. A non-zero fourth character indicates the removal of a data spike (following a predetermined cut-off value, $a(\lambda)=c(\lambda)=10$). A non-zero fifth character indicates c values were discarded because c values were associated with a variance that exceeded the cut-off variance value for c. A non-zero sixth character indicates a values were discarded because a values were associated with a variance that exceeded the

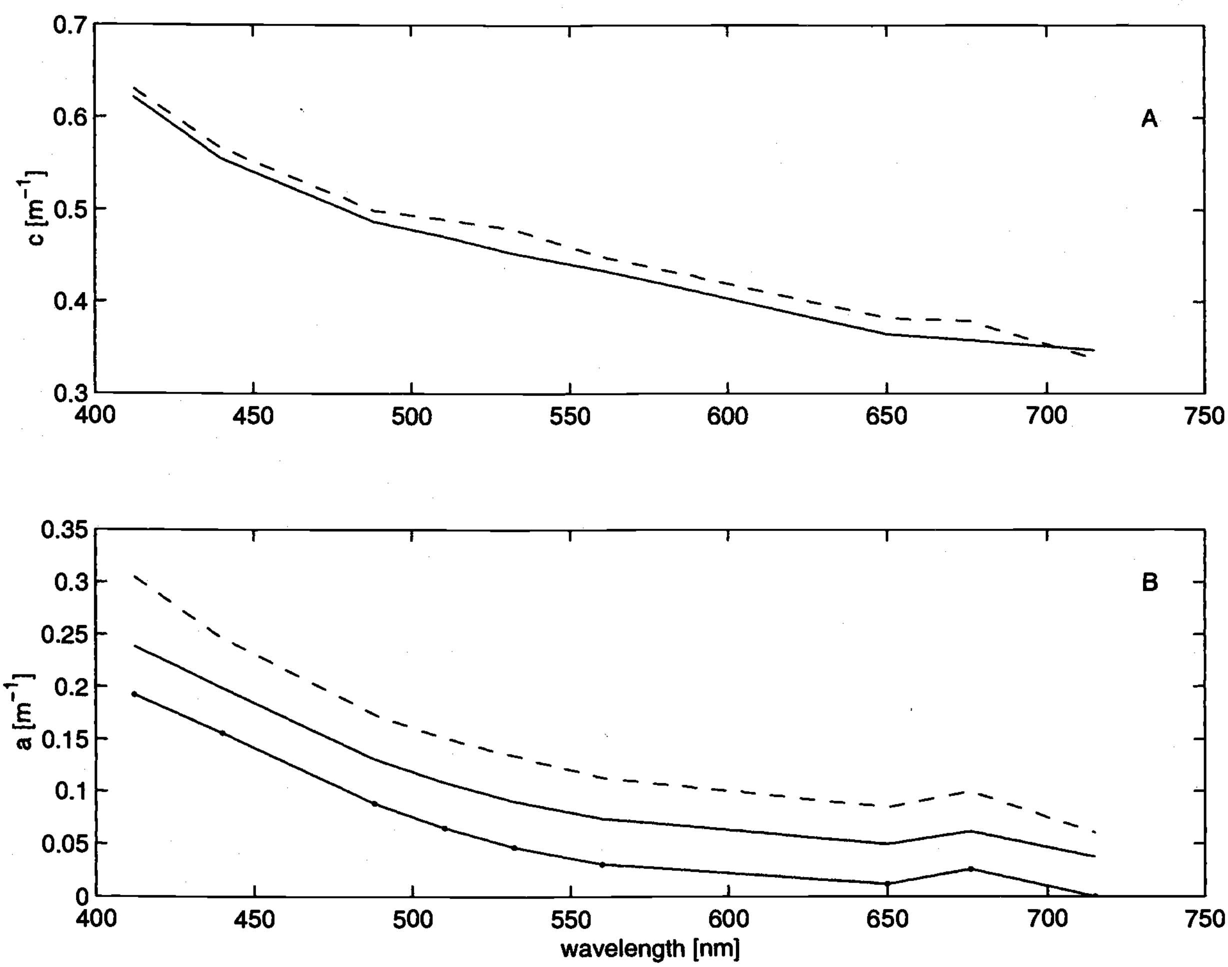

Figure 16: SeaSoar ac-9 attenuation (A) and absorption (B) spectra (e9608 Butterfly 2, line N-S at 20 m) that are temperature and salinity corrected (dashed) are then post-calibrated (solid). Absorption spectra are further corrected to remove errors due to scattering (dotted solid line)

cut-off variance value for a. A non-zero seventh character indicates a file has been edited to remove data merged with incorrect GPS values. A non-zero eighth character indicates the data has been adjusted to correct a "jump" in the data due to optical path clouding in the flow tubes.

For example, a data file having the 26th column and its first three elements,

101101001
1.0e+22
1.23

would indicate by the first row, (1) no missing values were inserted in the data file; (2) negative IOP values were found and removed; (3) data spikes were removed; (4) there were no c values were associated with an anomalously excessive variance; (5) a values were removed for having an associated anomalously excessive variance; (6) no GPS errors were found in the raw data file; (7) no adjustment in the data was performed to adjust for a "clouding" event. In the second row, a non-zero value indicates that missing values exist in the data file and are flagged by the value, 1.0e+22. In the third row, 1.23% of the original data file that was eliminated after the entire editing procedure.

While our rapid physical and bio-optical surveys involved the towed, undulating vehicle SeaSoar, the techniques described here for producing reliable multi-wavelength bio-optical measurements are equally valid for other towed systems (e.g., Guildline Instrument's Mini-BAT; Geological and Marine Instrumentation's Scanfish; Chelsea Instrument's Nu Shuttle and Aquashuttle) and autonomous underwater vehicles. These measurement platforms and bio-optical instruments of increasing capability (complexity) are being used ever more frequently. With proper care, they can be used to rapidly characterize three-dimensional physical and bio-optical property distributions.

4 Data Presentation

The final, processed and edited inherent optical property data files were used to generate the plots of representative spectra, contoured maps and contoured sections presented later in the report. Contour maps were created by gridding the data using "zgrid" (Crain, 1968, unpublished). Any grid point more than two grid points away from a data point was set to be undefined. The $a(676)$,$a(440)$ and $c(650)$ were chosen to show phytoplankton, combined contributions of absorbing components (non-phytoplankton particulate matter, phytoplankton and colored dissolved organic matter) and sediment distributions, respectively. The reader should note that the magnitude is proportional to the concentration of the absorbing substances. Bio-optical models can be applied to $a(676)$ to retrieve estimates of chlorophyll a concentrations in units of mg/m^3 (e.g. Morel and Bricaud, 1981; Cleveland, 1995).

4.1 Spectra

The volume of optical data associated with the SeaSoar surveys makes the display of a and c as a function of wavelength impractical. Therefore, only representative spectra from the beginning, middle and end of the E9608 and E9704 cruises are included in this report. The spectra are averages between the isopycnals $\sigma_t = 24.2 \pm 0.025$ kg/m^3, for the E9608 cruise and $\sigma_t = 25.4 \pm 0.025$ kg/m^3, for the E9704 cruise. These isopycnals roughly correspond to 20-30 meters depth.

4.2 Maps

Maps of inherent optical properties are presented for each parameter, $a(676)$, $a(440)$ and $c(650)$, at four different levels as a function of latitude and longitude. The four different levels were chosen to display: 1) representative surface (z = 5 m), 2) subsurface chlorophyll maxima ($\sigma_t = 24.6 \pm 0.025$ kg/m^3 (E9608) and $\sigma_t = 25.4 \pm 0.025$ kg/m^3 (E9704), z $\approx$ 20-30 m), 3) mid-depth (z = 45 m) and 4) near bottom sediment layer IOP distributions (z = 15 m above bottom). The four panels are presented clockwise, starting at the upper left, respectively. The top label is the survey pattern name, the wavelength and date.

4.3 Sections

The sections, or lines, of a survey pattern are presented as plots of $a(676)$, $a(440)$ and $c(650)$ as a function of depth (pressure) and latitude (cross-shelf distance). The top label identifies the survey pattern. The name, average longitude and time of the section are printed above each column of $a(676)$, $a(440)$ and $c(650)$.

5 Acknowledgements

The authors wish to thank: the Oregon State University Marine Technicians, M. Willis and L. Fayler, who were responsible for the highly successful SeaSoar operations. The officers and crew of the *R/V Endeavor* performed superbly, allowing us to tow SeaSoar through a region with considerable fishing activity and ship traffic. C. Moore (WET Labs, Inc.) provided valuable assistance with installing the ac-9 on SeaSoar. Thanks to S. Pegau and R. Zaneveld for providing their profiling ac-9 data for comparison with our SeaSoar ac-9 data and for helpful discussions on ac-9 data processing. Thanks to S. Pegau, C. Roesler, A. Barnard and E. Boss for helpful discussions on ac-9 data quality control. T. Ebling created the ac-9 realtime display and monitoring software by adapting the code originally written by N. Potter for use with T. Cowles's towed multiwavelength fluorescence instrument. This work was funded by the Office of Naval Research Grant N00014-95-1-0382.

6 References

Barth, J. A. and D. J. Bogucki, 2000. Spectral light absorption and attenuation measurements from a towed undulating vehicle. *Deep-Sea Res.I*, **47**, 363-342.

Barth, J. A., R. O'Malley, J. Fleischbein, R. L. Smith and A. Huyer, 1996. SeaSoar and CTD observations during Coastal Jet Separation cruise W9408A August to September 1994. College of Oceanic and Atmospheric Sciences, Oregon State University, Corvallis. **Ref. 96-1, Data Report 162**, November 1996, 309 pp.

Cleveland, J. S., 1995. Regional models for phytoplankton absorption as a function of chlorophyll *a* concentration. *J. Geophys. Res.*, **100**, C7, 13,333-13,344.

Crain, I., 1968. *Zgrid*: A Laplace interpolation method for the PLOT+ Graphics System. unpublished.

Dillon, T., J.A. Barth, A. Eerofeev and G.May, 2000. MicroSoar: A new instrument for measuring microscale turbulence from rapidly moving submerged platforms. *J. Atmos. Oceanic Technol.*, submitted.

Erofeev, A. Y., T. M. Dillon, J. A. Barth and G. H. May, 1998. MicroSoar microstructure observations during the Coastal Mixing and Optics experiment: R/V Endeavor Cruise from 25-Apr to 15-May 1997. College of Oceanic and Atmospheric Sciences, Oregon State University, Corvallis. **Ref. 98-3, Data Report 170**, September 1998.

Houghton R. W. and J. Marra, 1983. Physical/Biological Structure and Exchange Across the Thermohaline Shelf/Slope Front in the New York Bight. *J. Geophys. Res.*C7, **88**,4467-4481.

Moore, C. C., and L. Bruce, 1996. *ac-9 Protocols.* Internal Report, WET Labs, Inc., Philomath, OR, 42 pp.

Morel, A. and A. Bricaud, 1981. Theoretical results concerning light absorption in a discrete medium, and application to specific absorption of phytoplankton. *Deep-Sea Res.*, *Part A*, **28A**, 1375-1393.

O'Malley, J. A. Barth, A. Erofeev, J. Fleishbein, P. M. Kosro and S. D. Pierce, 1998. SeaSoar CTD observations during the Coastal Mixing and Optics Experiment: R/V Endeavor Cruises from 24-Aug to 1-Sep 1996 and 25-Apr to 15-May 1997. College of Oceanic and Atmospheric Sciences, Oregon State University, Corvallis. **Ref. 98-1, Data Report 168**, October 1996, 499 pp.

Pegau, W.S., D. G. Gray and J. R. V. Zaneveld, 1997. Absorption and attenuation of visible and near-infrared light in water: Dependence on temperature and salinity. *Applied Optics*, **36**, 6035-6046.

Pierce, S. D., J. A. Barth and P. M. Kosro, 1998. Acoustic Doppler current profiler observations during the Coastal Mixing and Optics experiment: R/V Endeavor Cruises from 14-Aug to 1-Sep 1996 and 25-Apr to 15-May 1997. College of Oceanic and Atmospheric Sciences, Oregon State University, Corvallis. **Ref. 98-2, Data Report 169**, September 1998.

Roesler C. S., J. Simeon and M. C. Talbot, 1997. Variability in vertical distributions of size fractionated component absorption and scattering coefficients in shallow continental shelf waters. *ASLO Aquatic Sciences Meeting, Santa Fe, New Mexico.*

Roesler C. S. and J. R. V. Zaneveld, 1994. High-resolution vertical profiles of spectral absorption, attenutaion and scattering coefficients in highly stratified waters. *SPIE Ocean Optics XII, Bergen, Norway*, **2258**, 309-319.

WET Labs, Inc., 1995. *ac-9 User's Guide*, Philomath, Oregon, 43 pp.

Zaneveld, J. R. V., W.S. Pegau and A. Barnard, 1997. Optical effects of a hurricane passage on the waters over the Northeast United States continental shelf. *ASLO Aquatic Sciences Meeting, Santa Fe, New Mexico*, p. 351.

7 Section Times and Cruise Tracks

7.1 E9608

E9608 Section Times

	section name	start time	stop time
Small Box 1	line1	15-Aug-96 23:20:18	16-Aug-96 01:59:54
	line1_2	16-Aug-96 01:59:55	16-Aug-96 02:23:46
	line2	16-Aug-96 02:39:56	16-Aug-96 04:19:04
	line2_3	16-Aug-96 04:19:05	16-Aug-96 04:44:54
	line3	16-Aug-96 04:44:55	16-Aug-96 07:01:37
	line3_4	16-Aug-96 07:01:38	16-Aug-96 07:30:59
	line4a	16-Aug-96 07:31:00	16-Aug-96 08:36:09
	line4b	16-Aug-96 09:39:42	16-Aug-96 10:35:54
	line4_5	16-Aug-96 10:35:55	16-Aug-96 11:13:50
	line5	16-Aug-96 11:13:51	16-Aug-96 13:10:14
	line5_6	16-Aug-96 13:10:15	16-Aug-96 13:38:06
	line6	16-Aug-96 13:38:07	16-Aug-96 15:27:16
Big Box 1	lineF	17-Aug-96 02:00:01	17-Aug-96 06:10:49
	lineE_F	17-Aug-96 06:10:50	17-Aug-96 07:00:21
	lineE	17-Aug-96 07:00:22	17-Aug-96 12:42:01
	lineD_E	17-Aug-96 12:50:43	17-Aug-96 13:42:58
	lineD	17-Aug-96 13:42:59	17-Aug-96 19:24:19
	lineC_D	17-Aug-96 19:24:20	17-Aug-96 20:11:58
	lineC	17-Aug-96 20:11:59	18-Aug-96 00:36:39
	lineB_C	18-Aug-96 00:36:40	18-Aug-96 01:28:16
	lineB	18-Aug-96 01:28:17	18-Aug-96 07:21:50
	bb1_sb2	18-Aug-96 08:28:01	18-Aug-96 09:07:44
Small Box 2	line1	18-Aug-96 09:35:18	18-Aug-96 11:31:21
	line1_2	18-Aug-96 11:31:22	18-Aug-96 11:59:06
	line2	18-Aug-96 11:59:07	18-Aug-96 13:44:25
	line2_3	18-Aug-96 13:44:26	18-Aug-96 14:12:57
	line3	18-Aug-96 14:12:58	18-Aug-96 16:06:00
	line3_4	18-Aug-96 17:07:09	18-Aug-96 17:35:17
	line4	18-Aug-96 18:02:09	18-Aug-96 19:42:21
	line4_5	18-Aug-96 19:42:22	18-Aug-96 20:06:23
	line5	18-Aug-96 21:06:45	18-Aug-96 23:12:05
	line5_6	18-Aug-96 23:12:06	18-Aug-96 23:46:51
	line6	18-Aug-96 23:46:52	19-Aug-96 01:45:26
	sb2_sb3	19-Aug-96 01:45:27	19-Aug-96 03:08:38
Small Box 3	line6	20-Aug-96 01:39:27	20-Aug-96 03:27:23
	line5_6	20-Aug-96 03:27:24	20-Aug-96 03:56:24
	line5	20-Aug-96 03:56:25	20-Aug-96 05:40:13
	line4_5	20-Aug-96 05:40:14	20-Aug-96 06:04:19
	line4	20-Aug-96 06:04:20	20-Aug-96 07:51:16
	line3_4	20-Aug-96 07:51:17	20-Aug-96 08:17:15
	line3	20-Aug-96 08:17:16	20-Aug-96 10:05:16
	line2_3	20-Aug-96 10:05:17	20-Aug-96 10:30:04
	line2	20-Aug-96 10:30:05	20-Aug-96 12:13:46
	line1_2	20-Aug-96 12:13:47	20-Aug-96 12:48:18
	line1	20-Aug-96 12:48:19	20-Aug-96 14:40:19

E9608 Section Times (continued)

	section name	start time	stop time
Big Box 2	lineA	20-Aug-96 17:03:21	20-Aug-96 22:18:46
	lineA_B	20-Aug-96 22:18:47	20-Aug-96 23:06:20
	lineB	20-Aug-96 23:06:21	21-Aug-96 04:53:03
	lineB_C	21-Aug-96 04:53:04	21-Aug-96 05:43:16
	lineC1	21-Aug-96 05:43:17	21-Aug-96 11:11:17
	lineC2	21-Aug-96 13:01:22	21-Aug-96 19:35:29
	lineC_D	21-Aug-96 19:35:30	21-Aug-96 20:23:40
	lineD	21-Aug-96 20:23:41	21-Aug-96 21:58:43
Small Box 4	line6	24-Aug-96 20:01:44	24-Aug-96 22:14:03
	line5_6	24-Aug-96 22:14:04	24-Aug-96 22:42:18
	line5	24-Aug-96 22:42:19	25-Aug-96 00:27:36
	line4_5	25-Aug-96 00:27:37	25-Aug-96 00:51:36
	line4	25-Aug-96 00:51:37	25-Aug-96 02:37:21
	line3_4	25-Aug-96 02:37:22	25-Aug-96 03:01:10
	line3	25-Aug-96 03:01:11	25-Aug-96 04:55:27
	line2_3	25-Aug-96 04:55:28	25-Aug-96 05:18:58
	line2	25-Aug-96 05:18:59	25-Aug-96 07:07:04
	line1_2	25-Aug-96 07:07:05	25-Aug-96 07:30:20
	line1	25-Aug-96 07:30:21	25-Aug-96 09:21:25
	sb4_sb5	25-Aug-96 09:21:26	25-Aug-96 11:34:55
Small Box 5	line6	25-Aug-96 11:34:56	25-Aug-96 13:31:44
	line5_6	25-Aug-96 13:31:45	25-Aug-96 13:59:09
	line5	25-Aug-96 13:59:10	25-Aug-96 15:52:39
	line4_5	25-Aug-96 15:52:40	25-Aug-96 16:17:11
	line4	25-Aug-96 16:17:12	25-Aug-96 18:14:59
	line3_4	25-Aug-96 18:15:00	25-Aug-96 18:38:20
	line3	25-Aug-96 18:38:21	25-Aug-96 20:24:41
	line2_3	25-Aug-96 20:24:42	25-Aug-96 20:51:21
	line2	25-Aug-96 20:51:22	25-Aug-96 22:48:44
	line1_2	25-Aug-96 22:48:45	25-Aug-96 23:14:43
	line1	25-Aug-96 23:14:44	26-Aug-96 01:05:56
	sb5_sb6	26-Aug-96 01:05:57	26-Aug-96 03:11:38
Small Box 6	line6	26-Aug-96 03:11:39	26-Aug-96 04:55:38
	line5_6	26-Aug-96 04:55:39	26-Aug-96 05:20:15
	line5	26-Aug-96 05:20:16	26-Aug-96 07:08:54
	line4_5	26-Aug-96 07:08:55	26-Aug-96 07:31:14
	line4	26-Aug-96 07:31:15	26-Aug-96 09:30:49
	line3_4	26-Aug-96 09:30:50	26-Aug-96 09:57:15
	line3	26-Aug-96 09:57:16	26-Aug-96 11:48:17
	line2_3	26-Aug-96 11:48:18	26-Aug-96 12:14:25
	line2	26-Aug-96 12:14:26	26-Aug-96 14:21:14
	line1_2	26-Aug-96 14:21:15	26-Aug-96 14:48:22
	line1	26-Aug-96 14:48:23	26-Aug-96 16:53:29
Butterfly 1	weA	26-Aug-96 23:59:40	27-Aug-96 00:59:48
	weB	27-Aug-96 04:05:59	27-Aug-96 05:25:22
	en	27-Aug-96 05:25:23	27-Aug-96 07:16:07
	ns	27-Aug-96 07:16:08	27-Aug-96 09:46:25
	sw	27-Aug-96 09:46:26	27-Aug-96 11:12:19

E9608 Section Times (continued)

	section name	start time	stop time
Butterfly 2	we	27-Aug-96 11:12:20	27-Aug-96 14:15:11
	en0	27-Aug-96 14:15:12	27-Aug-96 14:51:30
	en1	27-Aug-96 14:51:31	27-Aug-96 15:22:20
	en	27-Aug-96 15:22:21	27-Aug-96 17:31:05
	ns	27-Aug-96 17:31:06	27-Aug-96 20:00:15
	sw	27-Aug-96 20:00:16	27-Aug-96 21:28:56
Butterfly 3	we	27-Aug-96 23:52:14	28-Aug-96 02:36:24
	en	28-Aug-96 02:36:25	28-Aug-96 04:48:56
	ns	28-Aug-96 04:48:57	28-Aug-96 07:19:26
	sw	28-Aug-96 07:19:27	28-Aug-96 08:51:39
Butterfly 4	line1_4	28-Aug-96 09:41:28	28-Aug-96 11:09:23
	ns	28-Aug-96 11:09:24	28-Aug-96 14:53:05
	sn	28-Aug-96 14:53:06	28-Aug-96 17:09:54
Solitons	a	28-Aug-96 17:09:55	28-Aug-96 17:50:39
	b	28-Aug-96 17:50:40	28-Aug-96 18:17:37
	b_c	28-Aug-96 18:17:38	28-Aug-96 18:22:15
	c	28-Aug-96 18:22:16	28-Aug-96 18:58:20
	d	28-Aug-96 18:58:21	28-Aug-96 19:26:34
	e	28-Aug-96 19:26:35	28-Aug-96 19:50:45
	f	28-Aug-96 19:50:46	28-Aug-96 20:15:42
	g	28-Aug-96 20:15:43	28-Aug-96 21:00:00
	h	28-Aug-96 21:00:01	28-Aug-96 22:22:00
	i	28-Aug-96 22:22:01	28-Aug-96 23:36:58
	j	28-Aug-96 23:36:59	29-Aug-96 00:02:32
	k	29-Aug-96 00:02:33	29-Aug-96 00:18:30
	l	29-Aug-96 00:18:31	29-Aug-96 00:23:41
Small Box 7	line6	29-Aug-96 04:00:03	29-Aug-96 05:53:19
	line5_6	29-Aug-96 05:53:20	29-Aug-96 06:21:21
	line5	29-Aug-96 06:55:17	29-Aug-96 09:03:37
	line4_5	29-Aug-96 09:03:38	29-Aug-96 09:28:10
	line4	29-Aug-96 09:28:11	29-Aug-96 11:33:18
	line3_4	29-Aug-96 11:33:19	29-Aug-96 11:59:58
	line3	29-Aug-96 11:59:59	29-Aug-96 13:52:43
	line2_3	29-Aug-96 13:52:44	29-Aug-96 14:18:42
	line2	29-Aug-96 14:18:43	29-Aug-96 16:14:56
	line1_2	29-Aug-96 16:14:57	29-Aug-96 16:42:12
	line1	29-Aug-96 16:42:13	29-Aug-96 18:50:35
	sb7_sb8	29-Aug-96 18:50:36	29-Aug-96 21:17:35
Small Box 8	line6	29-Aug-96 21:17:36	29-Aug-96 23:24:30
	line5_6	29-Aug-96 23:24:31	29-Aug-96 23:53:13
	line5	29-Aug-96 23:53:14	30-Aug-96 01:44:01
	line4_5	30-Aug-96 01:44:02	30-Aug-96 02:09:33
	line4	30-Aug-96 02:09:34	30-Aug-96 04:10:58
	line3_4	30-Aug-96 04:10:59	30-Aug-96 04:38:14
	line3	30-Aug-96 04:38:15	30-Aug-96 06:52:04
	line2_3	30-Aug-96 06:52:05	30-Aug-96 07:19:44
	line2	30-Aug-96 07:19:45	30-Aug-96 09:16:53
	line1_2	30-Aug-96 09:16:54	30-Aug-96 09:43:08
	line1	30-Aug-96 10:06:17	30-Aug-96 12:10:57

E9608 Section Times (continued)

	section name	start time	stop time
Small Box 9	line6	30-Aug-96 14:52:14	30-Aug-96 16:51:13
	line5_6	30-Aug-96 16:51:14	30-Aug-96 17:19:02
	line5	30-Aug-96 17:19:03	30-Aug-96 19:23:28
	line4_5	30-Aug-96 19:23:29	30-Aug-96 19:53:05
	line4	30-Aug-96 19:53:06	30-Aug-96 21:45:12
	line3_4	30-Aug-96 21:45:13	30-Aug-96 22:08:56
	line3	30-Aug-96 22:08:57	30-Aug-96 23:59:22
	line2_3	30-Aug-96 23:59:23	31-Aug-96 00:26:12
	line2	31-Aug-96 00:26:13	31-Aug-96 02:29:09
	line1_2	31-Aug-96 02:29:10	31-Aug-96 02:57:00
	line1	31-Aug-96 02:57:01	31-Aug-96 04:53:39
	sb9_bb3	31-Aug-96 04:53:40	31-Aug-96 05:49:02
Big Box 3	lineC0	31-Aug-96 05:49:03	31-Aug-96 08:02:39
	lineC1	31-Aug-96 09:00:40	31-Aug-96 14:28:56
	lineC_Ds	31-Aug-96 14:28:57	31-Aug-96 15:19:51
	lineDs	31-Aug-96 15:23:45	31-Aug-96 19:00:59
	lineD_Es	31-Aug-96 19:01:00	31-Aug-96 20:06:29
	lineEs	31-Aug-96 20:06:30	31-Aug-96 23:29:47
	lineE_Fs	31-Aug-96 23:29:48	01-Sep-96 00:21:49
	lineF	01-Sep-96 00:21:50	01-Sep-96 04:46:06
	lineE_Fn	01-Sep-96 04:46:07	01-Sep-96 05:37:24
	lineEn	01-Sep-96 05:37:25	01-Sep-96 06:13:59
	lineD_En	01-Sep-96 06:14:00	01-Sep-96 07:05:38
	lineDn	01-Sep-96 07:05:39	01-Sep-96 07:45:11
	lineC_Dn	01-Sep-96 07:45:12	01-Sep-96 08:32:33
	lineC2	01-Sep-96 08:32:34	01-Sep-96 11:08:14

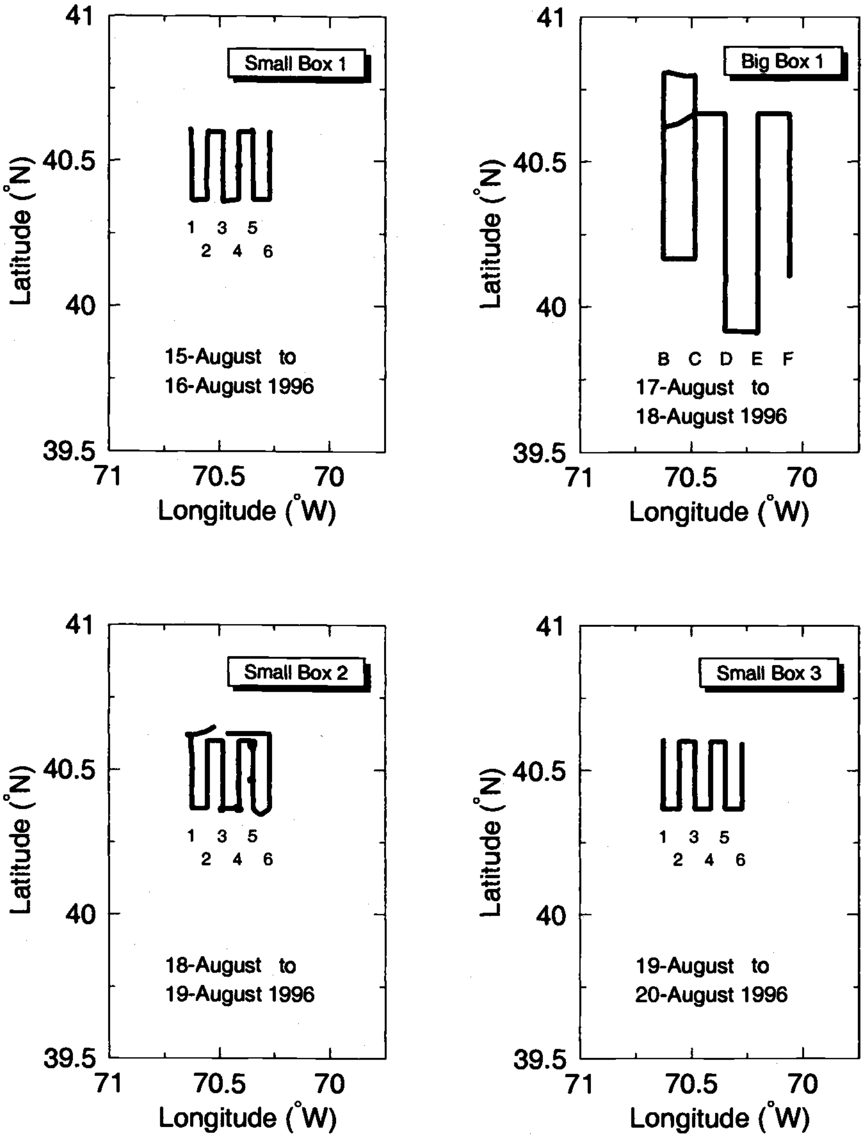

Figure 17: a: Cruise tracks during the E9608 SeaSoar surveys.

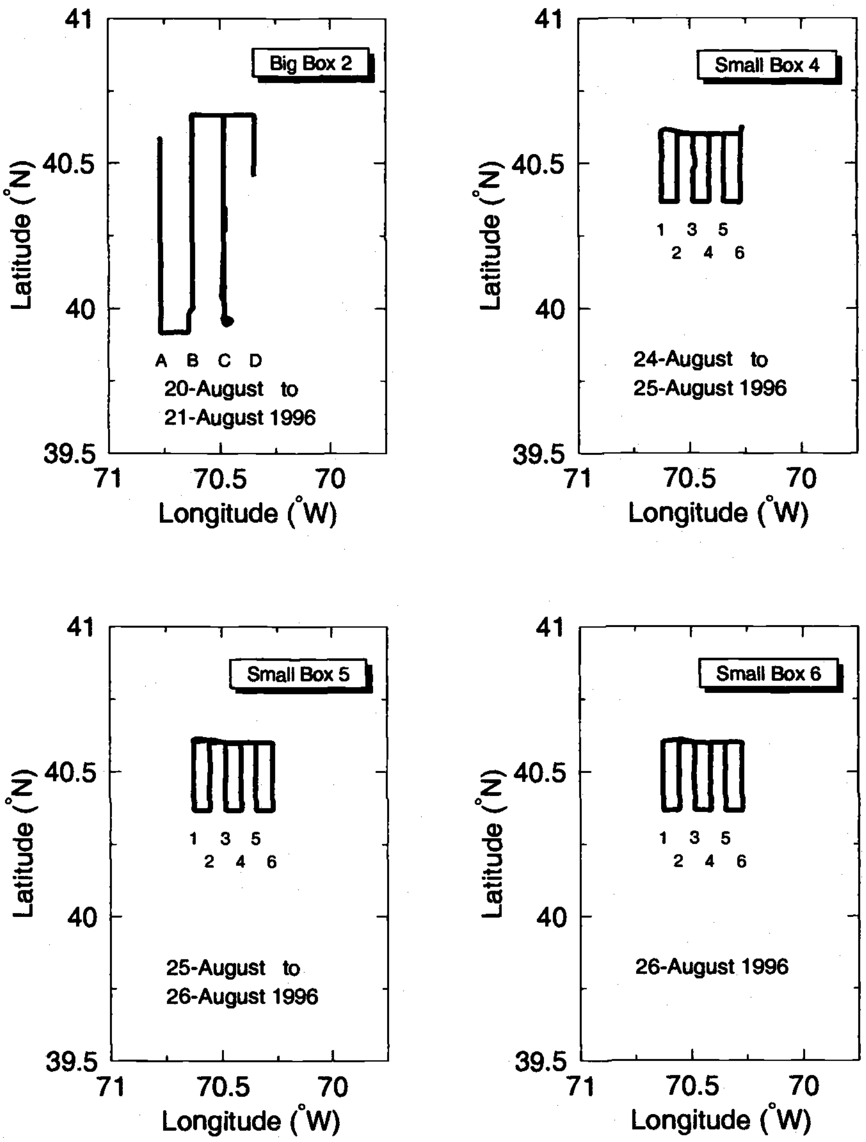

Figure 18: b: Cruise tracks during the E9608 SeaSoar surveys.

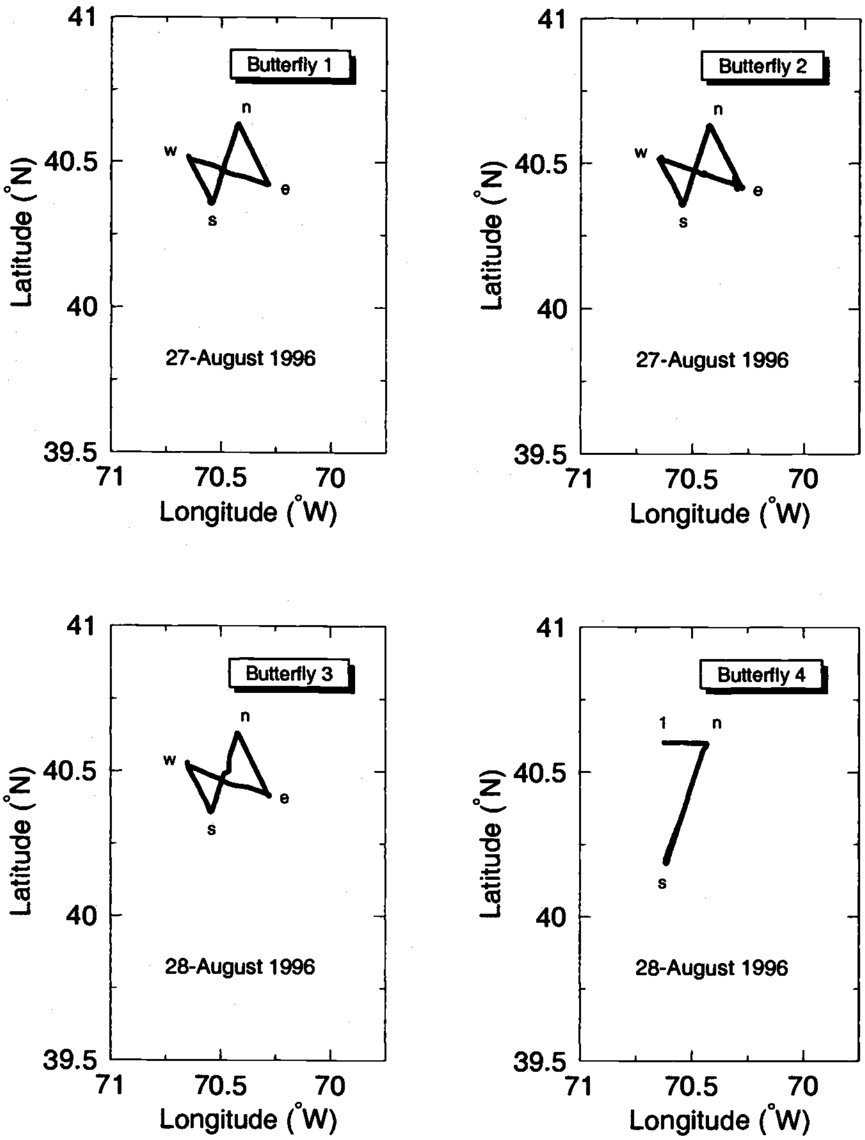

Figure 19: c: Cruise tracks during the E9608 SeaSoar surveys.

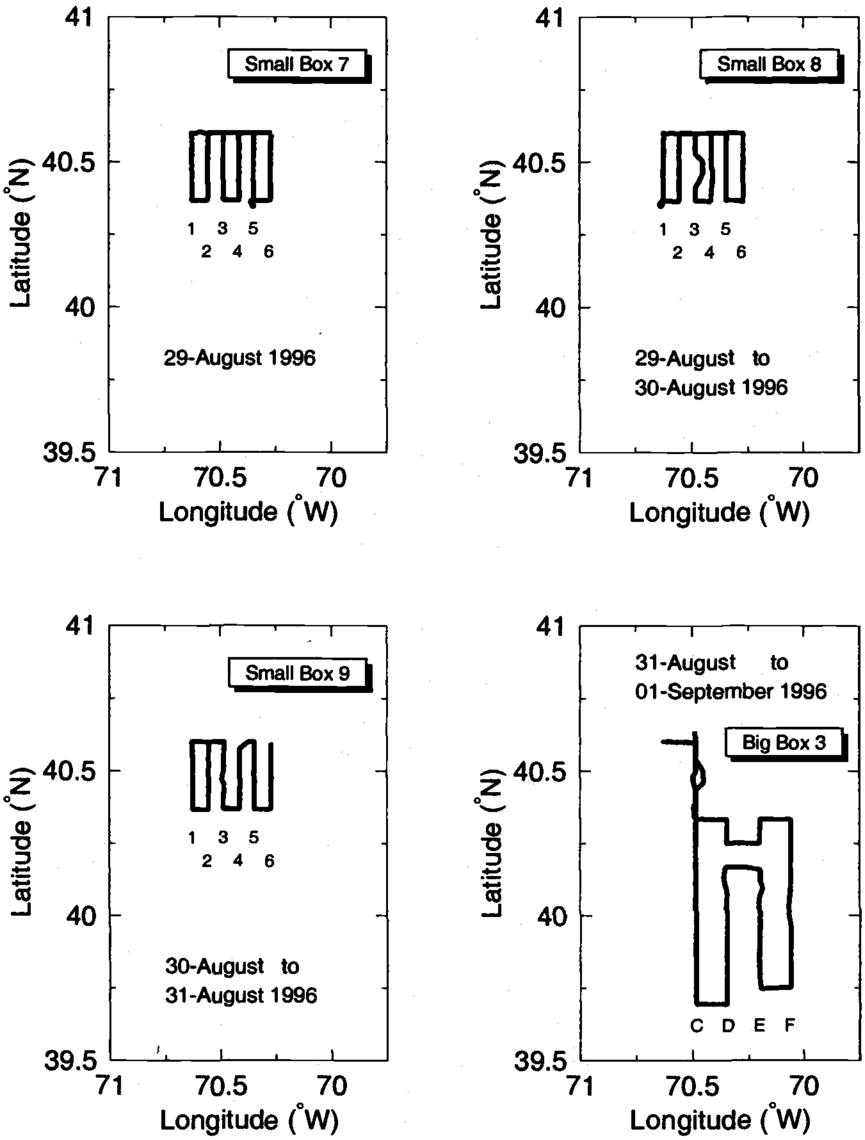

Figure 20: d: Cruise tracks during the E9608 SeaSoar surveys.

7.2 E9704

E9704 Section Times

	section name	start time	stop time
Small Box 1	line6	27-Apr-97 00:45:09	27-Apr-97 03:36:16
	line5_6	27-Apr-97 03:36:17	27-Apr-97 04:17:47
	line5	27-Apr-97 04:17:48	27-Apr-97 07:18:30
	line4_5	27-Apr-97 07:18:31	27-Apr-97 07:45:10
	line4	27-Apr-97 07:45:11	27-Apr-97 09:35:28
	line3_4	27-Apr-97 09:35:29	27-Apr-97 10:01:16
	line3	27-Apr-97 10:01:17	27-Apr-97 12:31:48
Small Box 2	lineB	27-Apr-97 22:27:00	28-Apr-97 01:37:23
	line1	28-Apr-97 01:46:28	28-Apr-97 03:49:47
	line1-2	28-Apr-97 03:49:48	28-Apr-97 04:19:01
	line2	28-Apr-97 04:19:02	28-Apr-97 06:24:10
	line2_3	28-Apr-97 06:24:11	28-Apr-97 06:53:27
	line3	28-Apr-97 06:53:28	28-Apr-97 09:29:11
	line3_4	28-Apr-97 09:29:12	28-Apr-97 09:57:09
	line4	28-Apr-97 09:57:10	28-Apr-97 11:52:14
	line4_5	28-Apr-97 11:52:15	28-Apr-97 12:20:59
	line5	28-Apr-97 12:21:00	28-Apr-97 14:36:18
Small Box 3	line6a	29-Apr-97 01:13:35	29-Apr-97 03:27:24
	line6b	29-Apr-97 03:36:08	29-Apr-97 05:45:12
	line5_6	29-Apr-97 05:45:13	29-Apr-97 06:17:12
	line5	29-Apr-97 06:17:13	29-Apr-97 08:23:24
	line4_5	29-Apr-97 08:23:25	29-Apr-97 08:51:37
	line4	29-Apr-97 08:51:38	29-Apr-97 10:51:48
	line3_4	29-Apr-97 10:51:49	29-Apr-97 11:21:16
	line3	29-Apr-97 11:21:17	29-Apr-97 13:27:57
	line2_3	29-Apr-97 13:27:58	29-Apr-97 13:55:47
	line2	29-Apr-97 13:55:48	29-Apr-97 16:06:58
	line1_2	29-Apr-97 16:06:59	29-Apr-97 16:36:19
	line1	29-Apr-97 16:36:20	29-Apr-97 18:40:47
	sb3_sb4	29-Apr-97 18:40:48	29-Apr-97 20:54:07
Small Box 4	line6	29-Apr-97 20:54:08	29-Apr-97 22:57:04
	line5_6	29-Apr-97 22:57:05	29-Apr-97 23:28:05
	line5	29-Apr-97 23:28:06	30-Apr-97 00:55:17
Small Box 5	lineE	02-May-97 12:38:20	02-May-97 17:34:53
	lineE_6	02-May-97 17:34:54	02-May-97 18:05:51
	line6	02-May-97 18:05:52	02-May-97 20:17:31
	line5	02-May-97 20:55:32	02-May-97 22:46:31
	line4_5	02-May-97 22:46:32	02-May-97 23:18:52
	line4	02-May-97 23:18:53	03-May-97 01:13:32
	line3_4	03-May-97 01:13:33	03-May-97 01:45:46
	line3	03-May-97 01:45:47	03-May-97 04:08:59
	line2_3	03-May-97 04:09:00	03-May-97 04:43:35
	line2	03-May-97 04:43:36	03-May-97 06:47:04
	line1_2	03-May-97 06:47:05	03-May-97 07:17:57
	line1	03-May-97 07:17:58	03-May-97 09:23:40
	sb5_sb6	03-May-97 09:23:41	03-May-97 11:45:42

E9704 Section Times (continued)

	section name	start time	stop time
Small Box 6	line6	03-May-97 11:45:43	03-May-97 13:50:16
	line5_6	03-May-97 13:50:17	03-May-97 14:20:46
	line5	03-May-97 14:20:47	03-May-97 16:26:08
	line4_5	03-May-97 16:26:09	03-May-97 16:53:30
	line4	03-May-97 16:53:31	03-May-97 19:08:28
	line3_4	03-May-97 19:08:29	03-May-97 19:41:59
	line3	03-May-97 19:42:00	03-May-97 21:35:08
	line2_3	03-May-97 21:35:09	03-May-97 22:06:51
	line2	03-May-97 22:06:52	04-May-97 00:49:17
	line1_2	04-May-97 00:49:18	04-May-97 01:23:13
	line1	04-May-97 01:23:14	04-May-97 02:09:45
Big Box 1	lineA	04-May-97 12:36:20	04-May-97 19:04:37
	lineA_B	04-May-97 19:04:38	04-May-97 20:04:36
	lineB	04-May-97 20:04:37	05-May-97 01:42:15
	lineB_C	05-May-97 01:42:16	05-May-97 02:43:33
	lineC	05-May-97 02:43:34	05-May-97 08:16:20
	lineC_D	05-May-97 08:16:21	05-May-97 09:16:59
	lineD	05-May-97 09:17:00	05-May-97 16:04:09
	lineD_E	05-May-97 16:04:10	05-May-97 17:06:16
	lineE1	05-May-97 17:06:17	05-May-97 20:48:29
	lineE	05-May-97 17:06:17	06-May-97 00:32:47
	lineE2	05-May-97 21:49:09	06-May-97 00:32:47
	lineE_F	06-May-97 00:32:48	06-May-97 01:24:53
	lineF	06-May-97 03:37:07	06-May-97 10:15:19
	lineF_G	06-May-97 10:15:20	06-May-97 11:10:33
	lineG	06-May-97 11:10:34	06-May-97 17:32:19
	bb1_sb7a	06-May-97 17:32:20	06-May-97 19:58:08
	bb1_sb7b	06-May-97 19:58:09	06-May-97 20:33:16
Small Box 7	line6	06-May-97 20:33:17	06-May-97 22:38:39
	line5_6	06-May-97 22:38:40	06-May-97 23:09:59
	line5	06-May-97 23:10:00	07-May-97 01:09:38
	line4_5	07-May-97 01:09:39	07-May-97 01:39:37
	line4	07-May-97 01:39:38	07-May-97 03:44:06
	line3_4	07-May-97 03:44:07	07-May-97 04:16:01
	line3a	07-May-97 04:16:02	07-May-97 06:37:09
	line3b	07-May-97 06:37:10	07-May-97 08:40:52
	line2_3	07-May-97 08:40:53	07-May-97 09:08:56
	line2	07-May-97 09:08:57	07-May-97 11:06:37
	line1_2	07-May-97 11:06:38	07-May-97 11:37:04
	line1	07-May-97 11:37:05	07-May-97 13:50:55

E9704 Section Times (continued)

	section name	start time	stop time
Small Box 8	line1a	07-May-97 13:50:56	07-May-97 15:07:21
	bf1lineWE	07-May-97 15:07:22	07-May-97 17:30:08
	line6a	07-May-97 17:30:09	07-May-97 18:16:28
	line6b	07-May-97 18:16:29	07-May-97 19:33:38
	line6	07-May-97 18:16:29	08-May-97 07:01:54
	line6c	08-May-97 05:39:23	08-May-97 07:01:54
	line5_6	08-May-97 07:01:55	08-May-97 07:33:50
	line5	08-May-97 07:33:51	08-May-97 09:32:51
	line4_5	08-May-97 09:32:52	08-May-97 09:57:29
	line4	08-May-97 09:57:30	08-May-97 11:57:19
	line3_4	08-May-97 11:57:20	08-May-97 12:26:30
	line3a	08-May-97 12:26:31	08-May-97 13:04:50
	line3	08-May-97 18:57:28	08-May-97 20:48:19
	line2_3	08-May-97 20:48:20	08-May-97 21:16:07
	line2	08-May-97 21:16:08	08-May-97 23:14:50
	line1_2	08-May-97 23:14:51	08-May-97 23:41:51
	line1	08-May-97 23:41:52	09-May-97 01:57:21
Small Box 9	line1a	09-May-97 01:57:22	09-May-97 03:11:53
	bf2lineWE	09-May-97 03:11:54	09-May-97 05:34:20
	line6a	09-May-97 05:34:21	09-May-97 06:01:59
	line6	09-May-97 06:02:00	09-May-97 08:14:59
	line5_6	09-May-97 08:15:00	09-May-97 08:45:55
	line5	09-May-97 09:08:07	09-May-97 11:09:21
	line4_5	09-May-97 11:09:22	09-May-97 11:35:03
	line4	09-May-97 11:35:04	09-May-97 13:33:29
	line3_4	09-May-97 13:33:30	09-May-97 14:00:01
	line3	09-May-97 14:00:02	09-May-97 16:16:43
	line2_3	09-May-97 16:16:44	09-May-97 16:44:59
	line2	09-May-97 16:45:00	09-May-97 18:32:48
	line1_2	09-May-97 18:32:49	09-May-97 19:03:17
	line1	09-May-97 19:03:18	09-May-97 21:11:56
Small Box 10	line1a	09-May-97 21:41:01	09-May-97 22:43:54
	bf3lineWE	09-May-97 22:43:55	10-May-97 01:01:16
	line6a	10-May-97 01:13:01	10-May-97 01:54:14
	line6	10-May-97 01:54:15	10-May-97 04:03:42
	line5_6	10-May-97 04:03:43	10-May-97 04:36:24
	line5	10-May-97 04:36:25	10-May-97 06:45:54
	line4_5	10-May-97 06:45:55	10-May-97 07:13:24
	line4	10-May-97 07:13:25	10-May-97 09:23:11
	line3_4	10-May-97 09:23:12	10-May-97 09:48:14
	line3	10-May-97 09:48:15	10-May-97 11:49:59
	line2_3	10-May-97 11:50:00	10-May-97 12:17:32
	line2	10-May-97 12:17:33	10-May-97 14:10:31
	line1_2	10-May-97 14:10:32	10-May-97 14:38:22
	line1	10-May-97 14:38:23	10-May-97 17:05:23

E9704 Section Times (continued)

	section name	start time	stop time
Small Box 11	line1	11-May-97 11:22:01	11-May-97 13:30:36
	line1_2	11-May-97 13:30:37	11-May-97 13:58:56
	line2	11-May-97 13:58:57	11-May-97 16:02:36
	line2_3	11-May-97 16:02:37	11-May-97 16:28:16
	line3	11-May-97 16:28:17	11-May-97 18:32:42
	line3_4	11-May-97 18:32:43	11-May-97 18:57:40
	line4	11-May-97 18:57:41	11-May-97 20:58:52
	line4_5	11-May-97 20:58:53	11-May-97 21:23:36
	line5	11-May-97 21:23:37	11-May-97 23:28:16
	line5_6	11-May-97 23:28:17	11-May-97 23:58:16
	line6	11-May-97 23:58:17	12-May-97 02:08:30
Small Box 12	line5_6	12-May-97 02:08:31	12-May-97 02:42:59
	line5	12-May-97 02:43:00	12-May-97 04:44:15
	line4_5	12-May-97 04:44:16	12-May-97 05:16:47
	line4	12-May-97 05:16:48	12-May-97 07:23:49
	line3_4	12-May-97 07:23:50	12-May-97 07:55:09
	line3	12-May-97 07:55:10	12-May-97 10:00:55
	line2_3	12-May-97 10:00:56	12-May-97 10:29:45
	line2	12-May-97 10:29:46	12-May-97 12:25:17
	line1_2	12-May-97 12:25:18	12-May-97 12:51:33
	line1	12-May-97 12:51:34	12-May-97 14:53:06
	sb12_bb2	12-May-97 14:53:07	12-May-97 15:59:34
Big Box 2	lineC	12-May-97 15:59:35	12-May-97 22:35:59
	lineA_C	12-May-97 22:36:00	13-May-97 00:26:26
	lineA	13-May-97 00:26:27	13-May-97 06:52:16
	lineA_B	13-May-97 06:52:17	13-May-97 07:48:21
	lineB	13-May-97 07:48:22	13-May-97 14:21:03
	lineC_D	13-May-97 17:57:27	13-May-97 18:59:24
	lineD	13-May-97 18:59:25	14-May-97 01:34:10
	lineD_E	14-May-97 01:34:11	14-May-97 02:31:03
	lineE	14-May-97 02:31:04	14-May-97 08:50:57
	lineE_F	14-May-97 08:50:58	14-May-97 09:45:29
	lineF	14-May-97 09:45:30	14-May-97 15:31:35
	lineF_G	14-May-97 15:31:36	14-May-97 16:29:04
	lineG	14-May-97 16:29:05	14-May-97 23:07:09

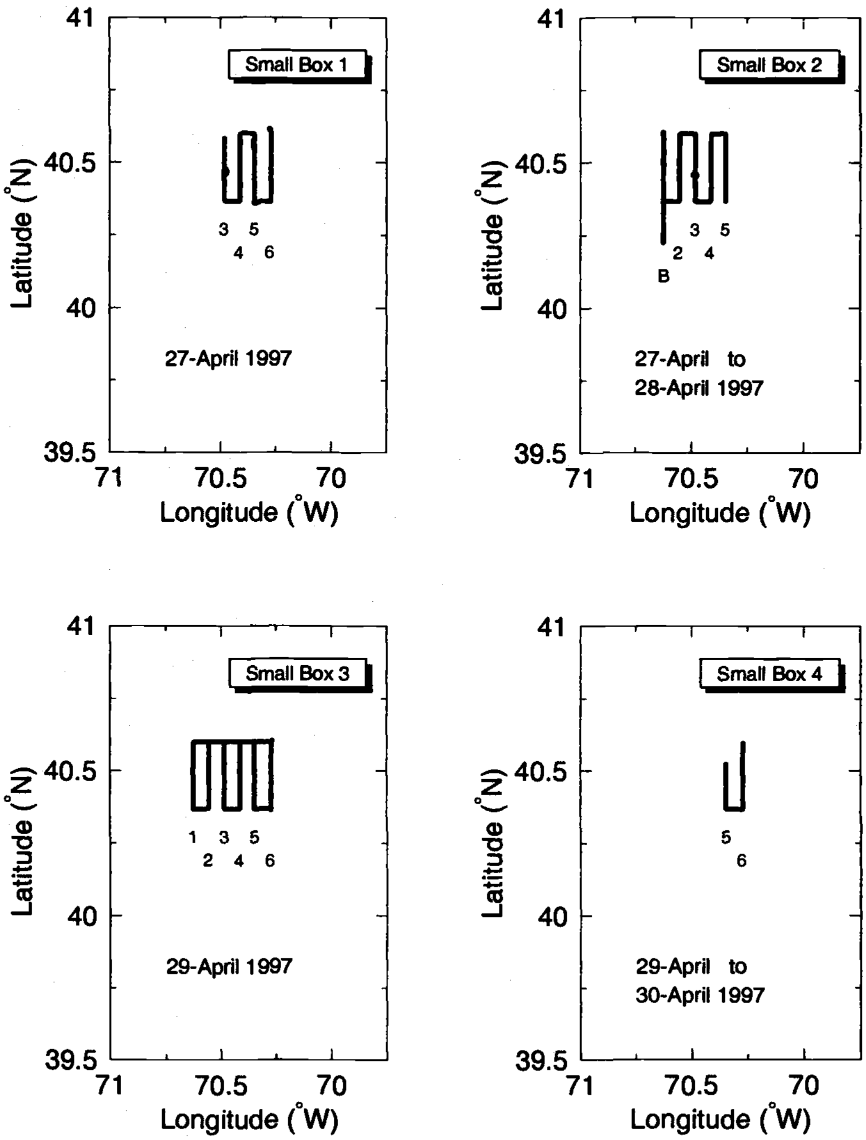

Figure 21: a: Cruise tracks during the E9704 SeaSoar surveys.

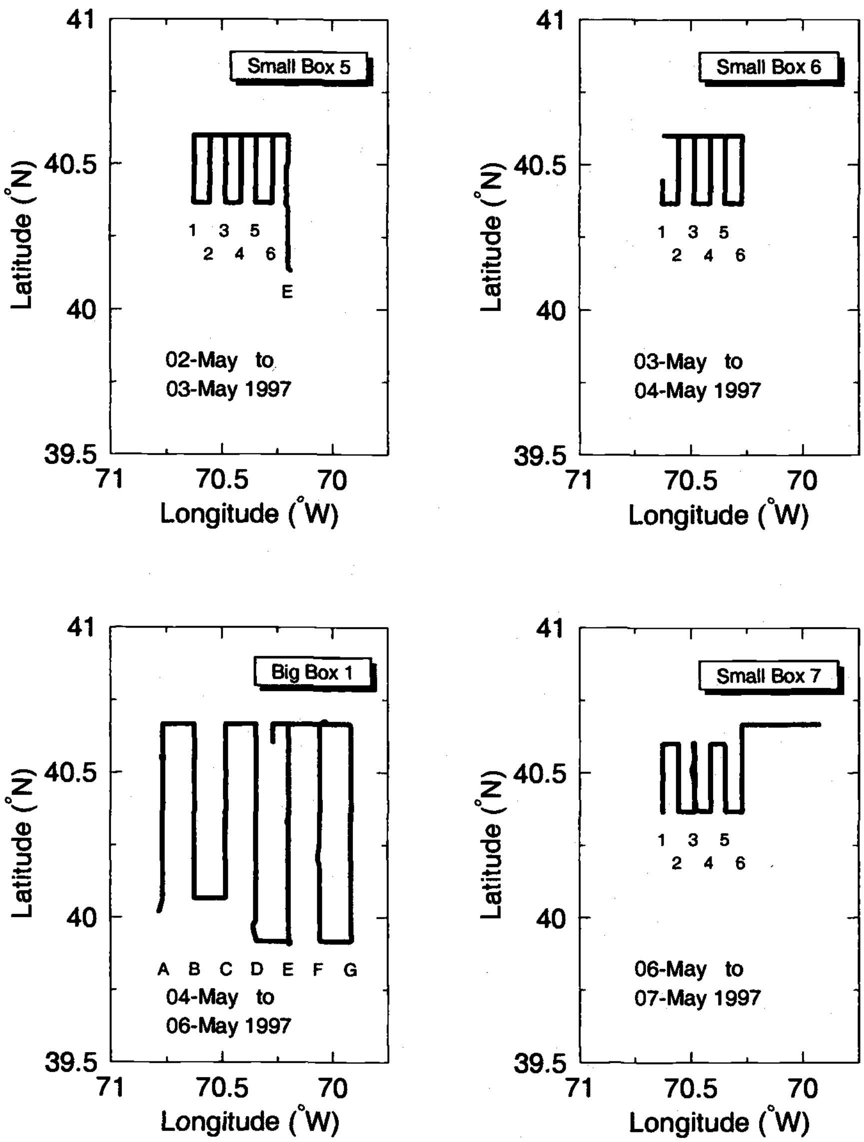

Figure 22: b: Cruise tracks during the E9704 SeaSoar surveys.

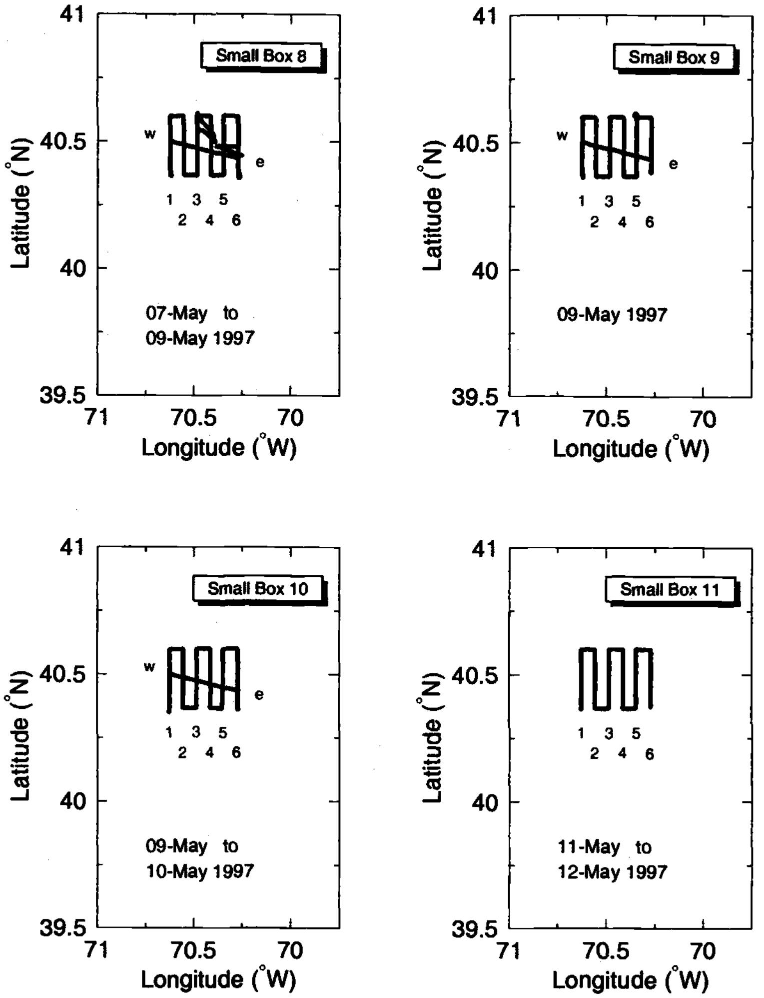

Figure 23: c: Cruise tracks during the E9704 SeaSoar surveys.

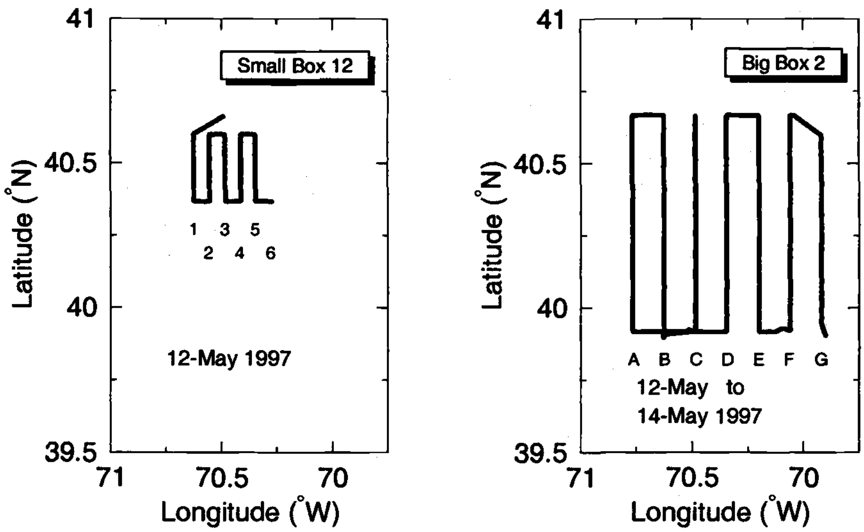

Figure 24: d: Cruise tracks during the E9704 SeaSoar surveys.

E9608 and E9704 Absorption and Attenuation Spectra

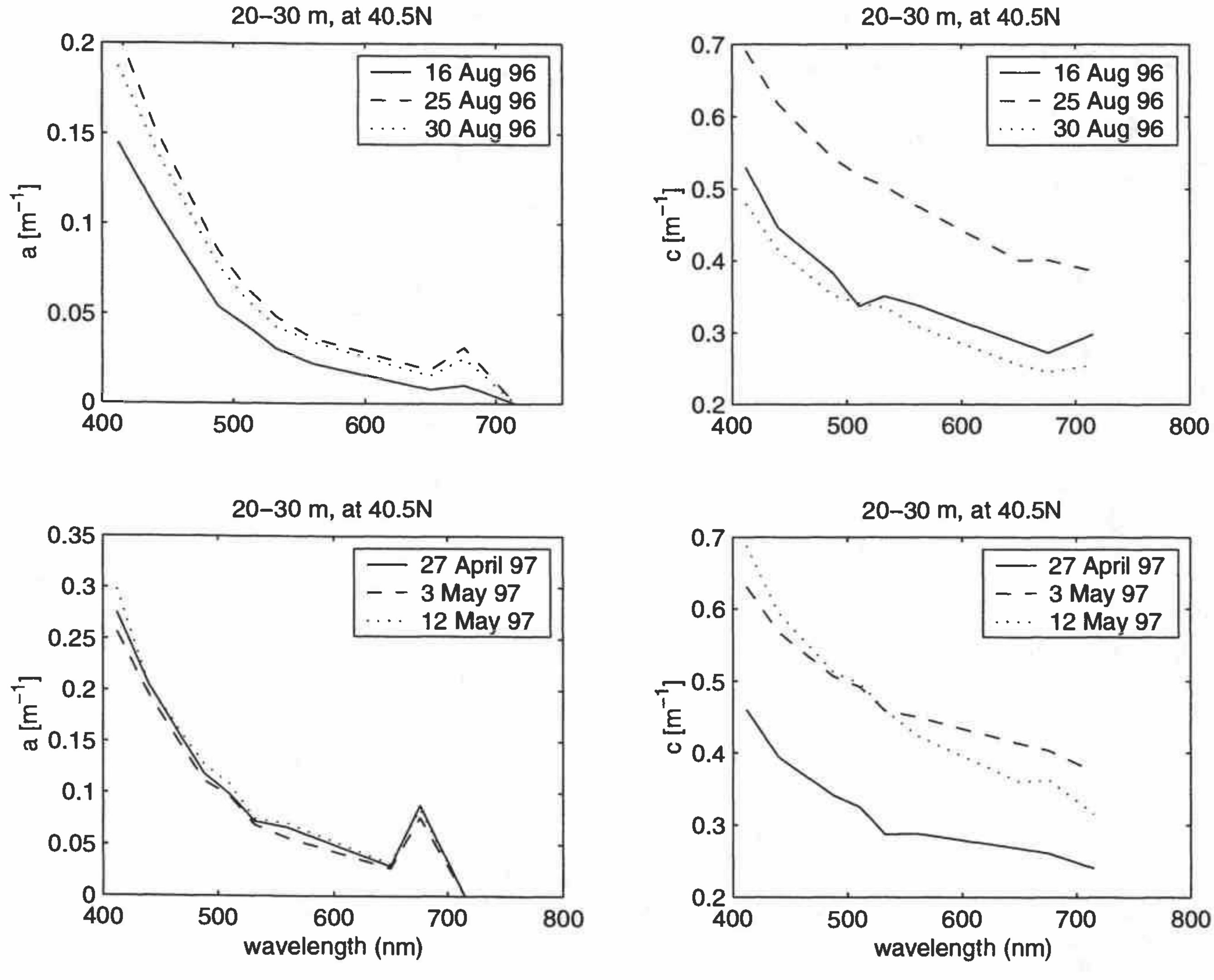
20–30 m, at 40.5N
a [m^-1]
16 Aug 96
25 Aug 96
30 Aug 96
0.2
0.15
0.1
0.05
0
400
500
600
700
20–30 m, at 40.5N
c [m^-1]
16 Aug 96
25 Aug 96
30 Aug 96
0.7
0.6
0.5
0.4
0.3
0.2
400
500
600
700
800
20–30 m, at 40.5N
a [m^-1]
27 April 97
3 May 97
12 May 97
0.35
0.3
0.25
0.2
0.15
0.1
0.05
0
400
500
600
700
800
wavelength (nm)
20–30 m, at 40.5N
c [m^-1]
27 April 97
3 May 97
12 May 97
0.7
0.6
0.5
0.4
0.3
0.2
400
500
600
700
800
wavelength (nm)

E9608 Bigbox Maps

E9608 Bigbox 1

17-Aug-96 02:02 to 18-Aug-96 05:21

Map view at 5 m

a(676) m^{-1}

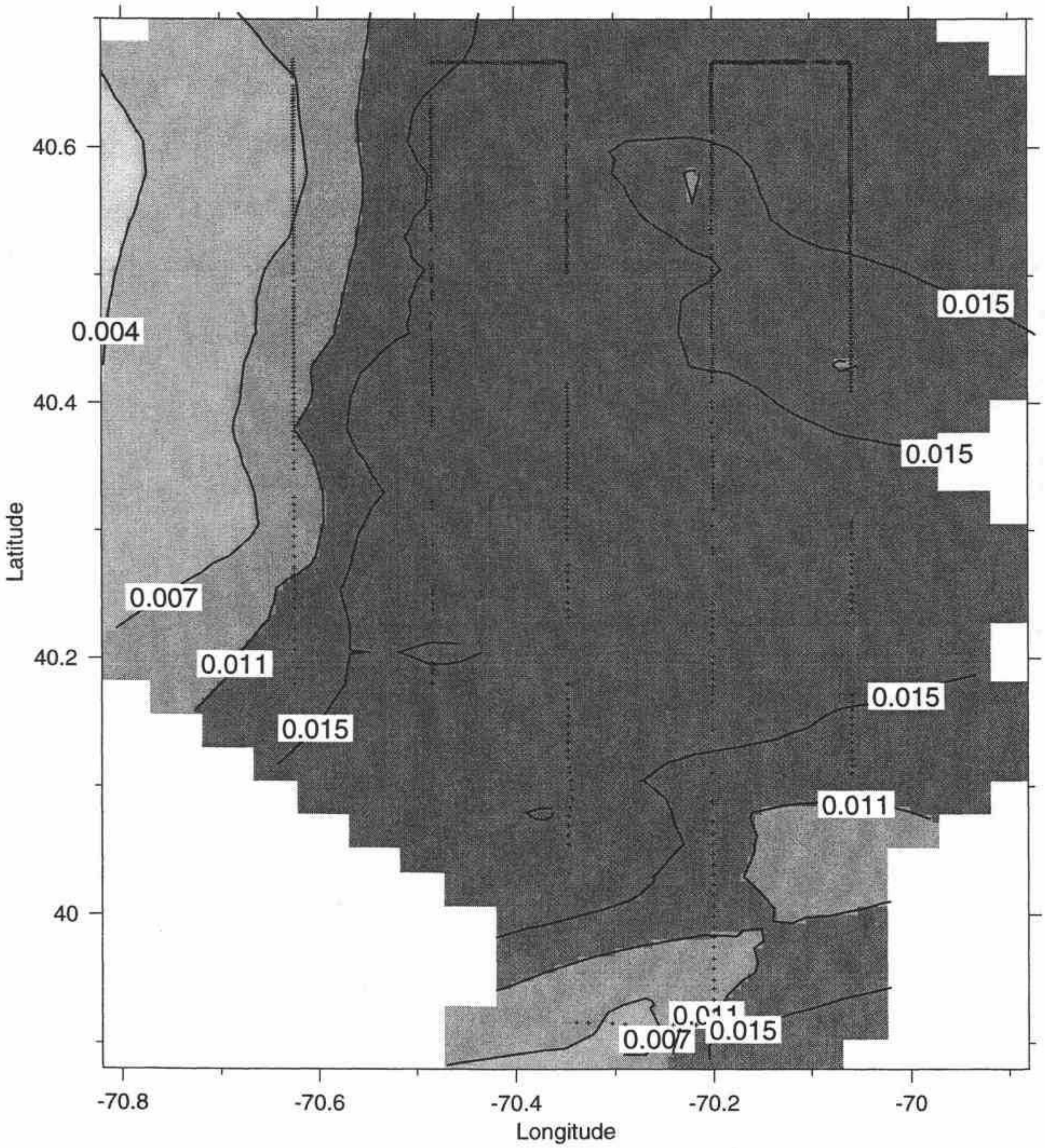

E9608 Bigbox 1
17-Aug-96 02:02 to 18-Aug-96 05:21
Map view at 45 m

a(676) m^{-1}

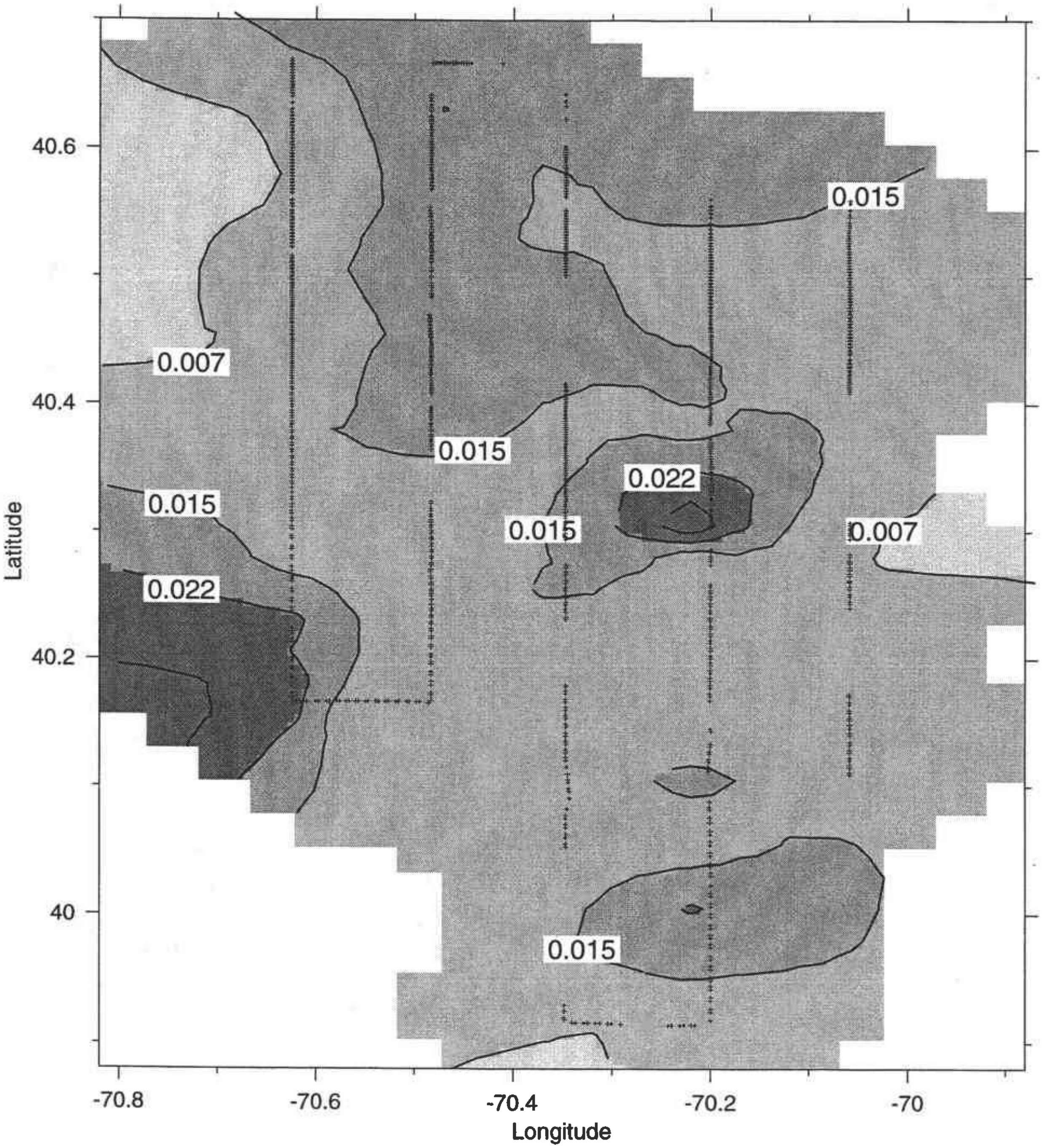

E9608 Bigbox 1

17-Aug-96 02:02 to 18-Aug-96 05:21

Map view at $\sigma_t = 24.6 \pm 0.025$ kg/m^3

a(676) m^{-1}

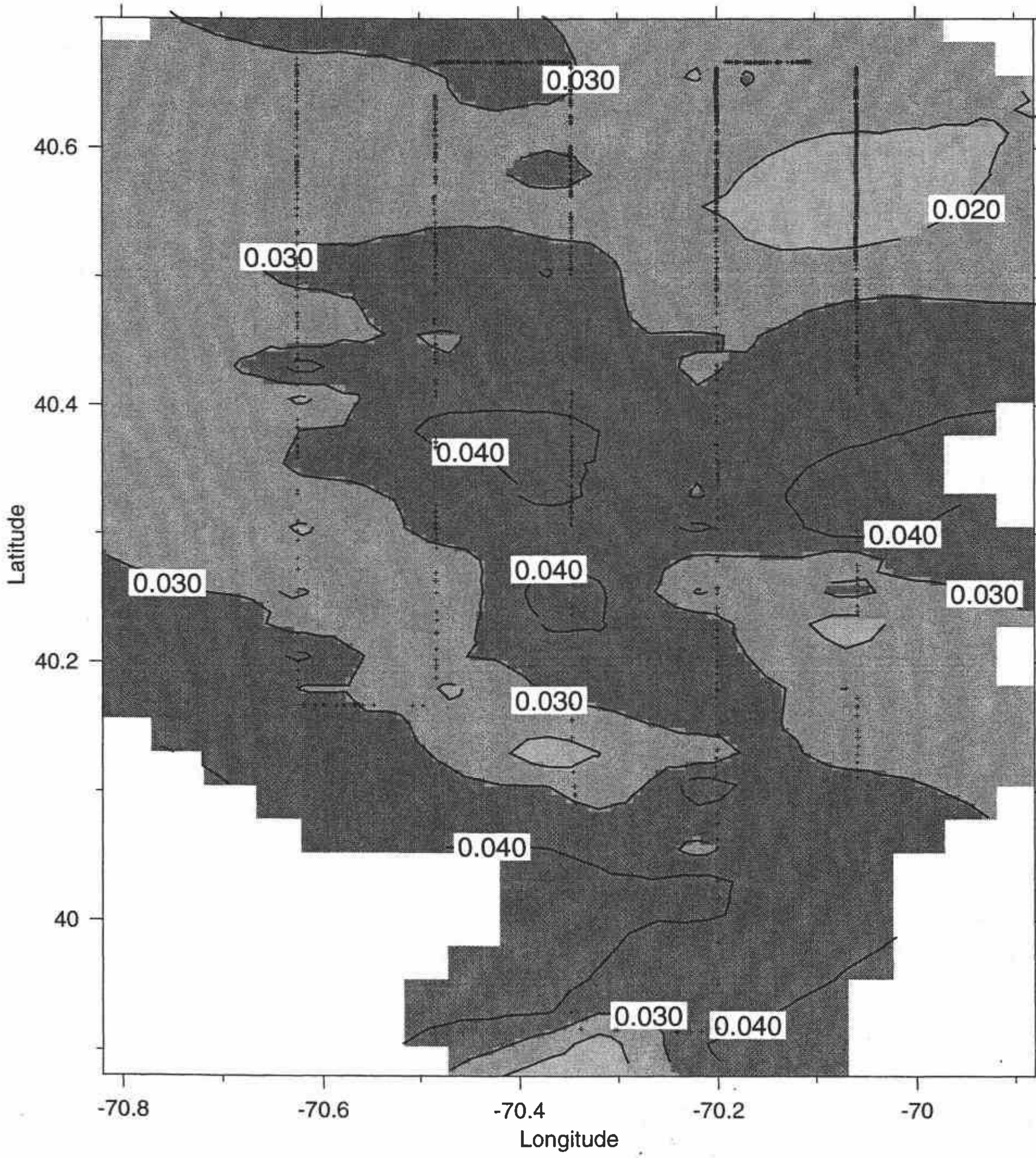

E9608 Bigbox 1

17-Aug-96 02:02 to 18-Aug-96 05:21

Map view at 10 m above bottom

a(676) m^{-1}

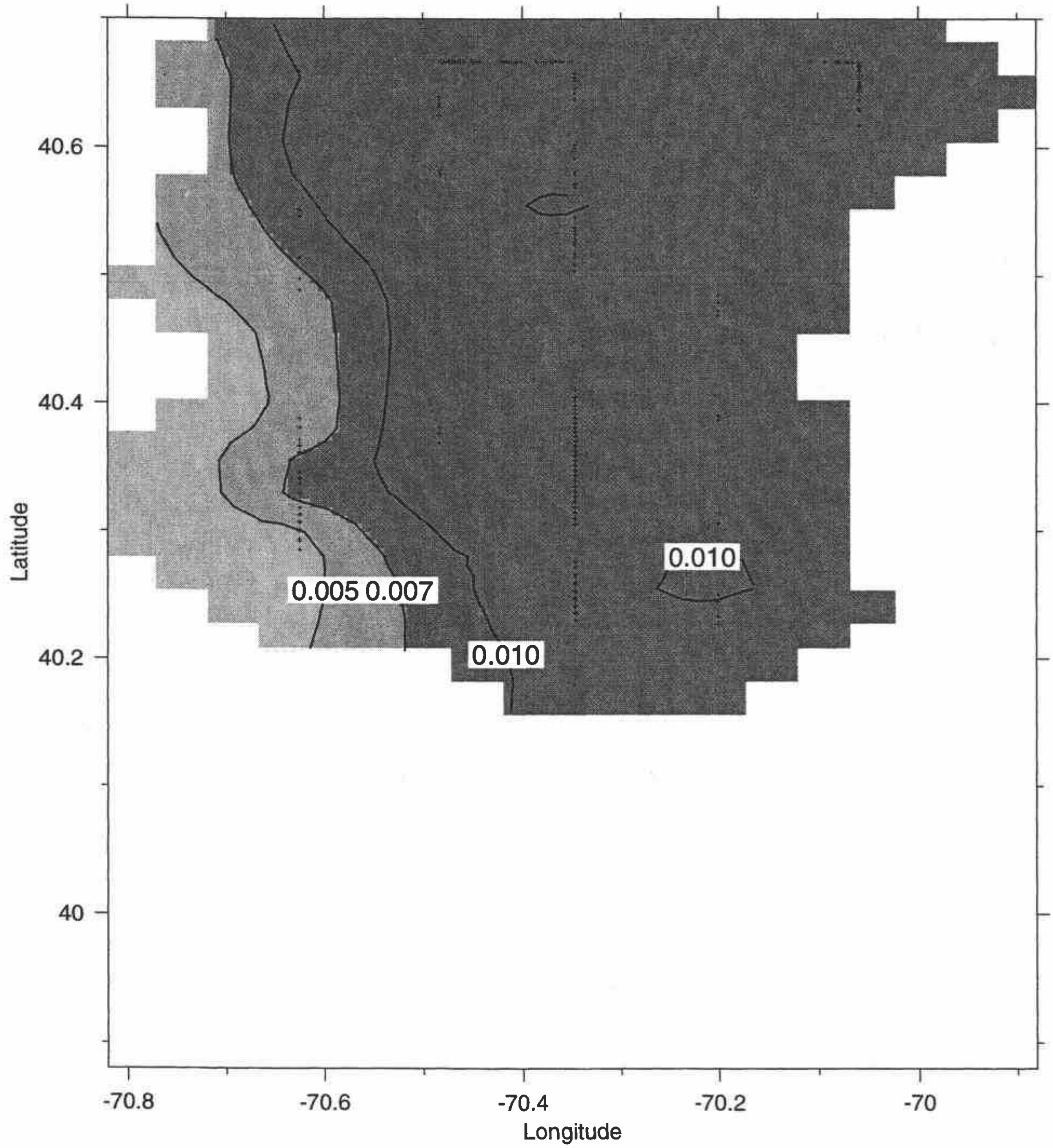

E9608 Bigbox 1
17-Aug-96 02:02 to 18-Aug-96 05:21
Map view at 5 m

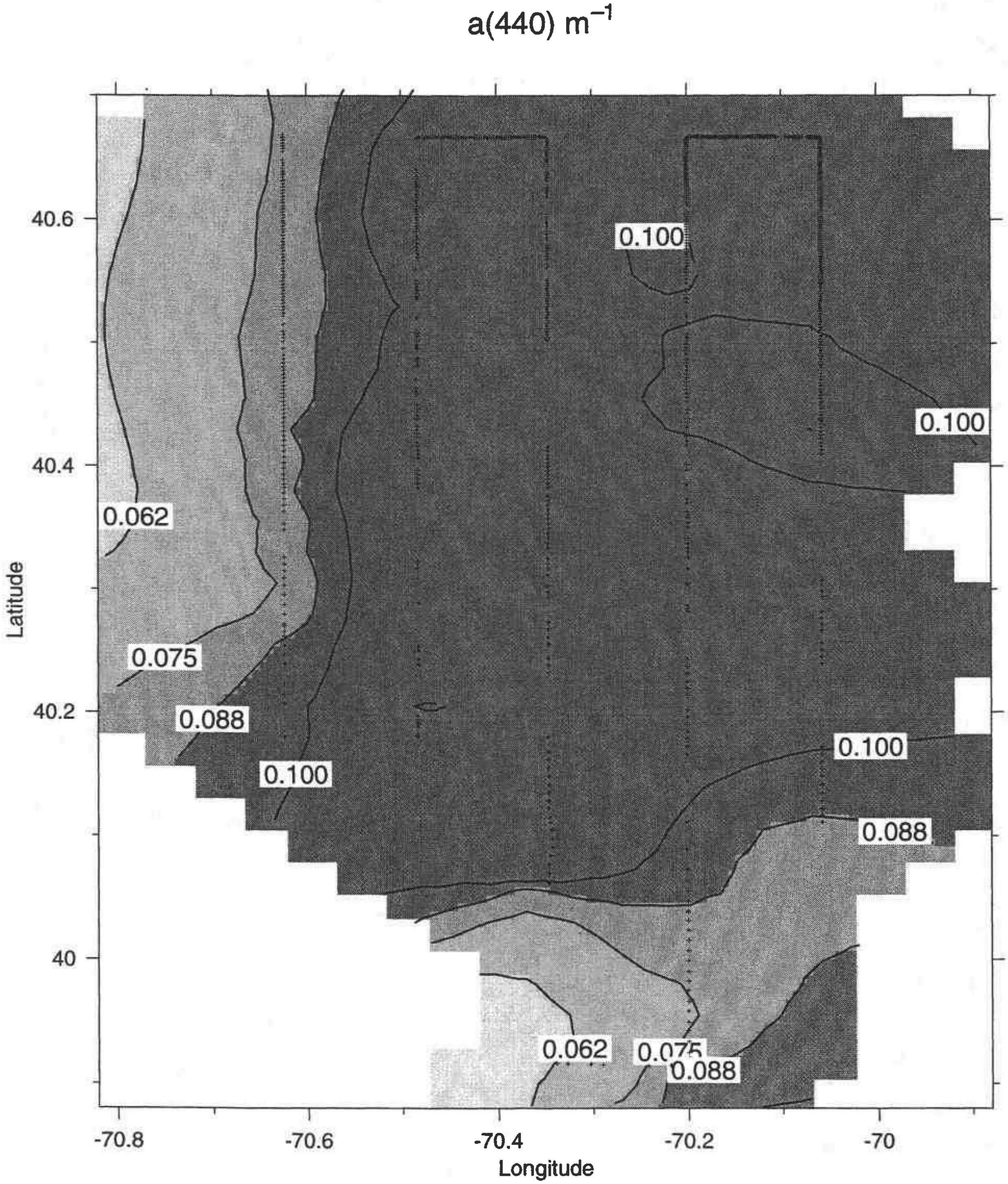

E9608 Bigbox 1

17-Aug-96 02:02 to 18-Aug-96 05:21

Map view at 45 m

a(440) m^{-1}

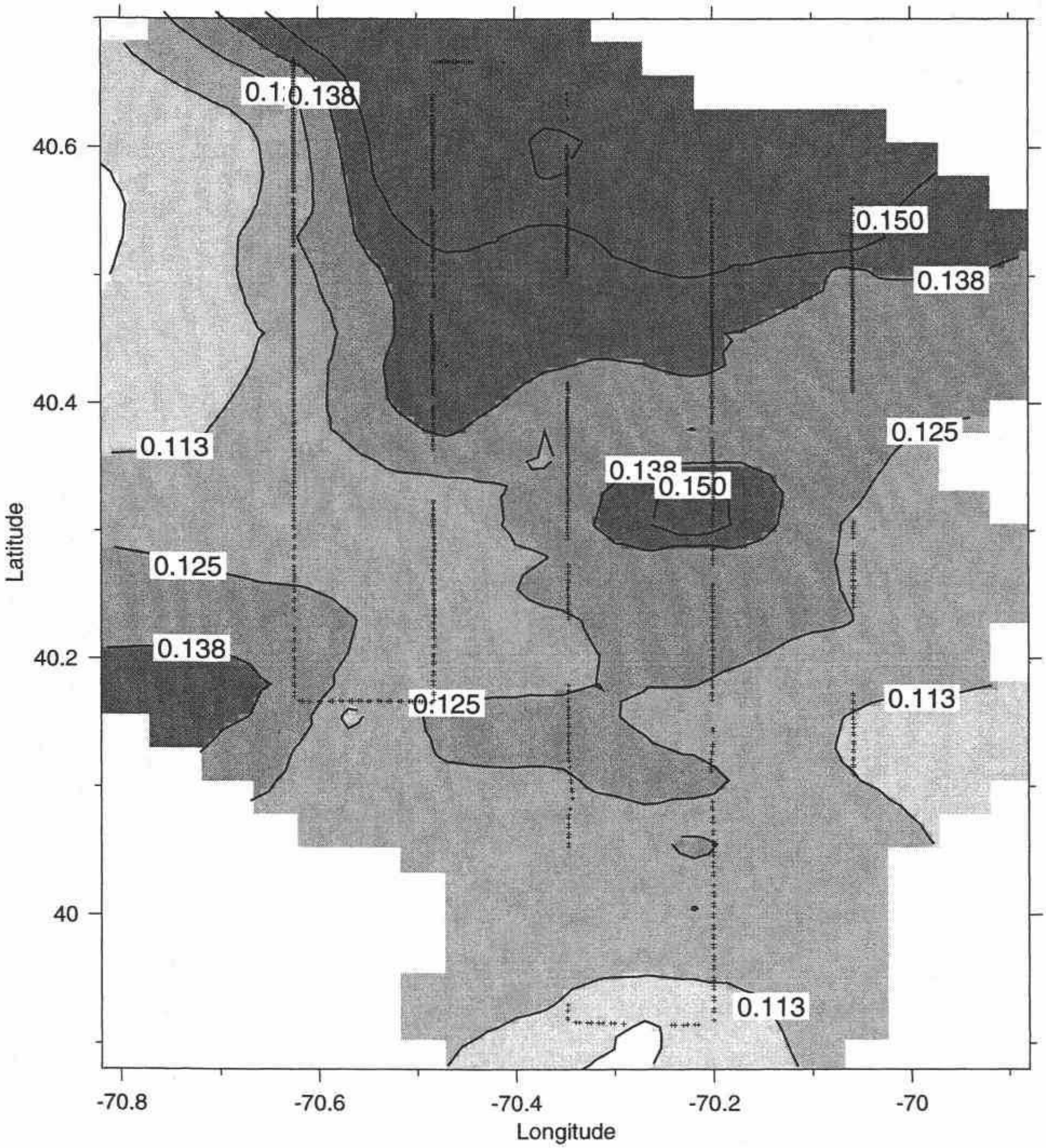

E9608 Bigbox 1

17-Aug-96 02:02 to 18-Aug-96 05:21

Map view at $\sigma_t = 24.6 \pm 0.025$ kg/m^3

a(440) m^{-1}

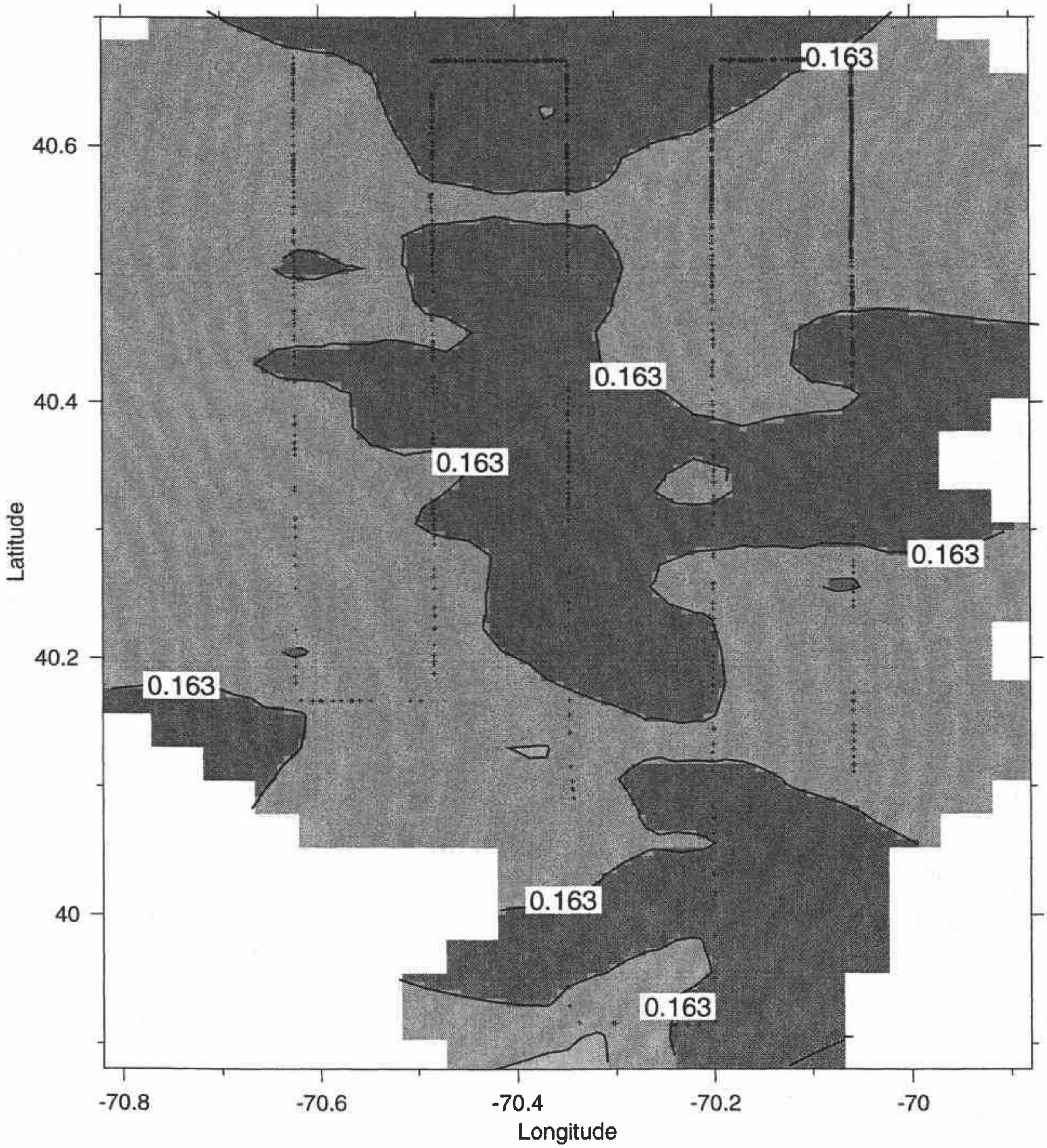

E9608 Bigbox 1

17-Aug-96 02:02 to 18-Aug-96 05:21

Map view at 10 m above bottom

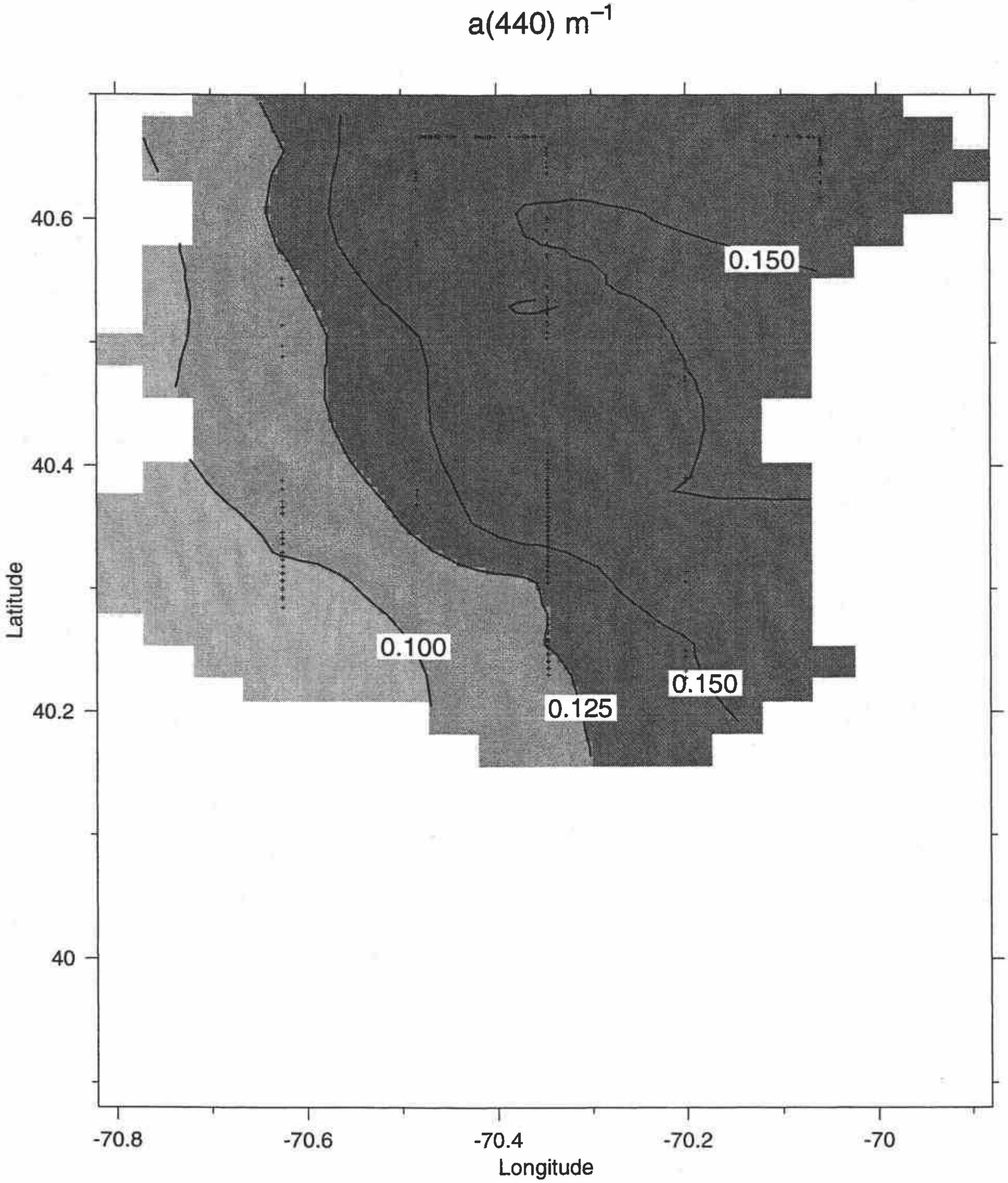

E9608 Bigbox 1

17-Aug-96 02:02 to 18-Aug-96 05:21

Map view at 5 m

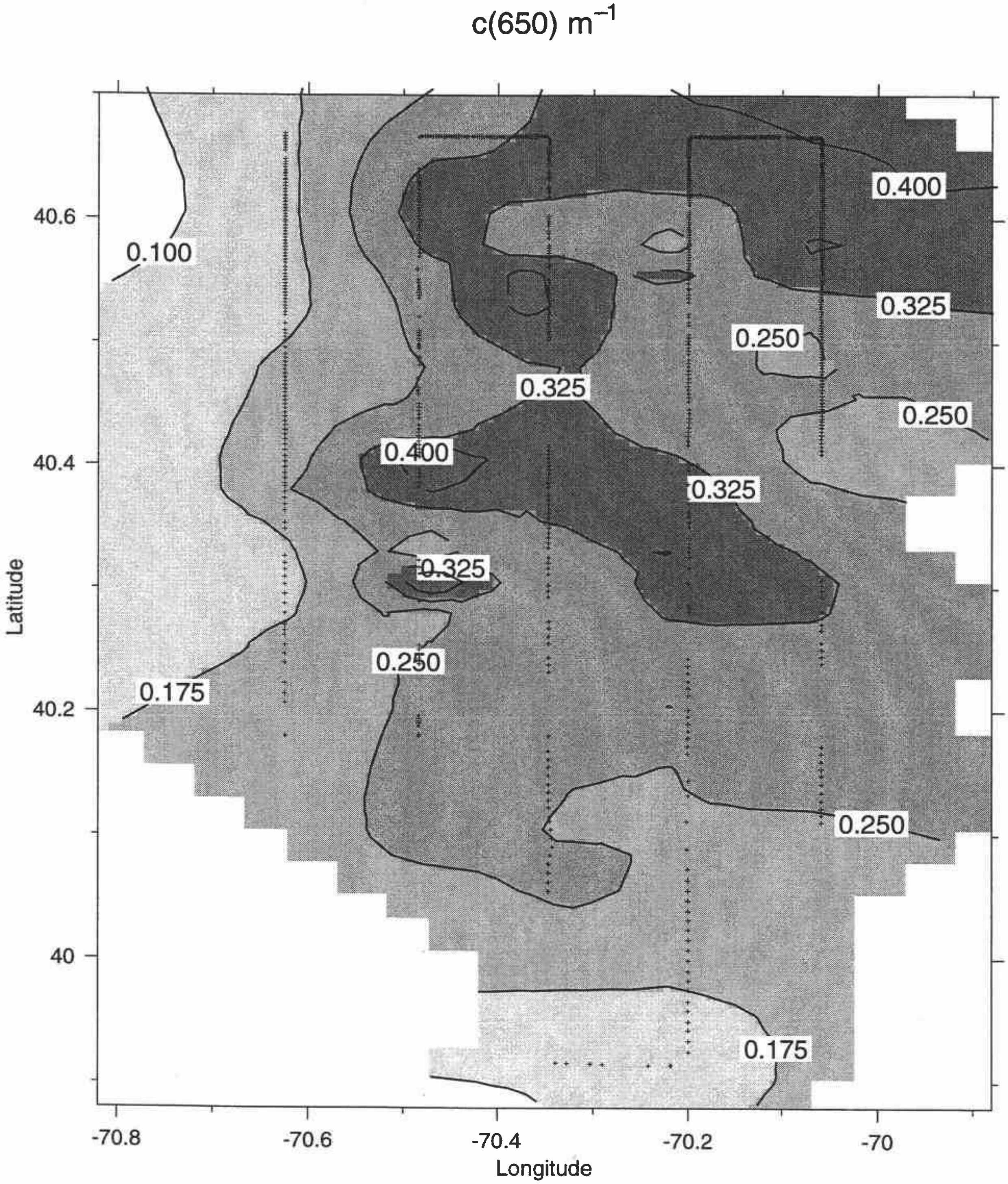

E9608 Bigbox 1

17-Aug-96 02:02 to 18-Aug-96 05:21

Map view at 45 m

c(650) m^{-1}

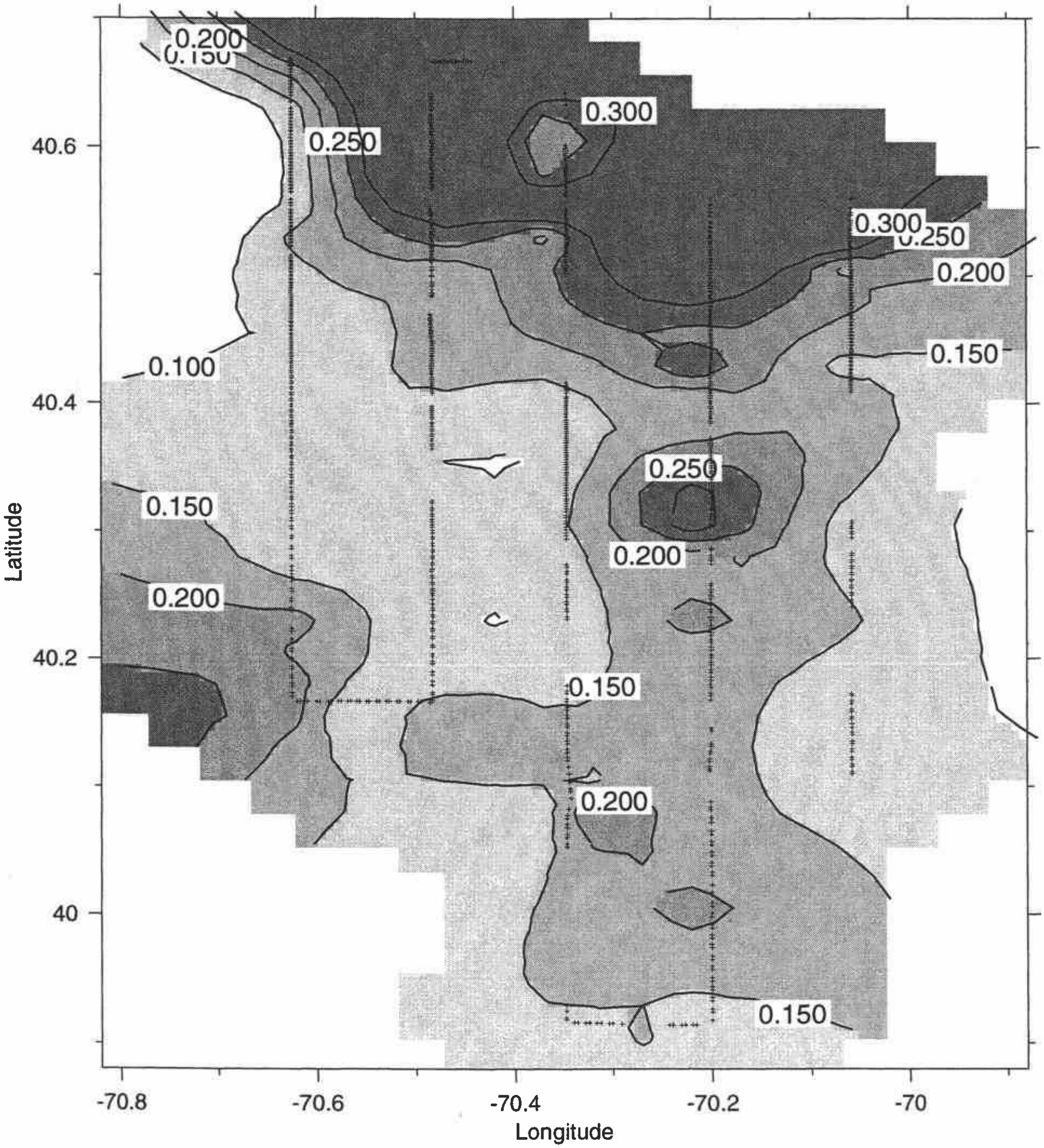

E9608 Bigbox 1

17-Aug-96 02:02 to 18-Aug-96 05:21

Map view at $\sigma_t = 24.6 \pm 0.025$ kg/m^3

c(650) m^{-1}

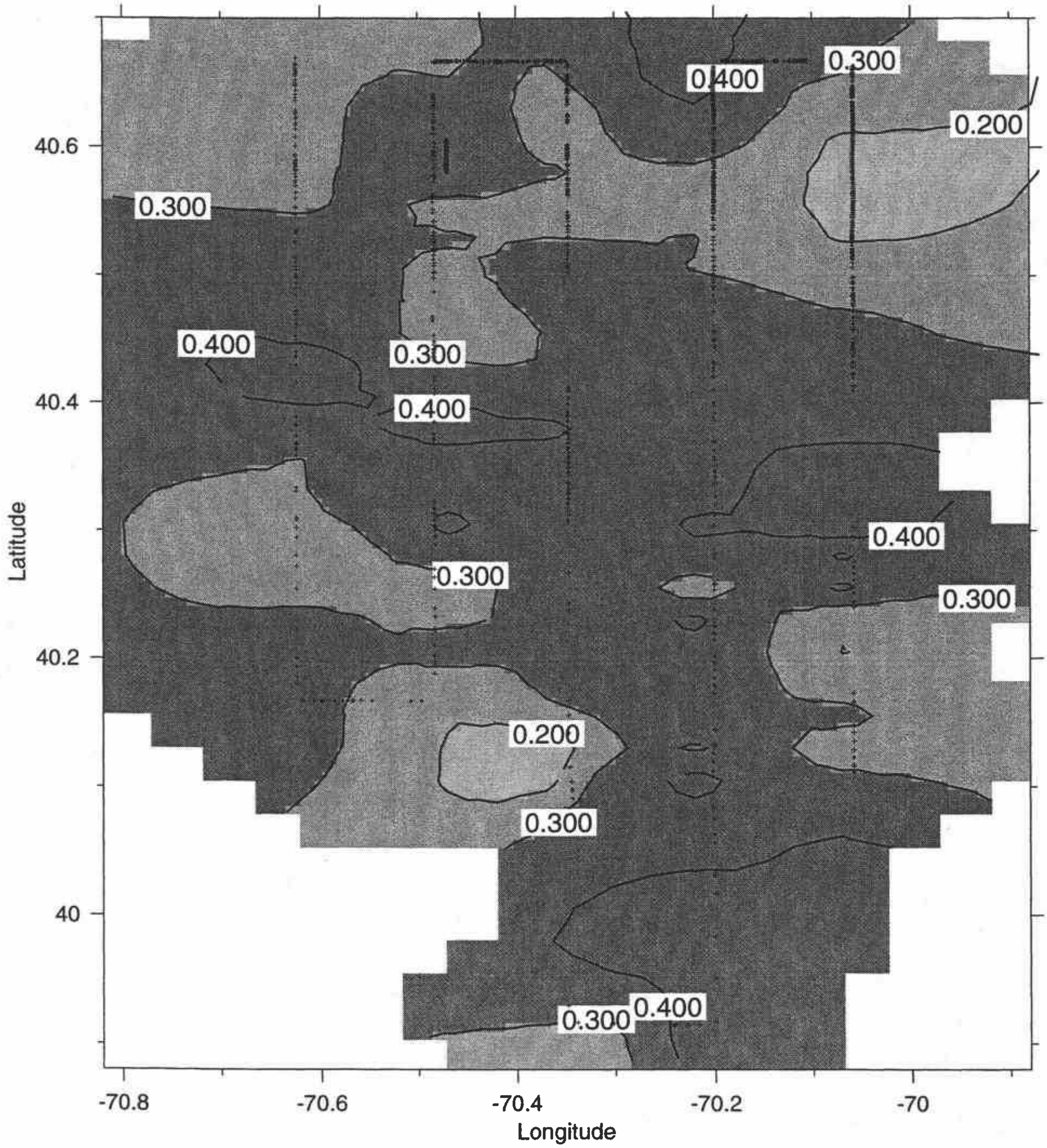

E9608 Bigbox 1

17-Aug-96 02:02 to 18-Aug-96 05:21

Map view at 10 m above bottom

c(650) m^{-1}

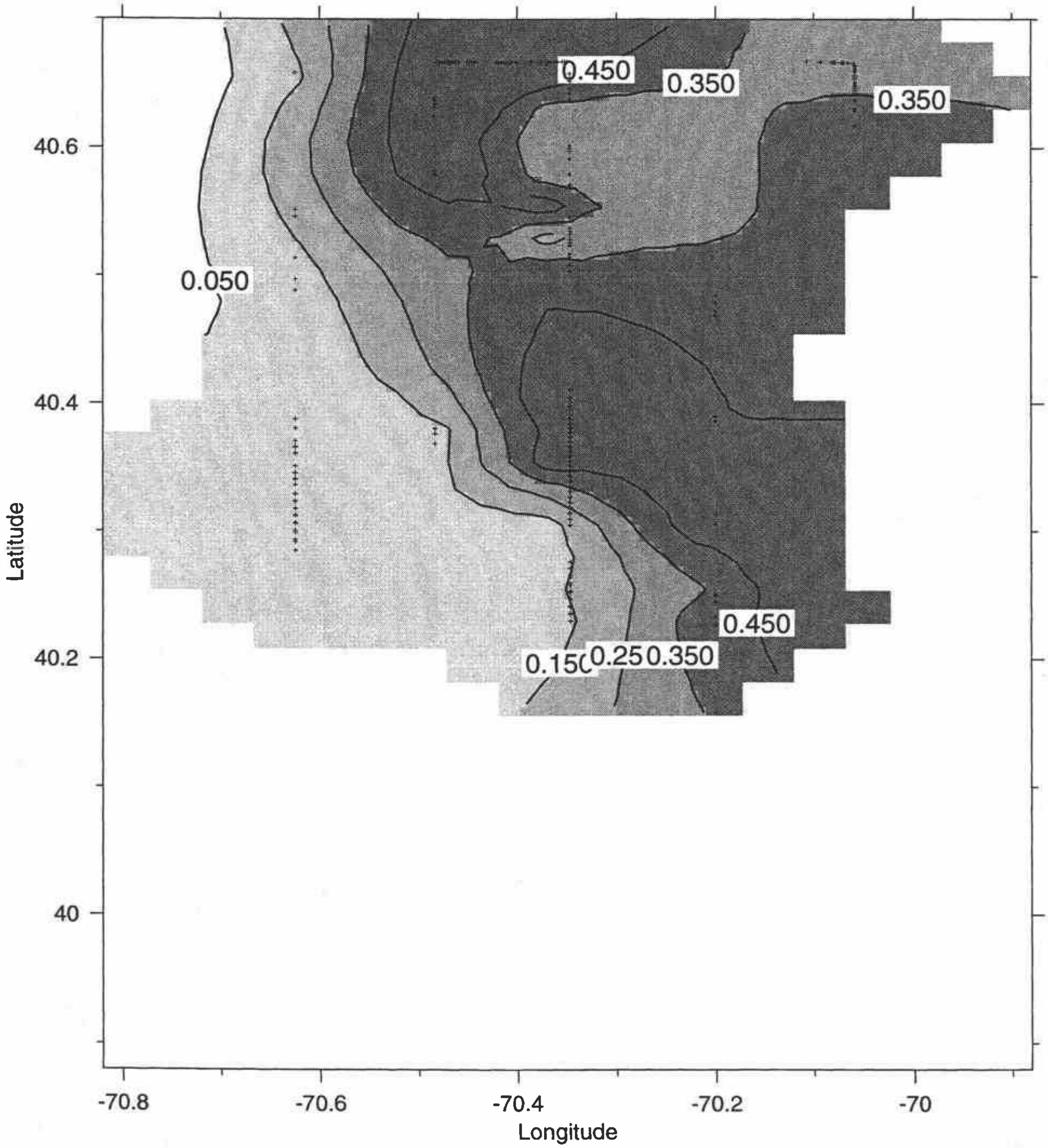

E9608 Bigbox 2

20-Aug-96 17:05 to 21-Aug-96 21:32

Map view at 5 m

a(676) m^{-1}

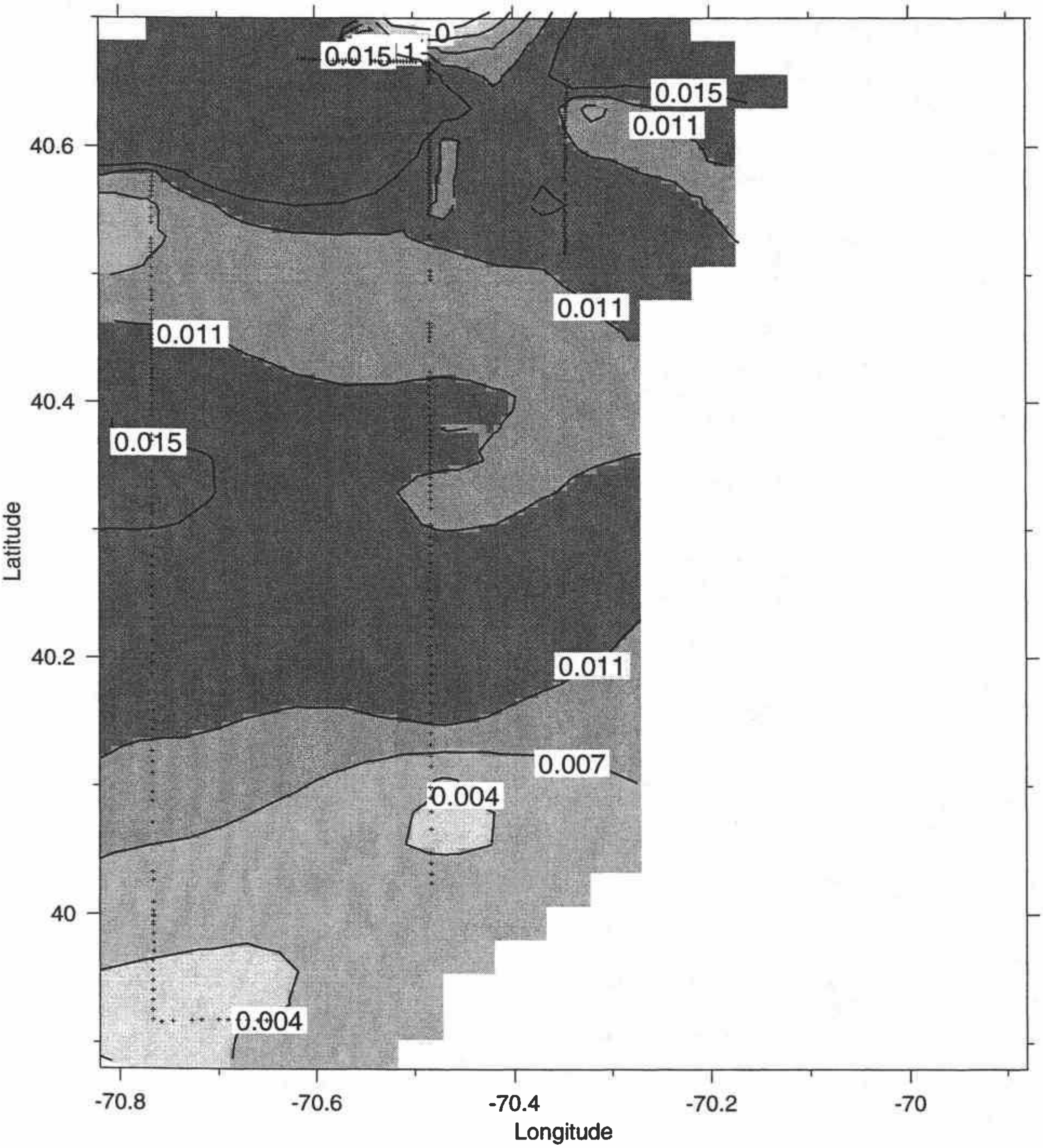

E9608 Bigbox 2

20-Aug-96 17:05 to 21-Aug-96 21:32

Map view at 45 m

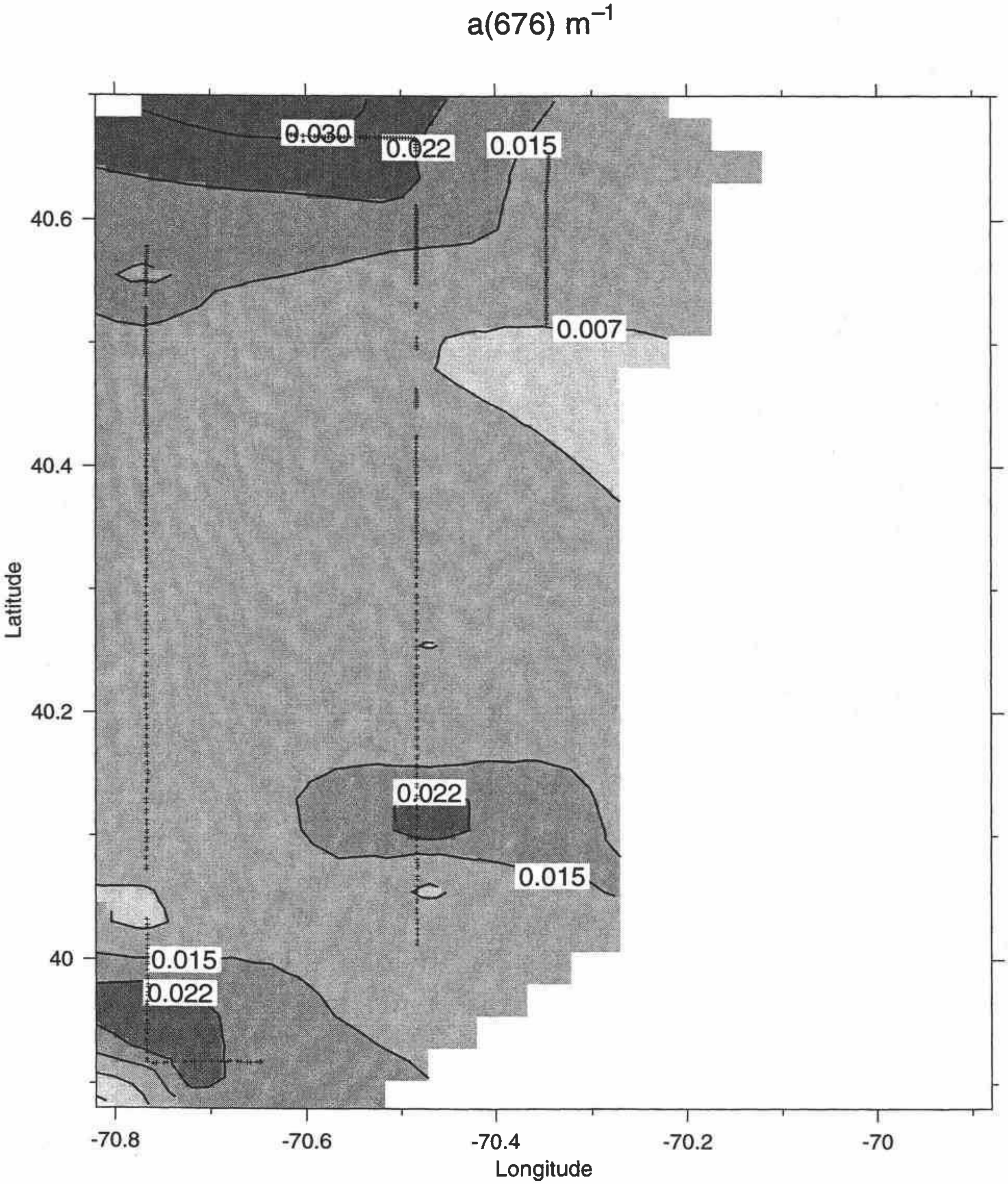

E9608 Bigbox 2

20-Aug-96 17:05 to 21-Aug-96 21:32

Map view at $\sigma_t = 24.6 \pm 0.025$ kg/m^3

a(676) m^{-1}

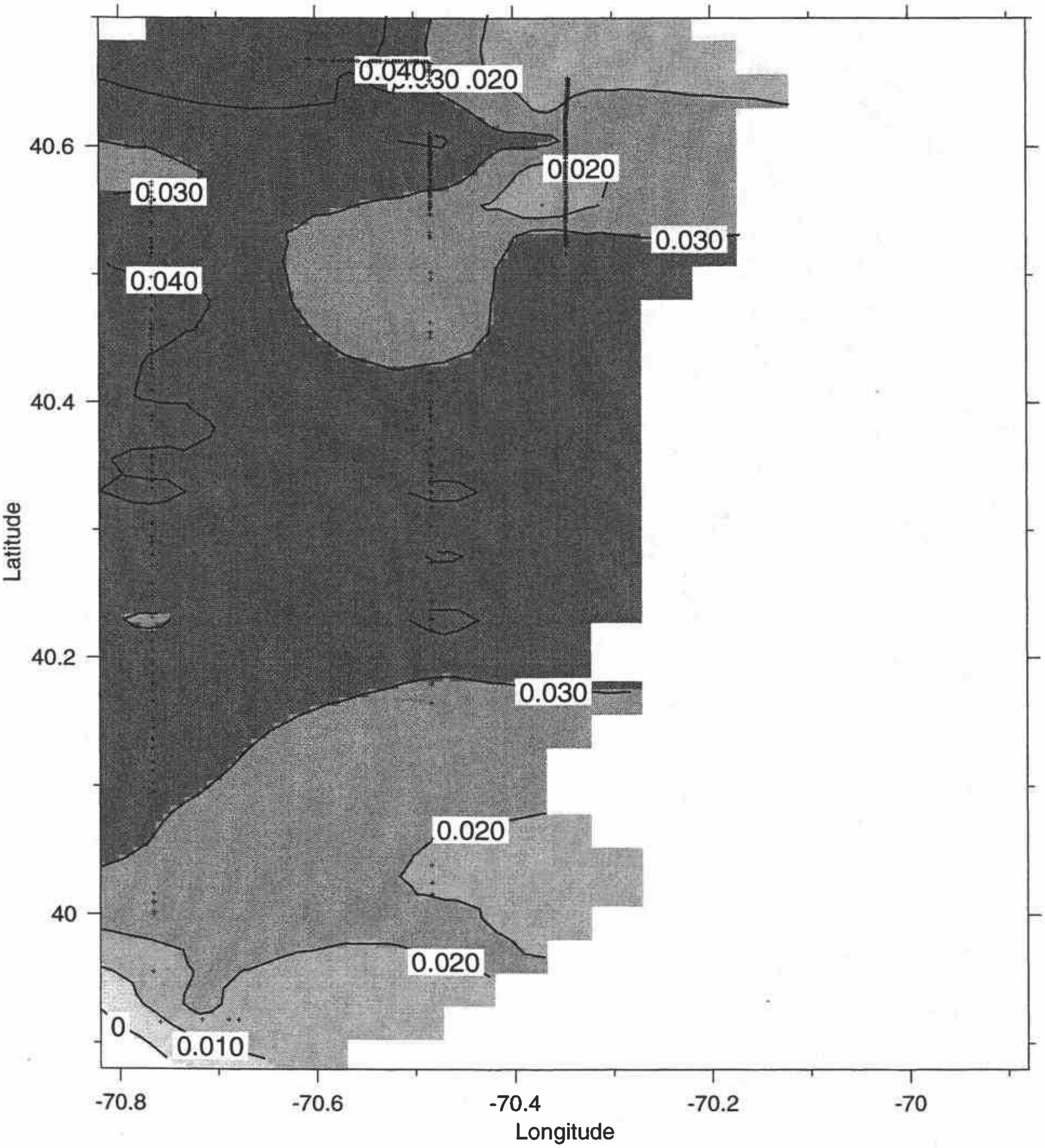

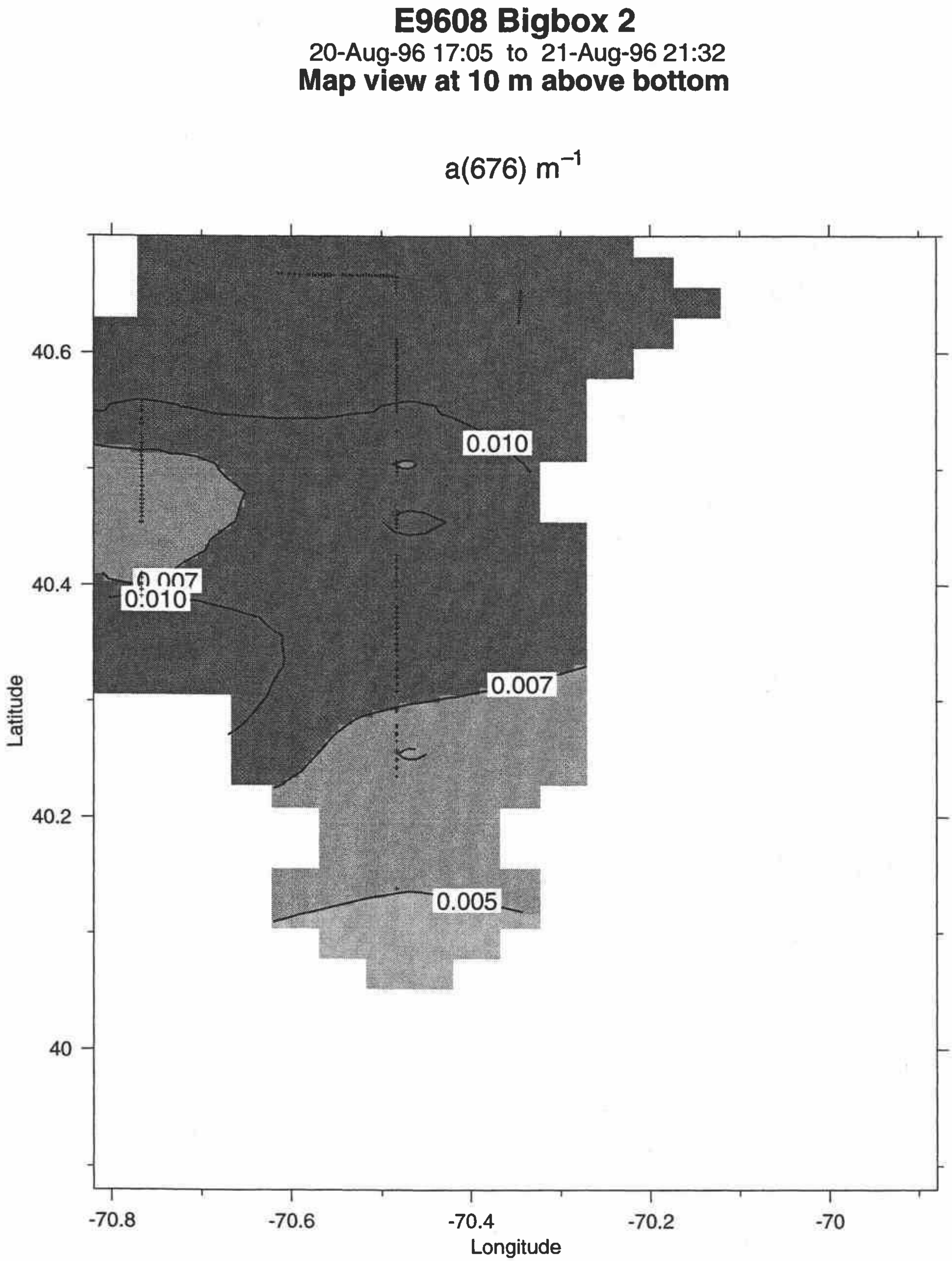

E9608 Bigbox 2
20-Aug-96 17:05 to 21-Aug-96 21:32
Map view at 10 m above bottom
a(676) m^{-1}
0.010
0.007
0.010
0.007
0.005
40.6
40.4
40.2
40
Latitude
-70.8
-70.6
-70.4
-70.2
-70
Longitude

E9608 Bigbox 2

20-Aug-96 17:05 to 21-Aug-96 21:32

Map view at 5 m

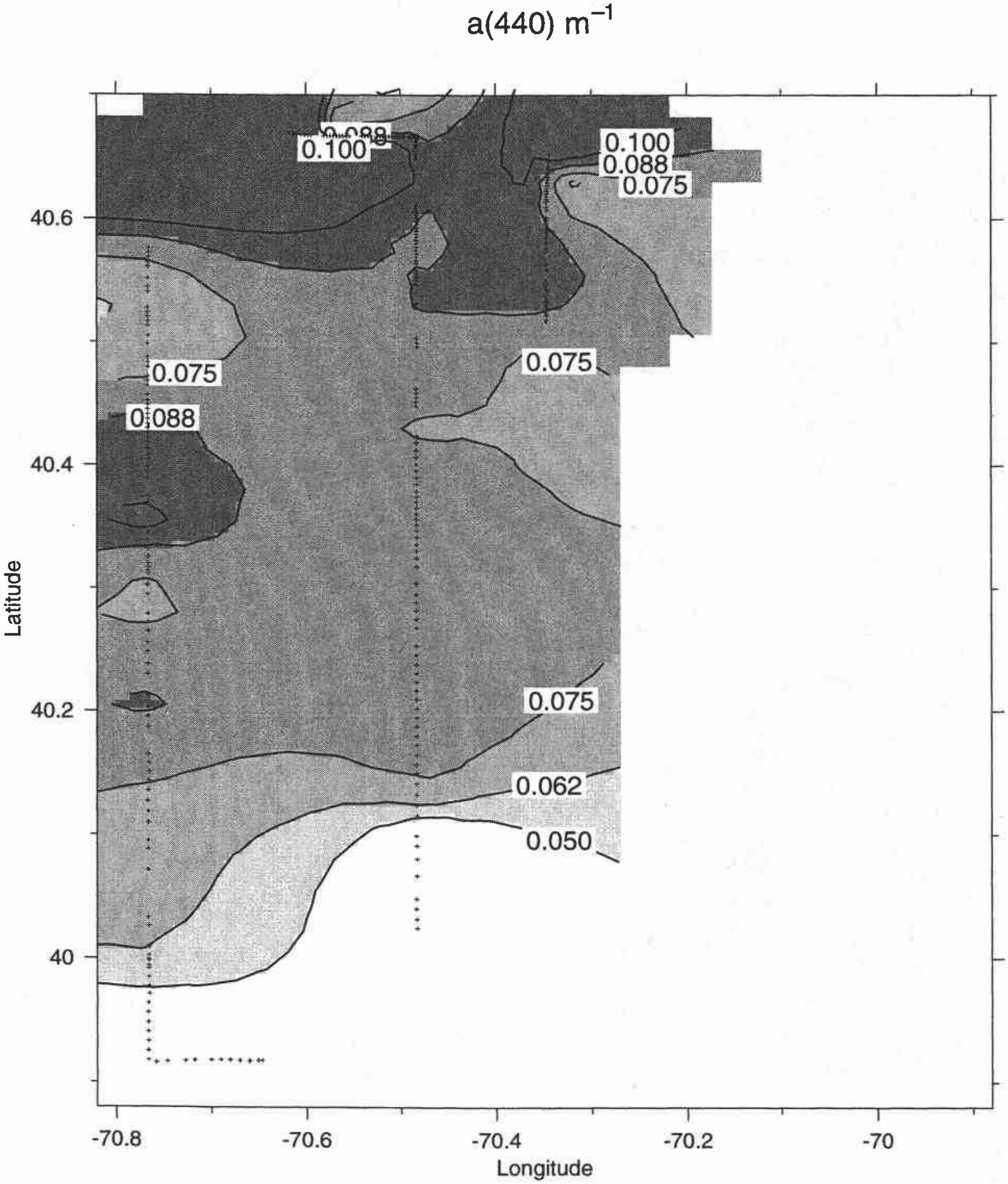

E9608 Bigbox 2

20-Aug-96 17:05 to 21-Aug-96 21:32

Map view at 45 m

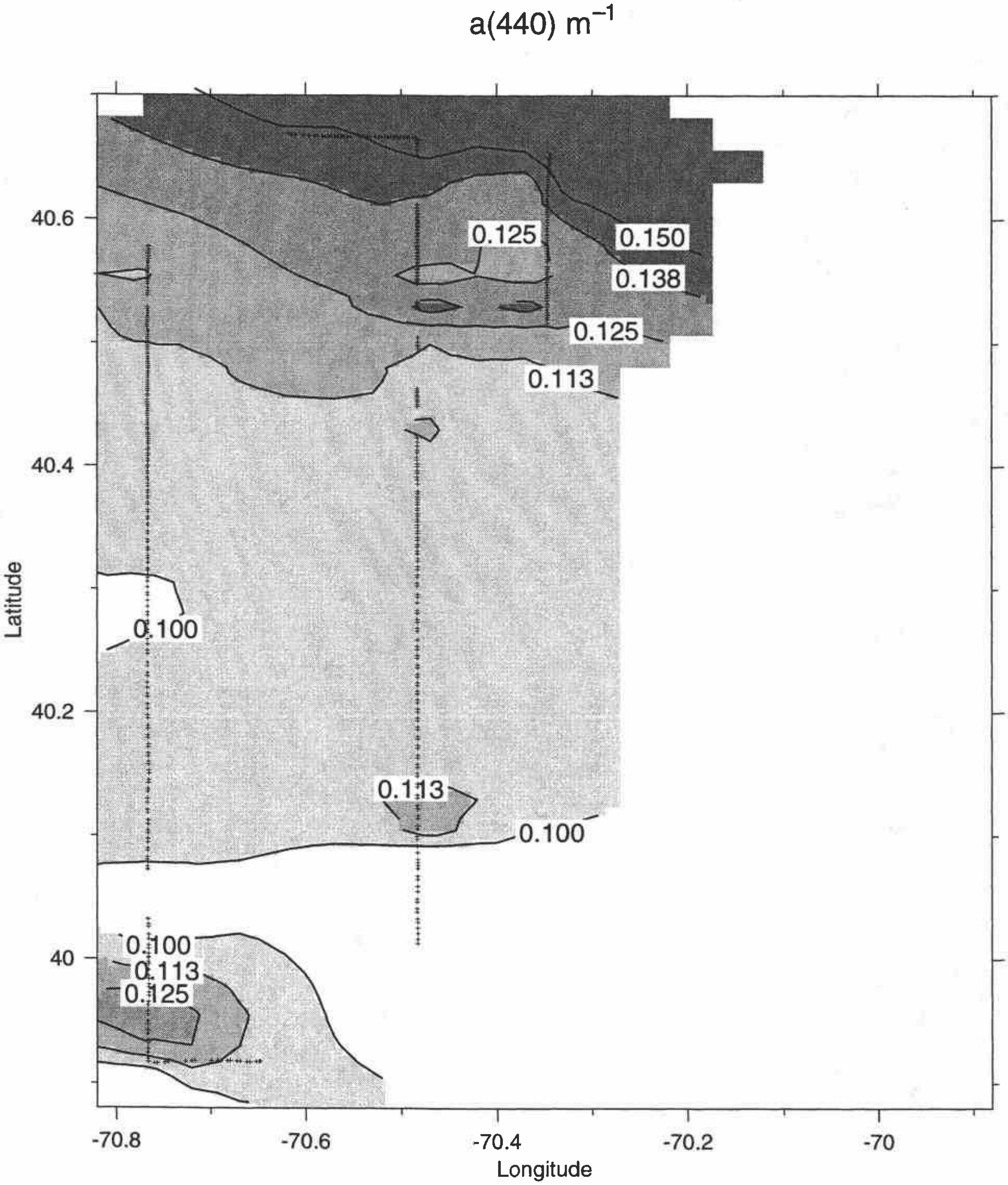

E9608 Bigbox 2

20-Aug-96 17:05 to 21-Aug-96 21:32

Map view at $\sigma_t = 24.6 \pm 0.025$ kg/m^3

a(440) m^{-1}

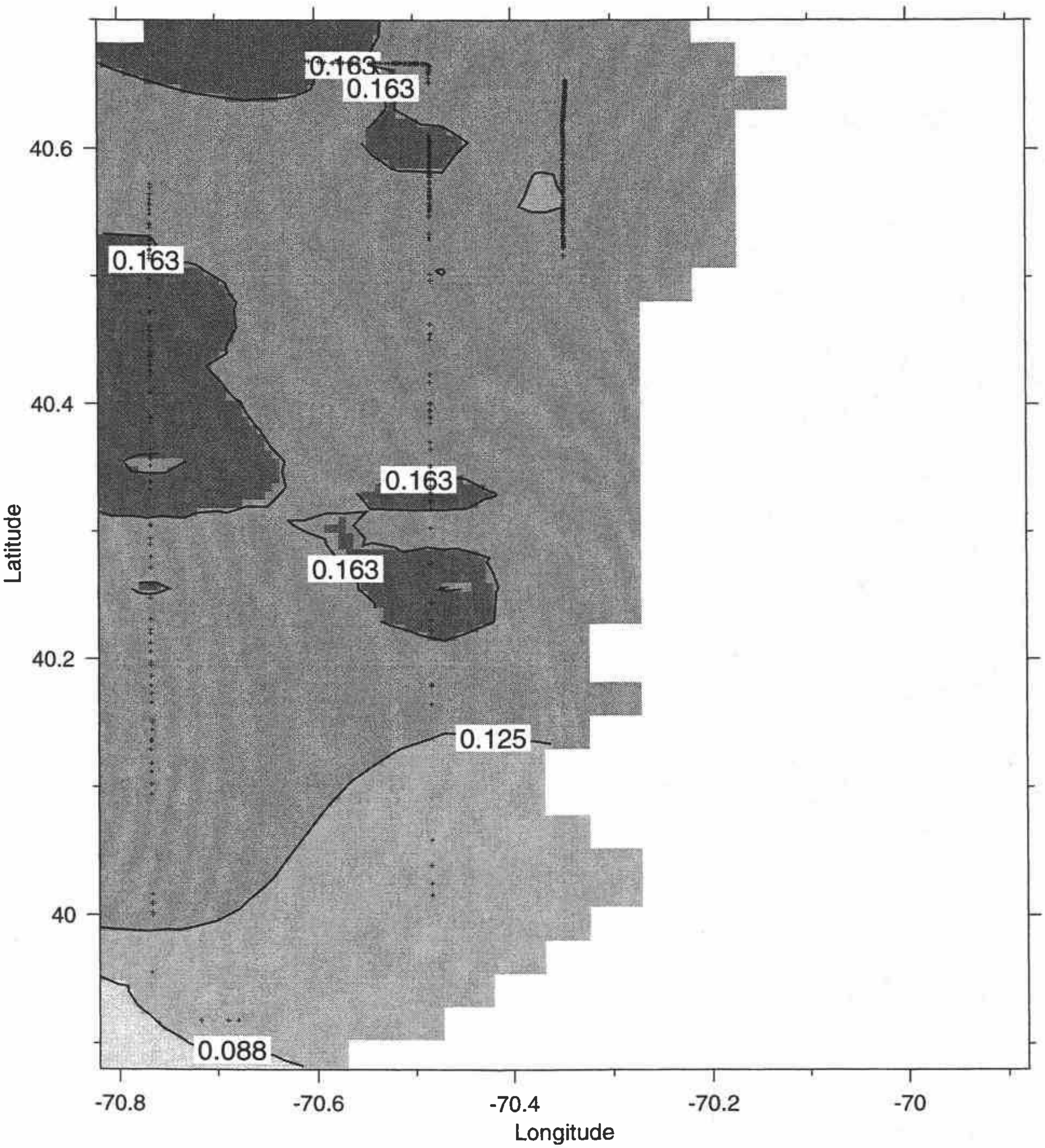

E9608 Bigbox 2

20-Aug-96 17:05 to 21-Aug-96 21:32

Map view at 10 m above bottom

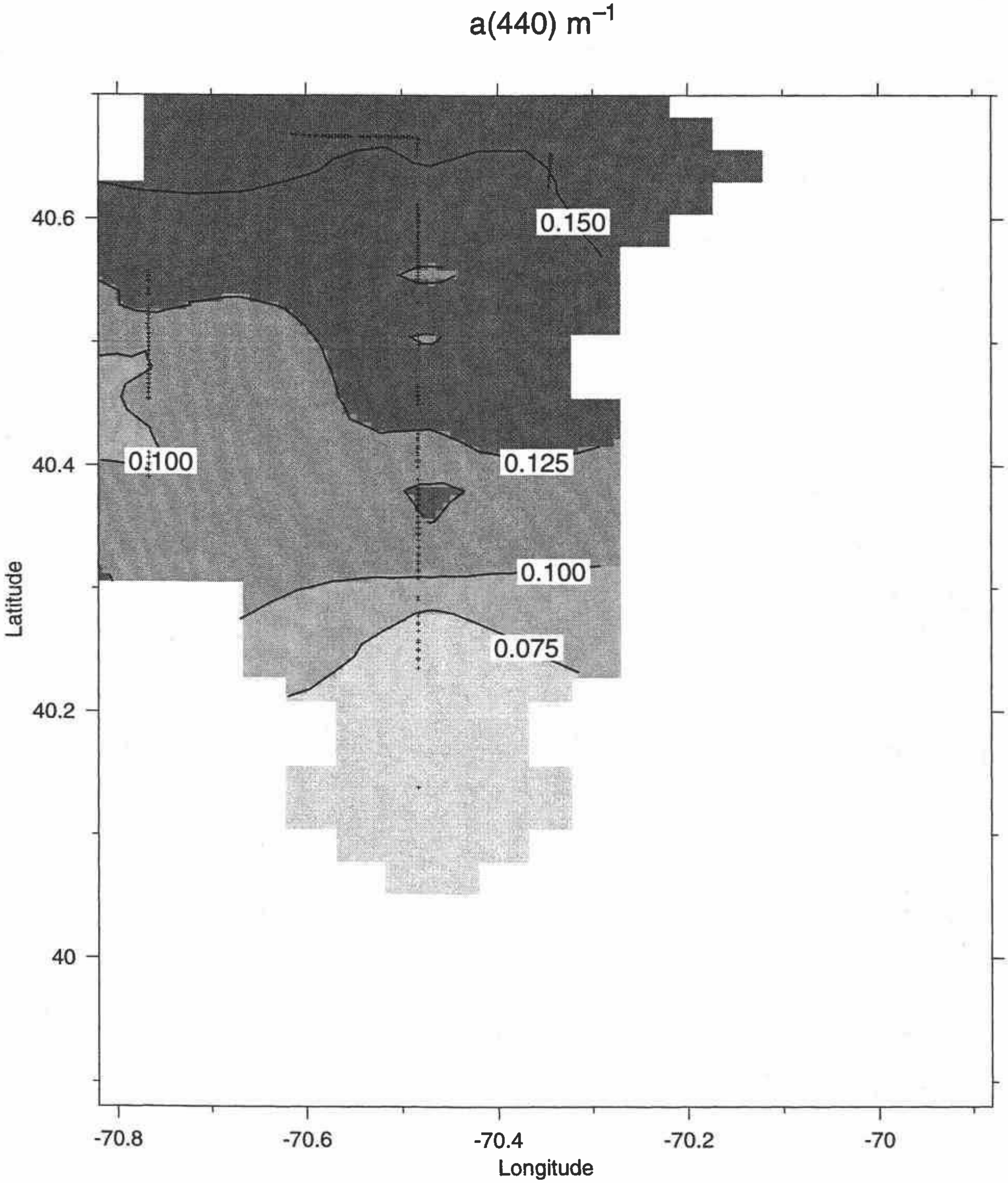

E9608 Bigbox 2

20-Aug-96 17:05 to 21-Aug-96 21:32

Map view at 5 m

c(650) m^{-1}

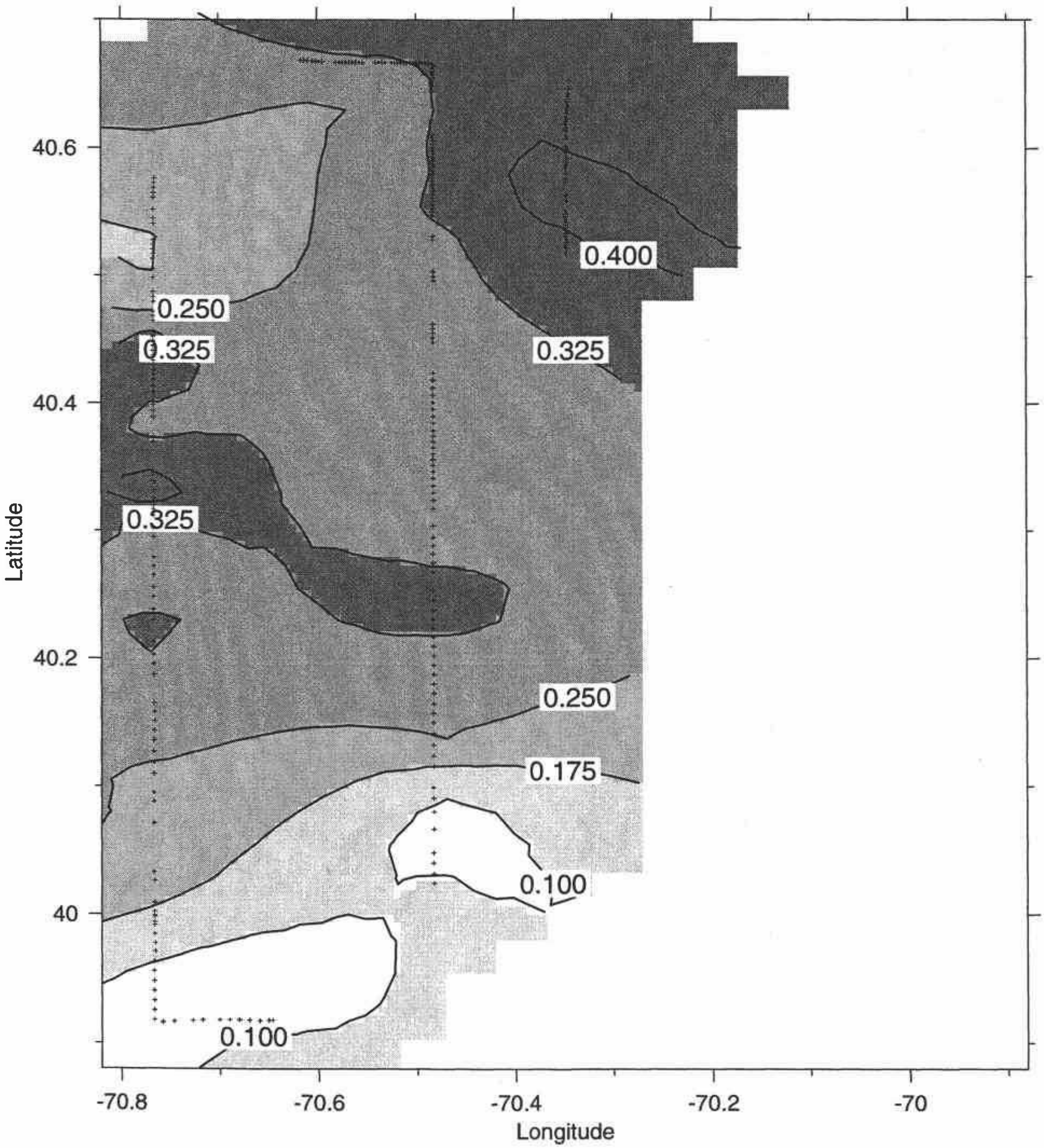

E9608 Bigbox 2

20-Aug-96 17:05 to 21-Aug-96 21:32

Map view at 45 m

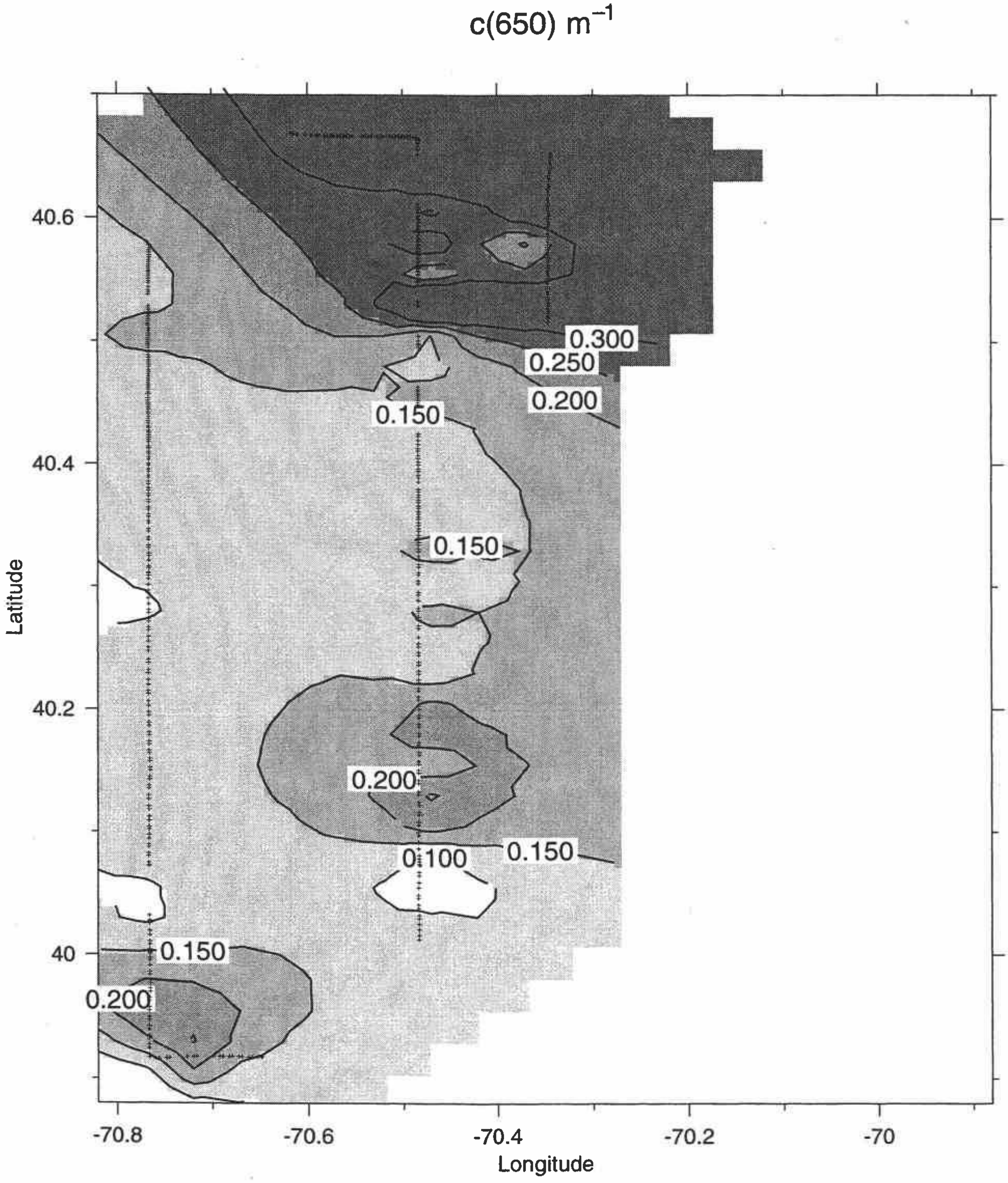

E9608 Bigbox 2

20-Aug-96 17:05 to 21-Aug-96 21:32

Map view at $\sigma_t = 24.6 \pm 0.025$ kg/m^3

c(650) m^{-1}

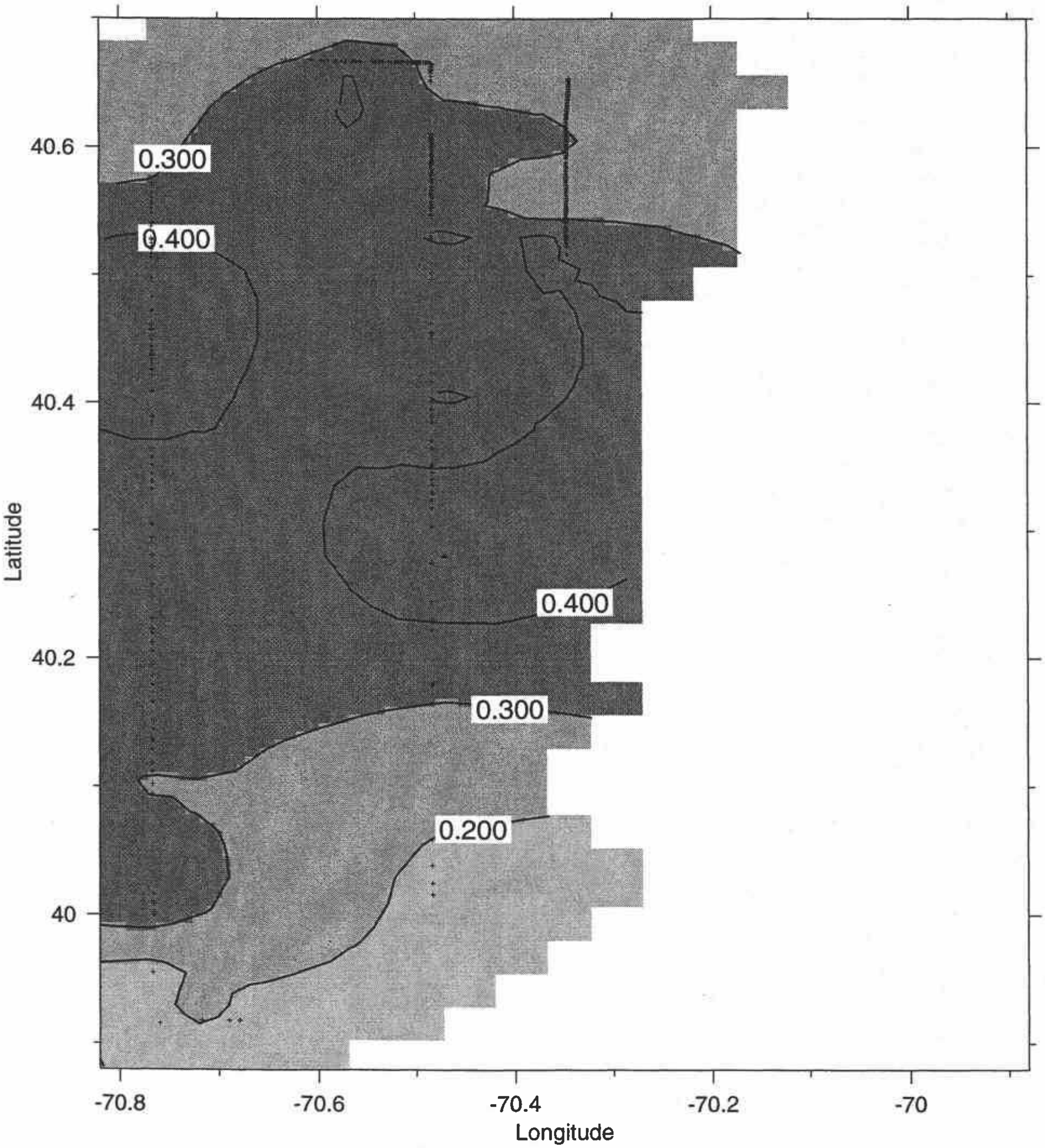

E9608 Bigbox 2

20-Aug-96 17:05 to 21-Aug-96 21:32

Map view at 10 m above bottom

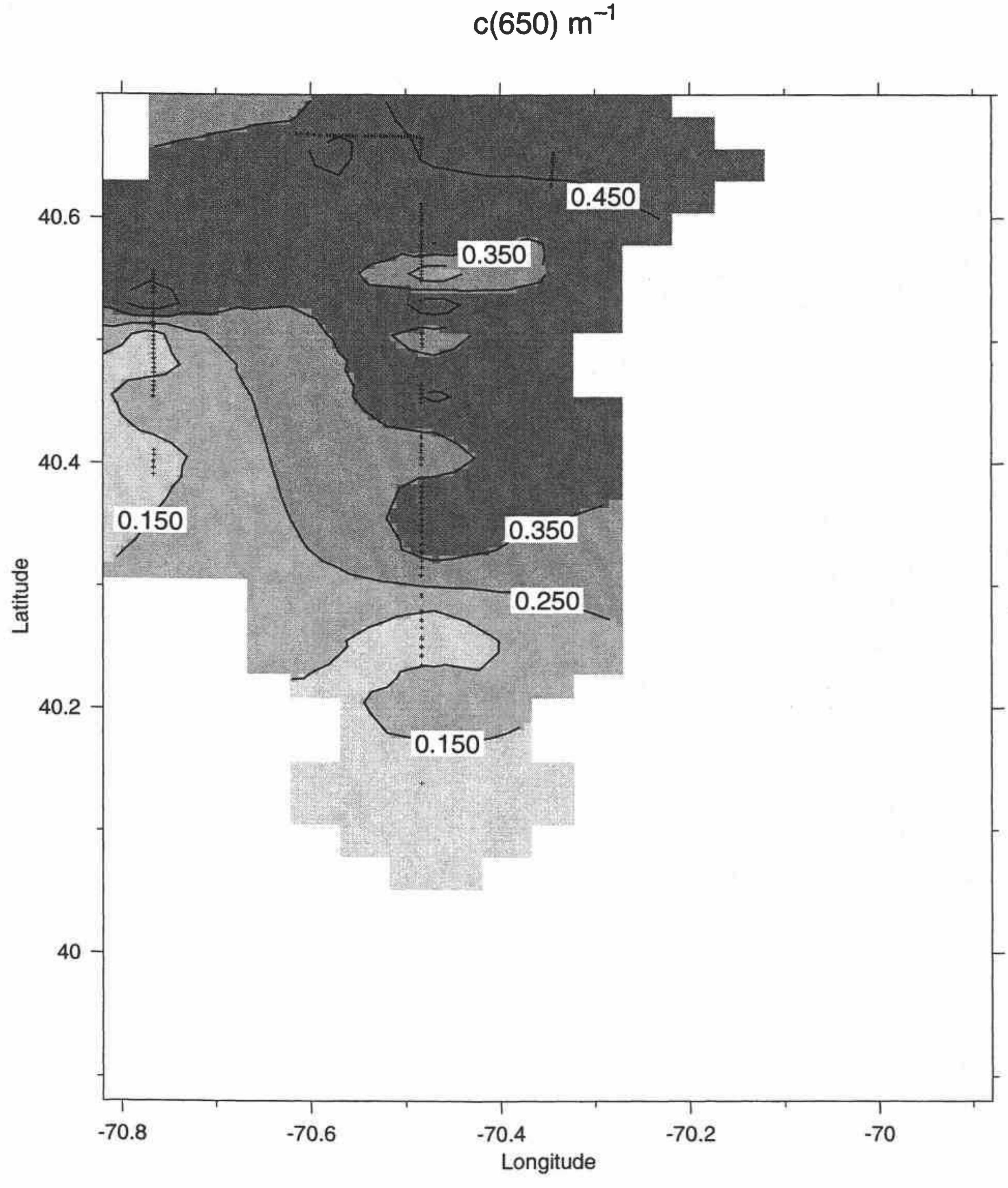

E9608 Bigbox 3

31-Aug-96 05:52 to 01-Sep-96 11:05

Map view at 5 m

a(676) m^{-1}

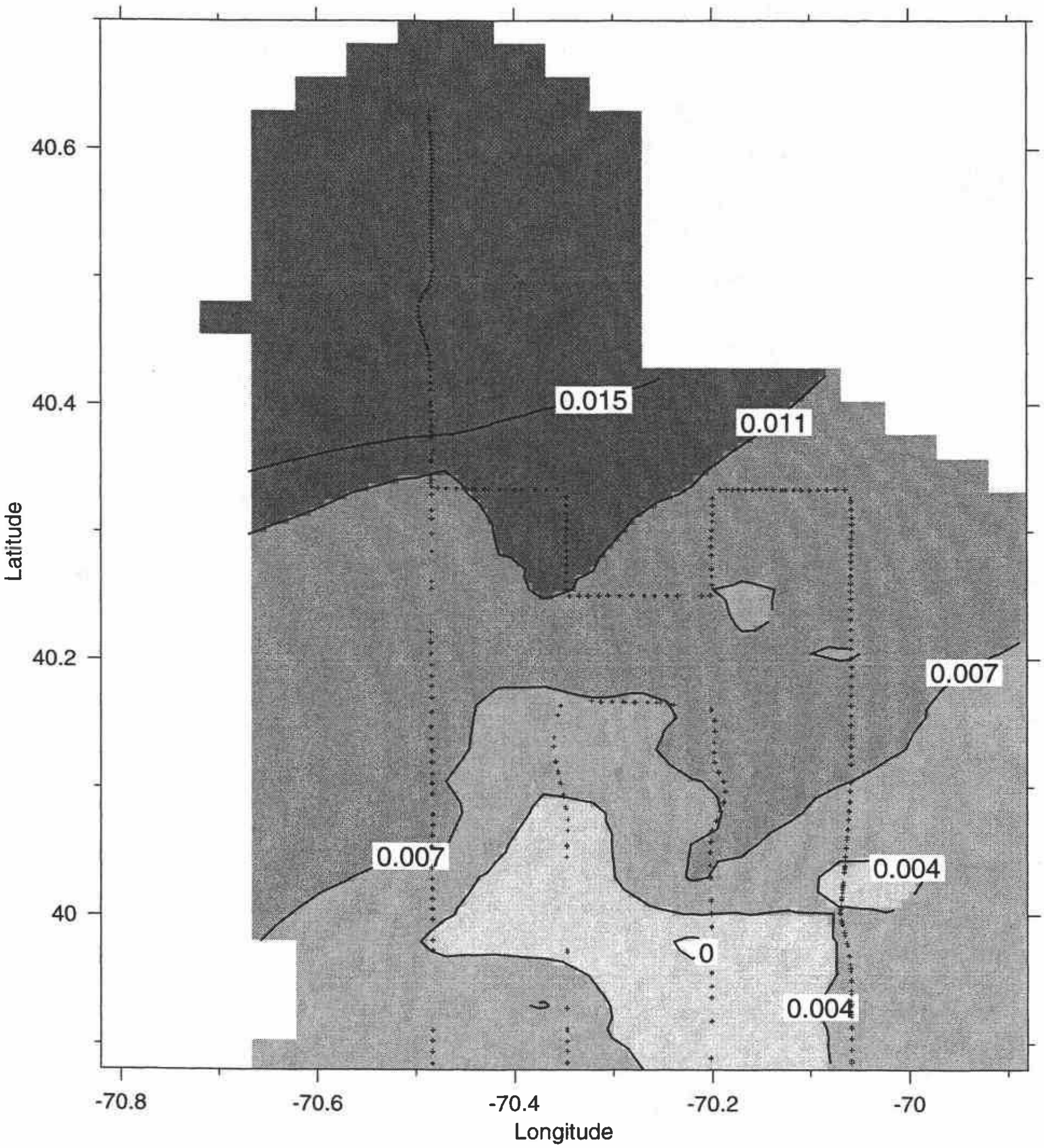

E9608 Bigbox 3

31-Aug-96 05:52 to 01-Sep-96 11:05

Map view at 45 m

a(676) m^{-1}

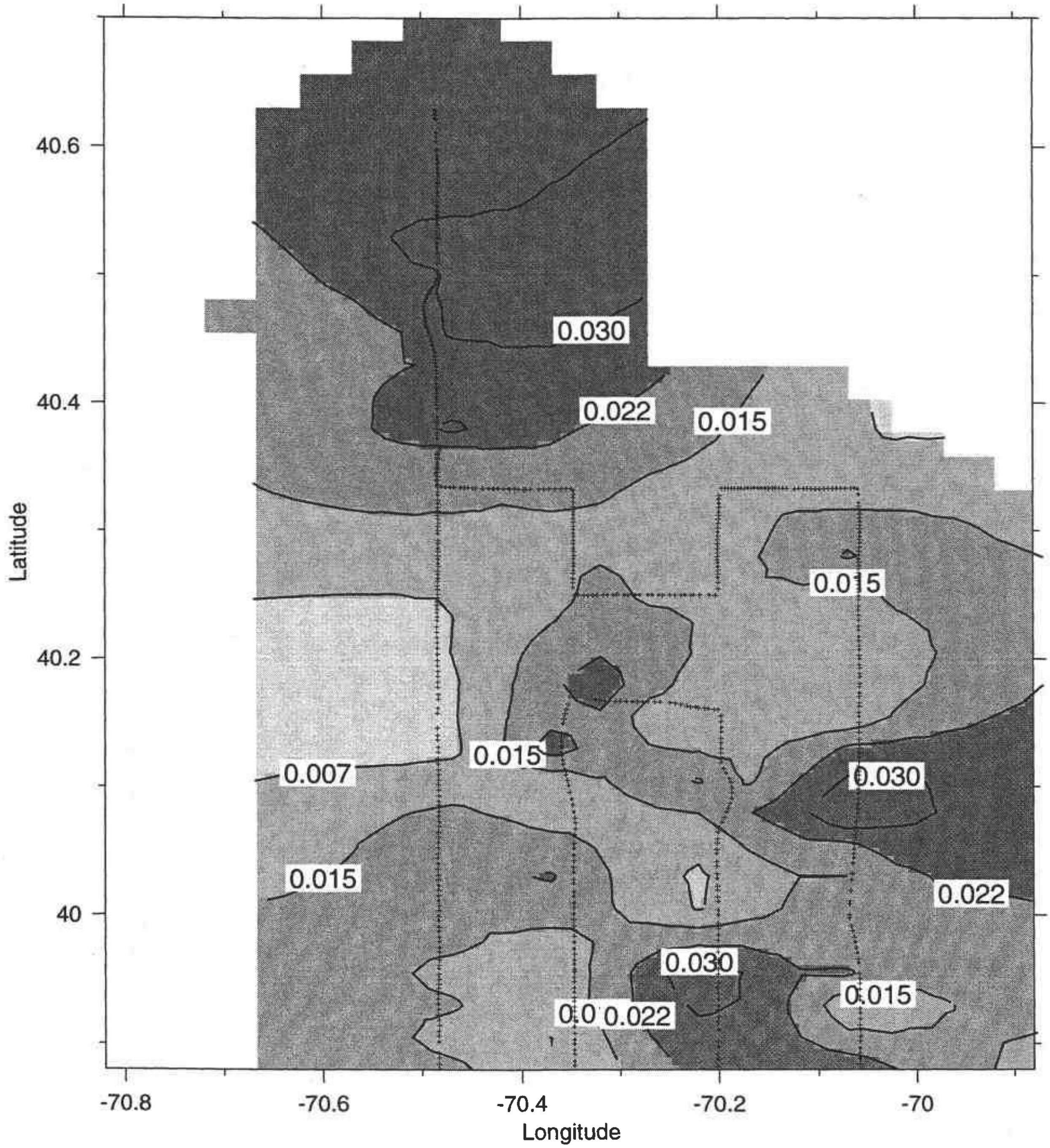

E9608 Bigbox 3

31-Aug-96 05:52 to 01-Sep-96 11:05

Map view at $\sigma_t = 24.6 \pm 0.025$ kg/m^3

a(676) m^{-1}

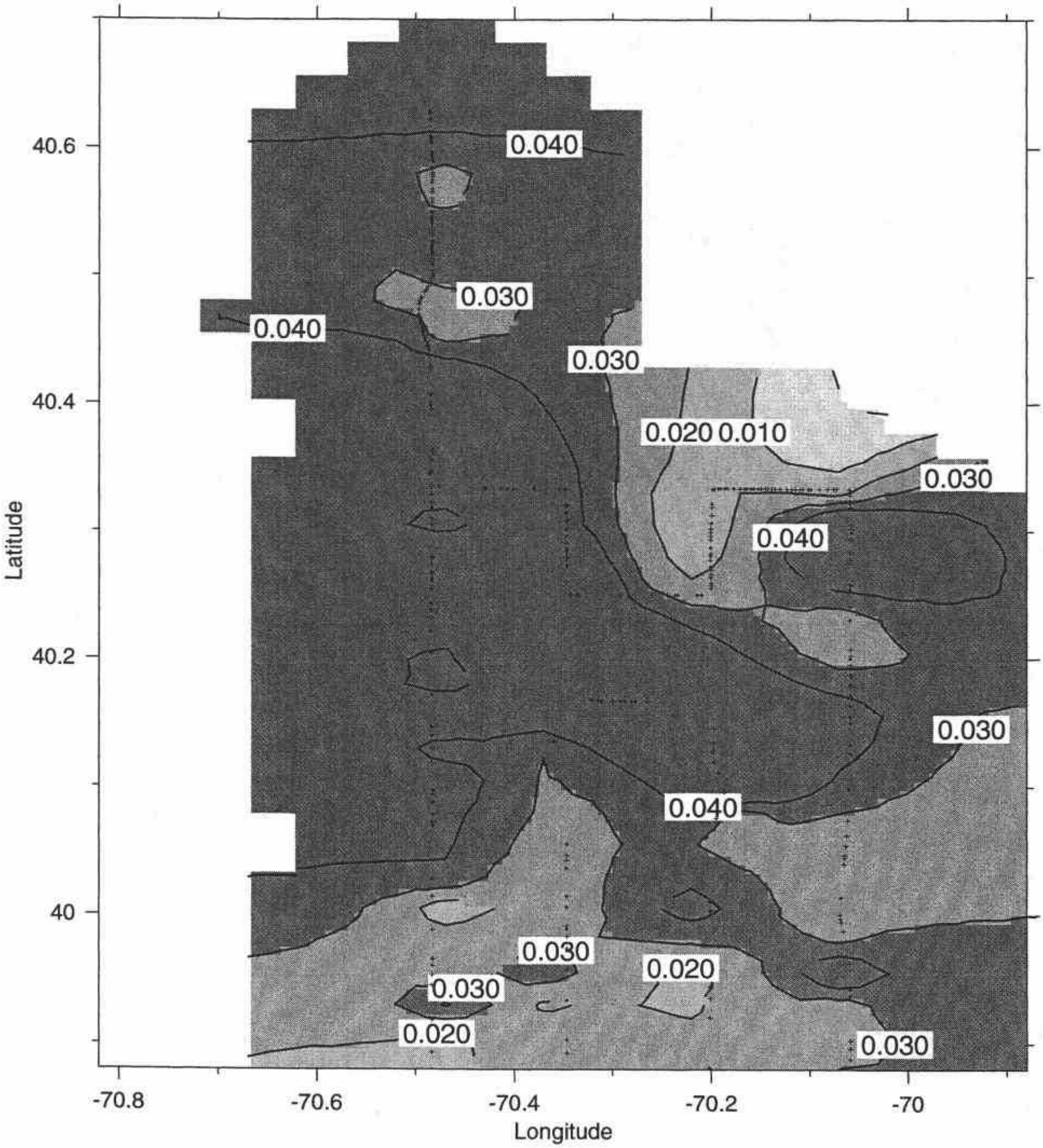

E9608 Bigbox 3

31-Aug-96 05:52 to 01-Sep-96 11:05

Map view at 10 m above bottom

$a(676)\ m^{-1}$

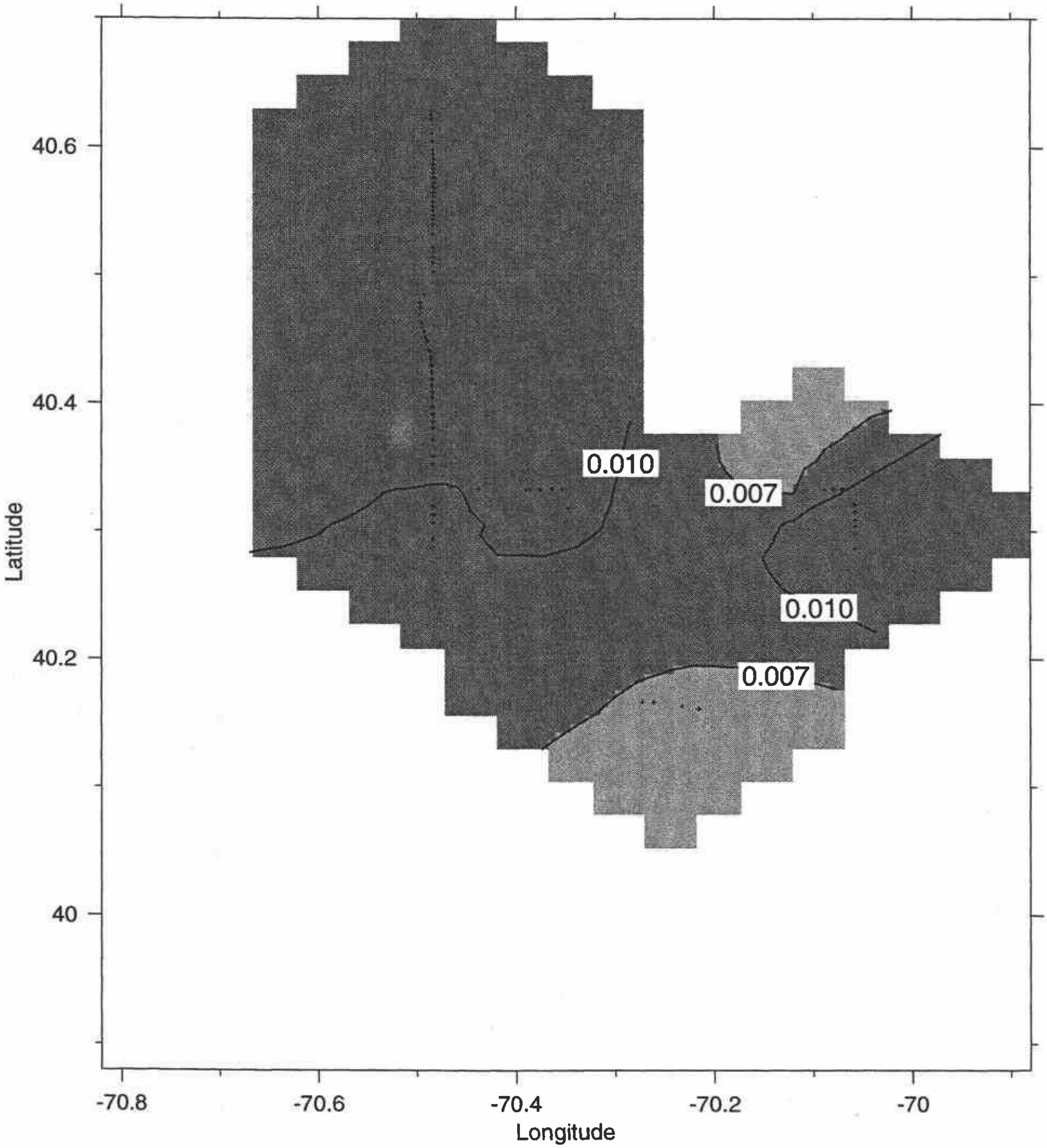

E9608 Bigbox 3

31-Aug-96 05:52 to 01-Sep-96 11:05

Map view at 5 m

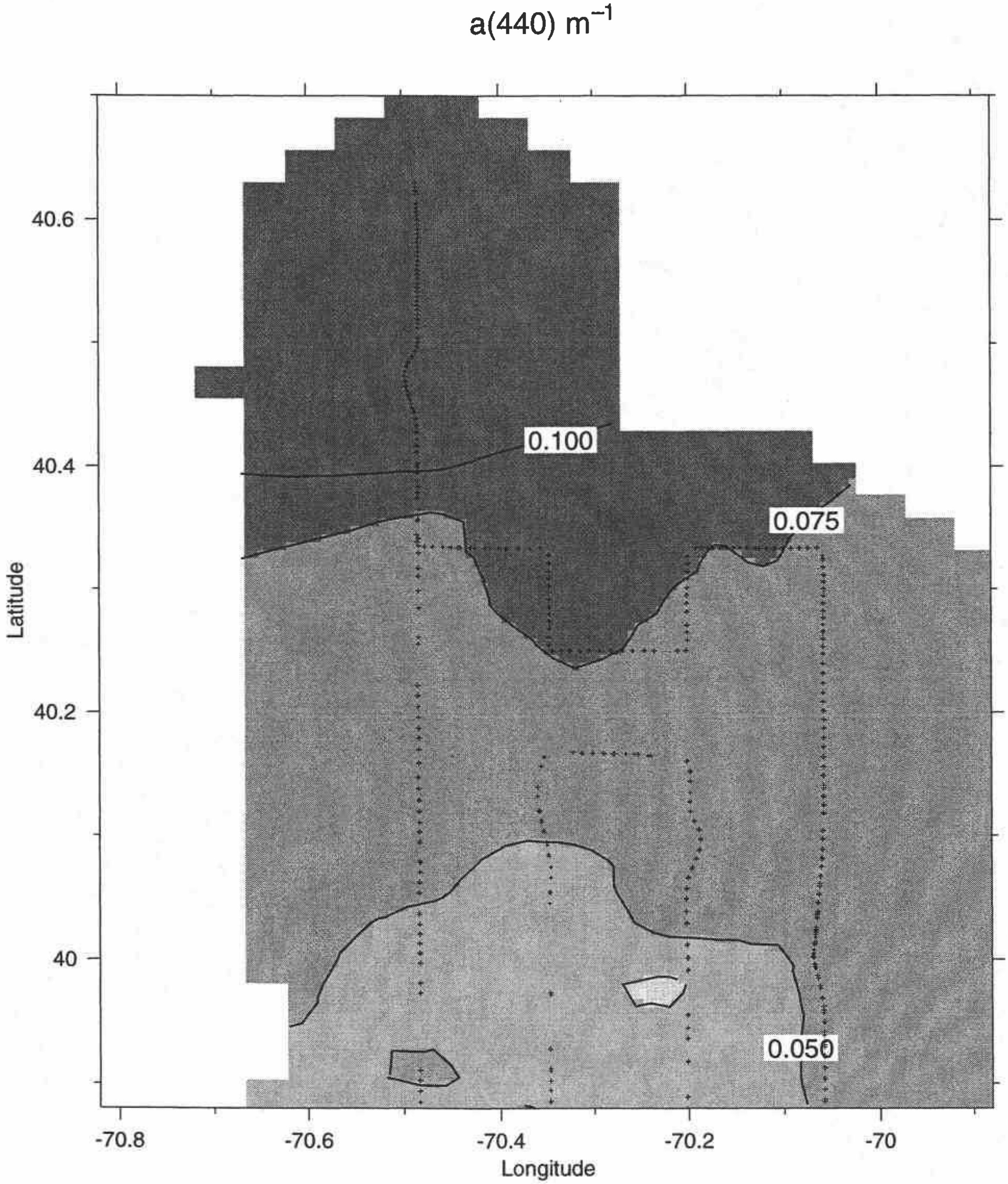

E9608 Bigbox 3

31-Aug-96 05:52 to 01-Sep-96 11:05

Map view at 45 m

a(440) m^{-1}

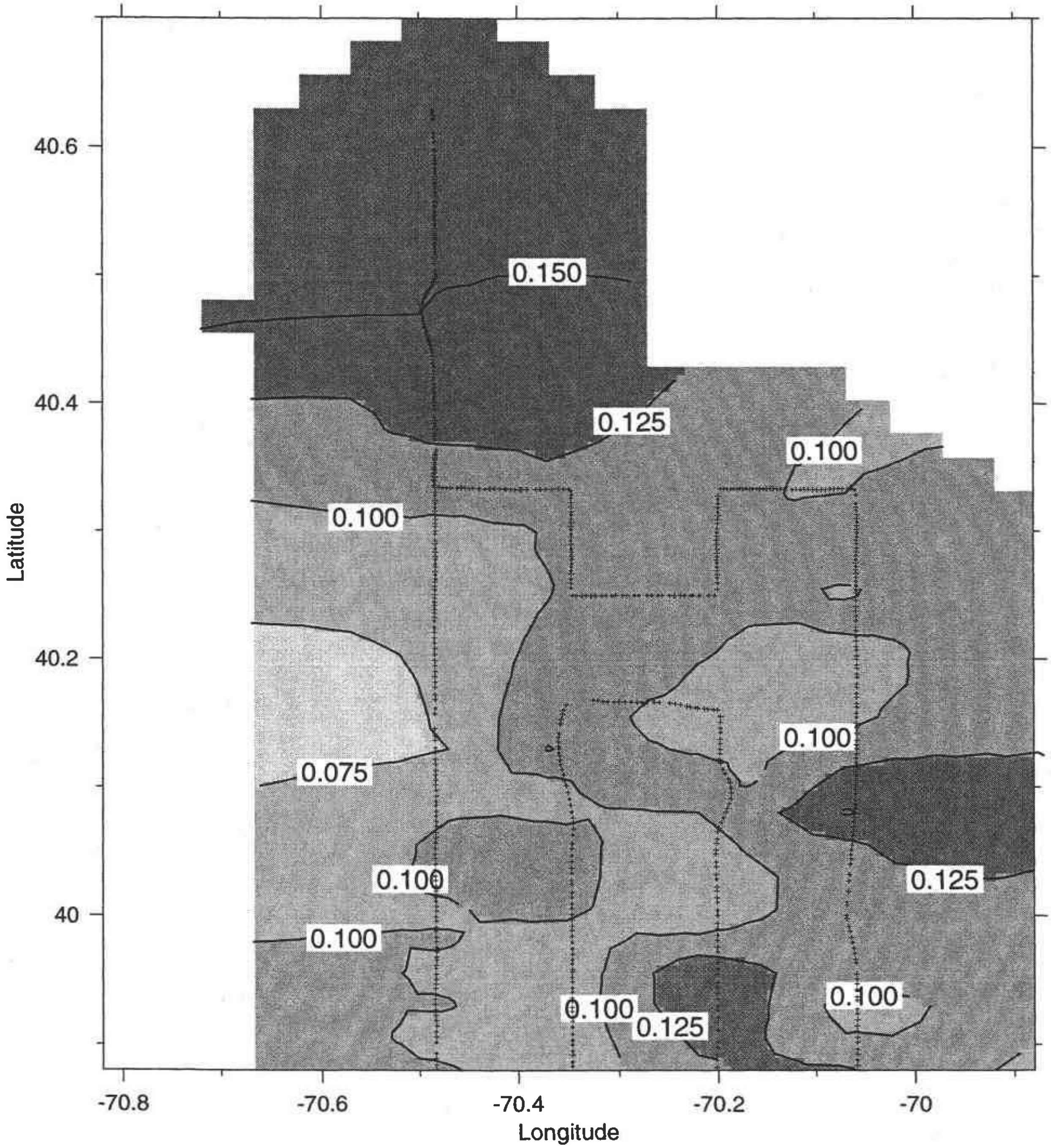

E9608 Bigbox 3

31-Aug-96 05:52 to 01-Sep-96 11:05

Map view at $\sigma_t = 24.6 \pm 0.025$ kg/m^3

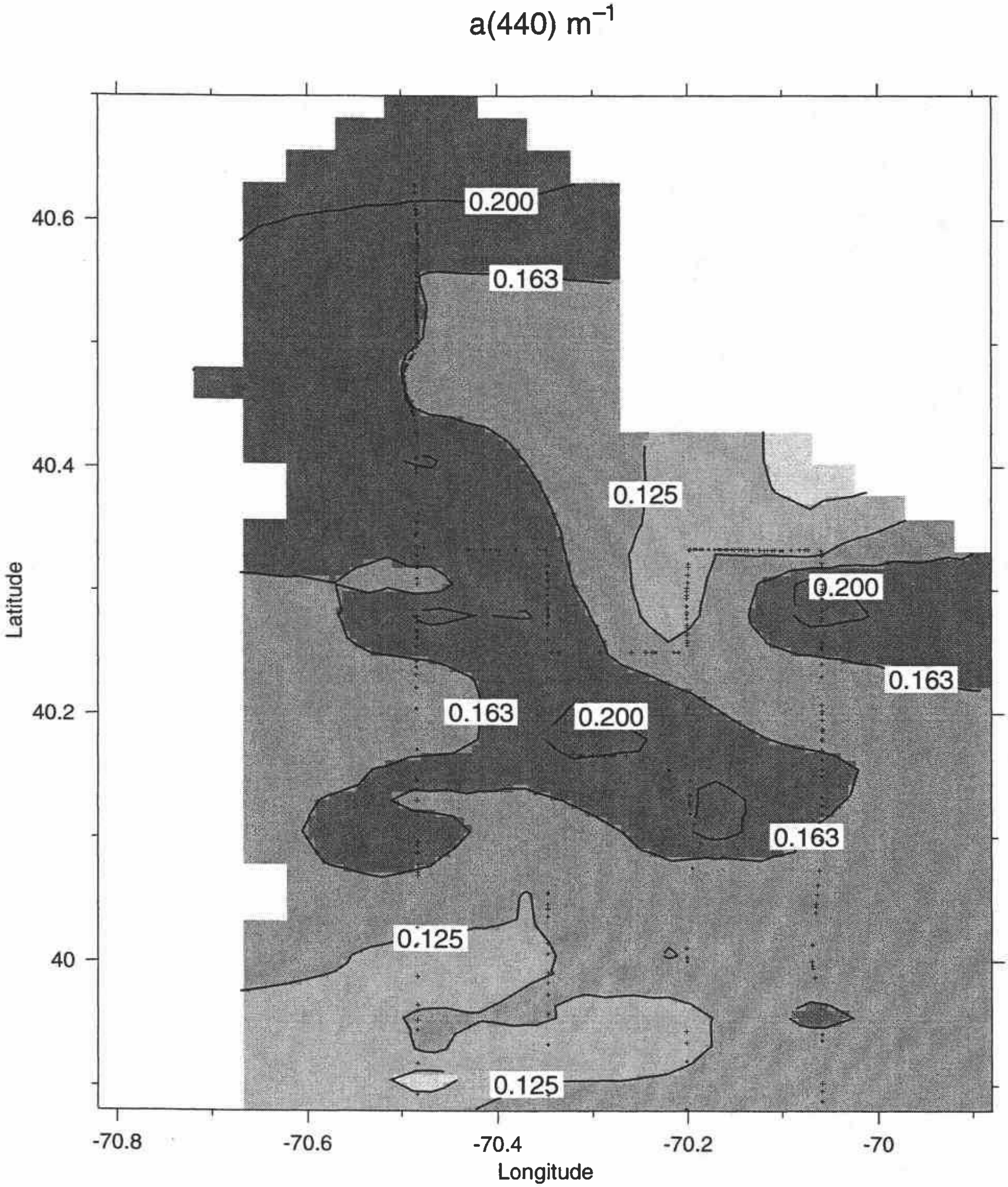

E9608 Bigbox 3

31-Aug-96 05:52 to 01-Sep-96 11:05

Map view at 10 m above bottom

a(440) m^{-1}

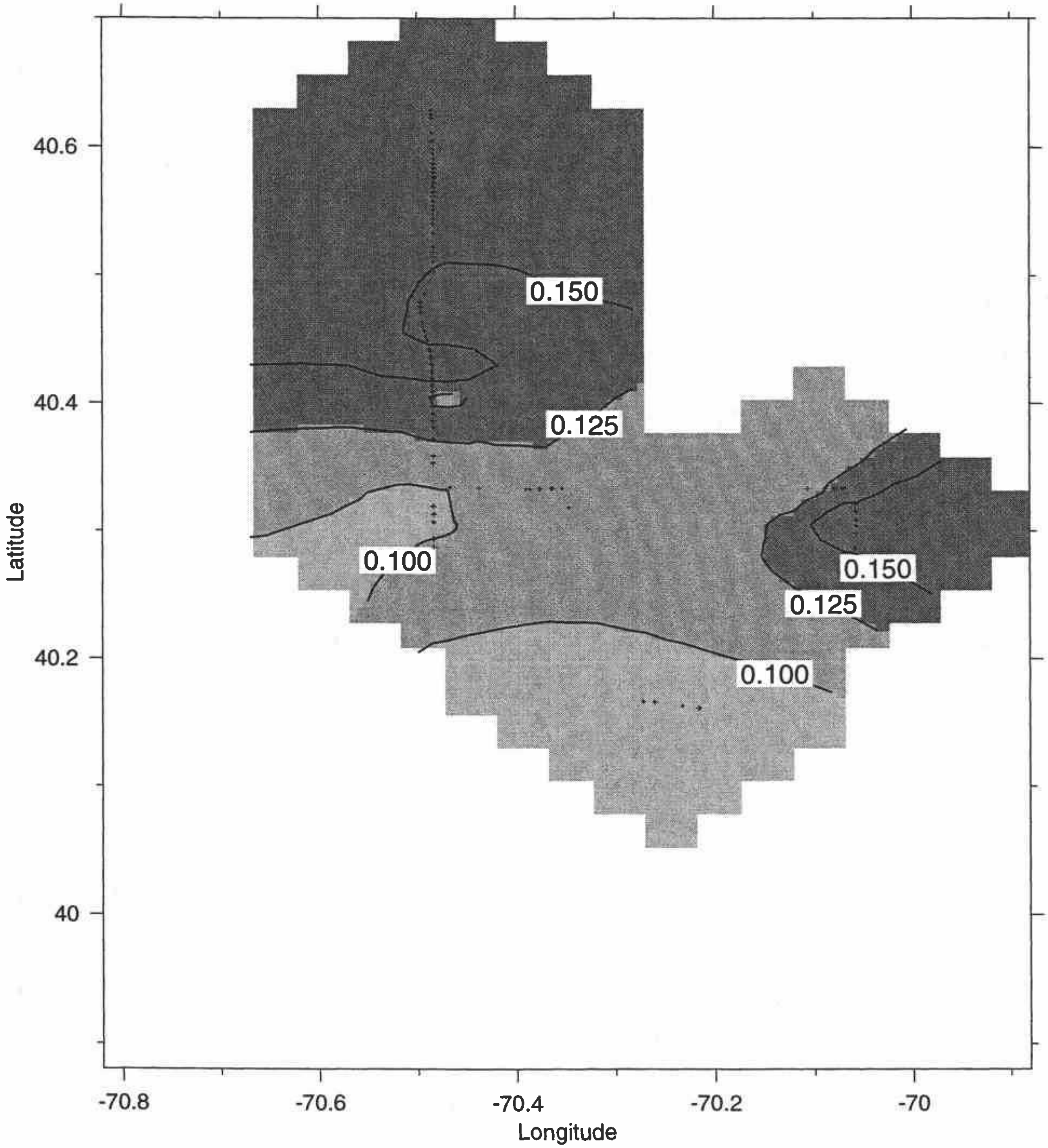

E9608 Bigbox 3

31-Aug-96 05:52 to 01-Sep-96 11:05

Map view at 5 m

c(650) m^{-1}

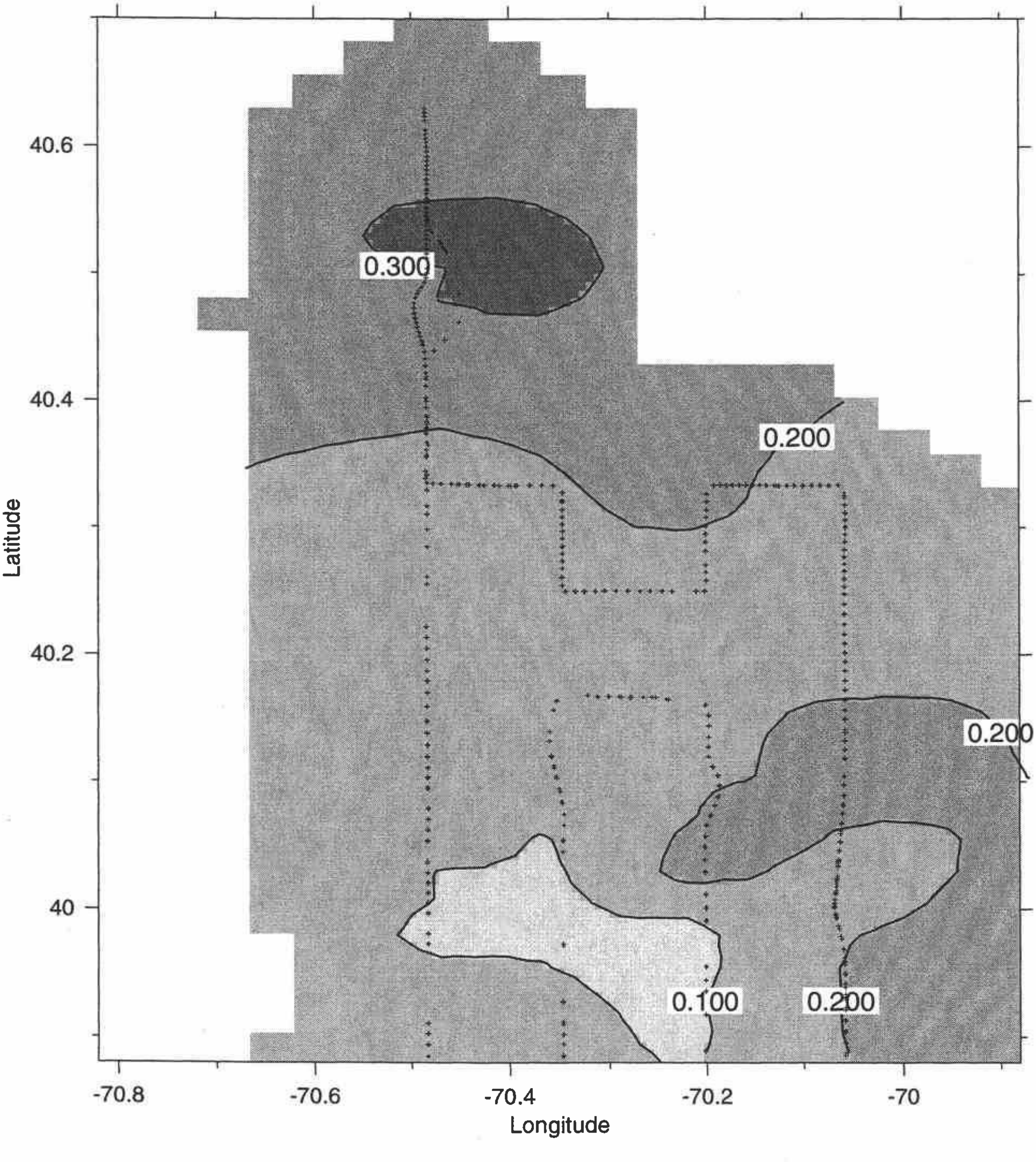

E9608 Bigbox 3

31-Aug-96 05:52 to 01-Sep-96 11:05

Map view at 45 m

c(650) m^{-1}

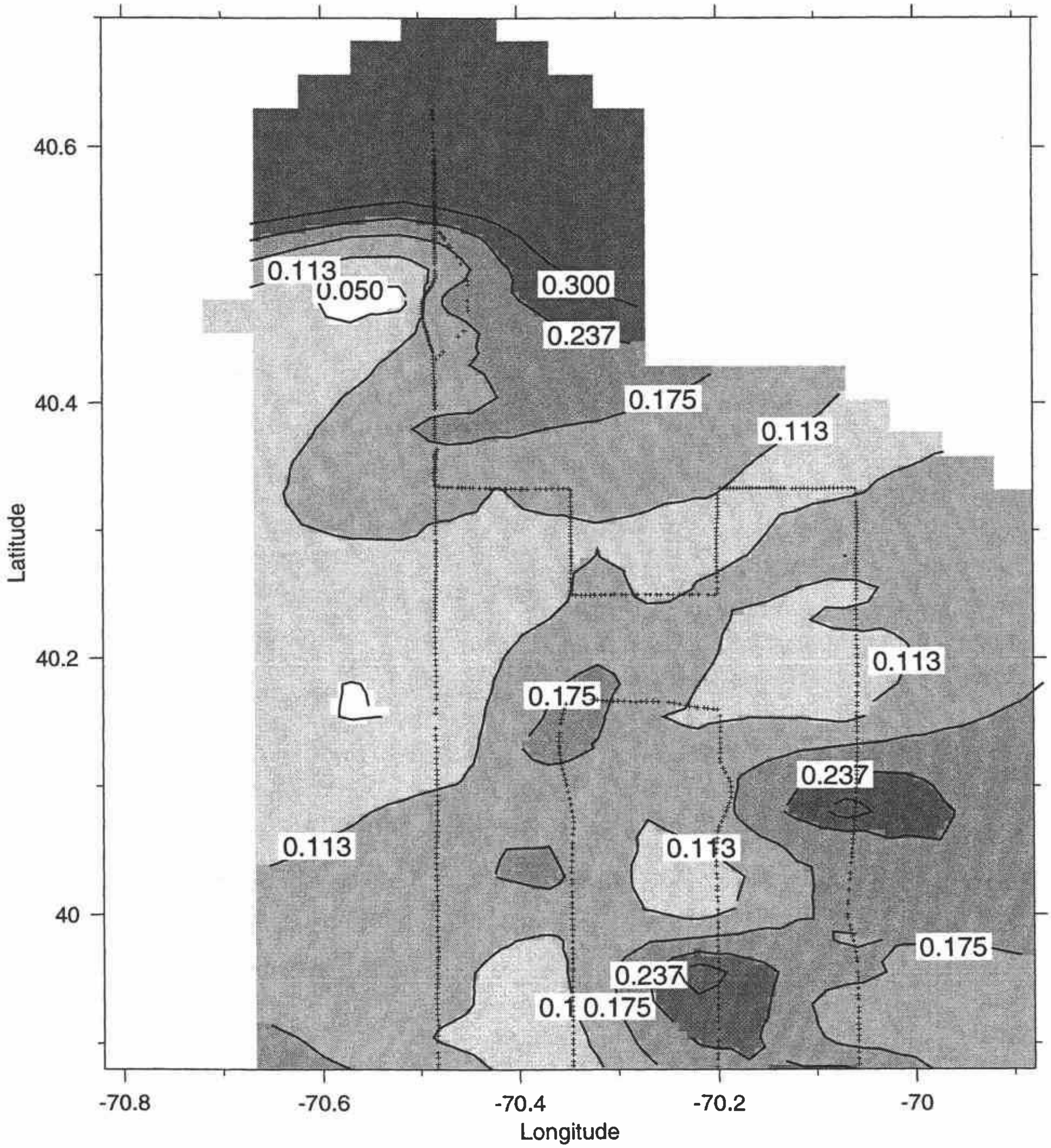

E9608 Bigbox 3

31-Aug-96 05:52 to 01-Sep-96 11:05

Map view at $\sigma_t = 24.6 \pm 0.025$ kg/m^3

c(650) m^{-1}

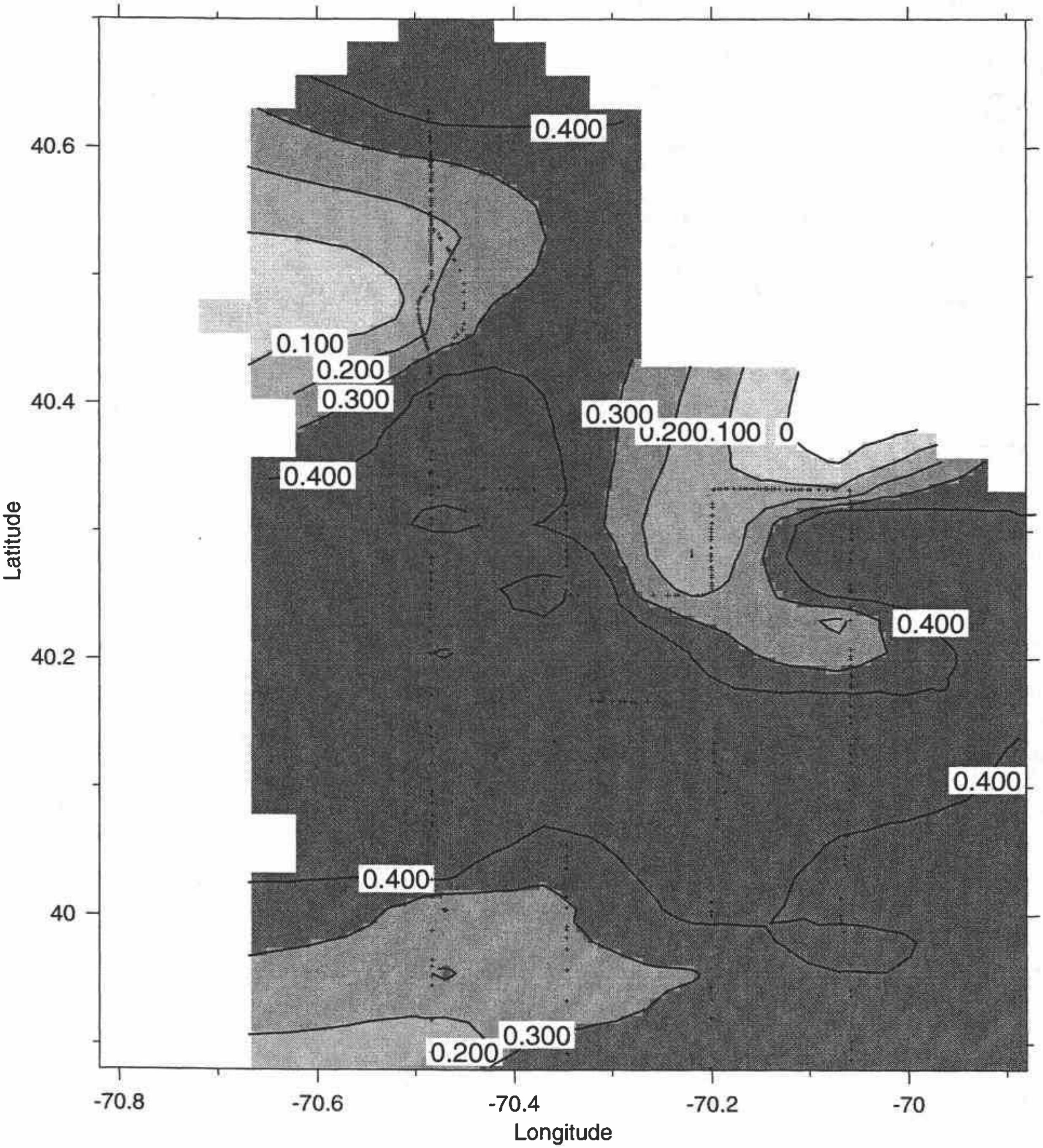

E9608 Bigbox 3

31-Aug-96 05:52 to 01-Sep-96 11:05

Map view at 10 m above bottom

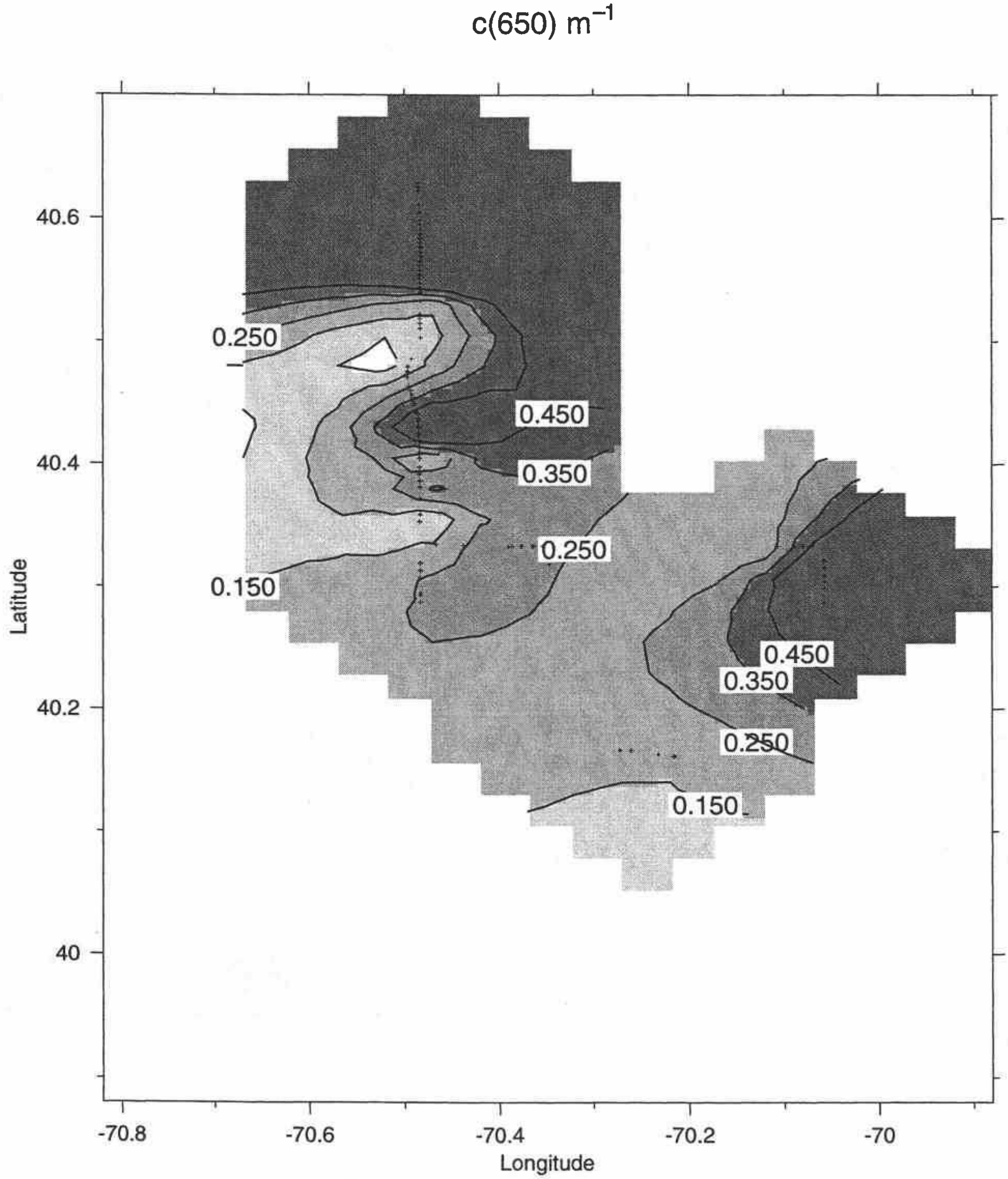

E9608 Smallbox Maps

E9608 Smallbox 1

15-Aug-96 23:26 to 16-Aug-96 15:26

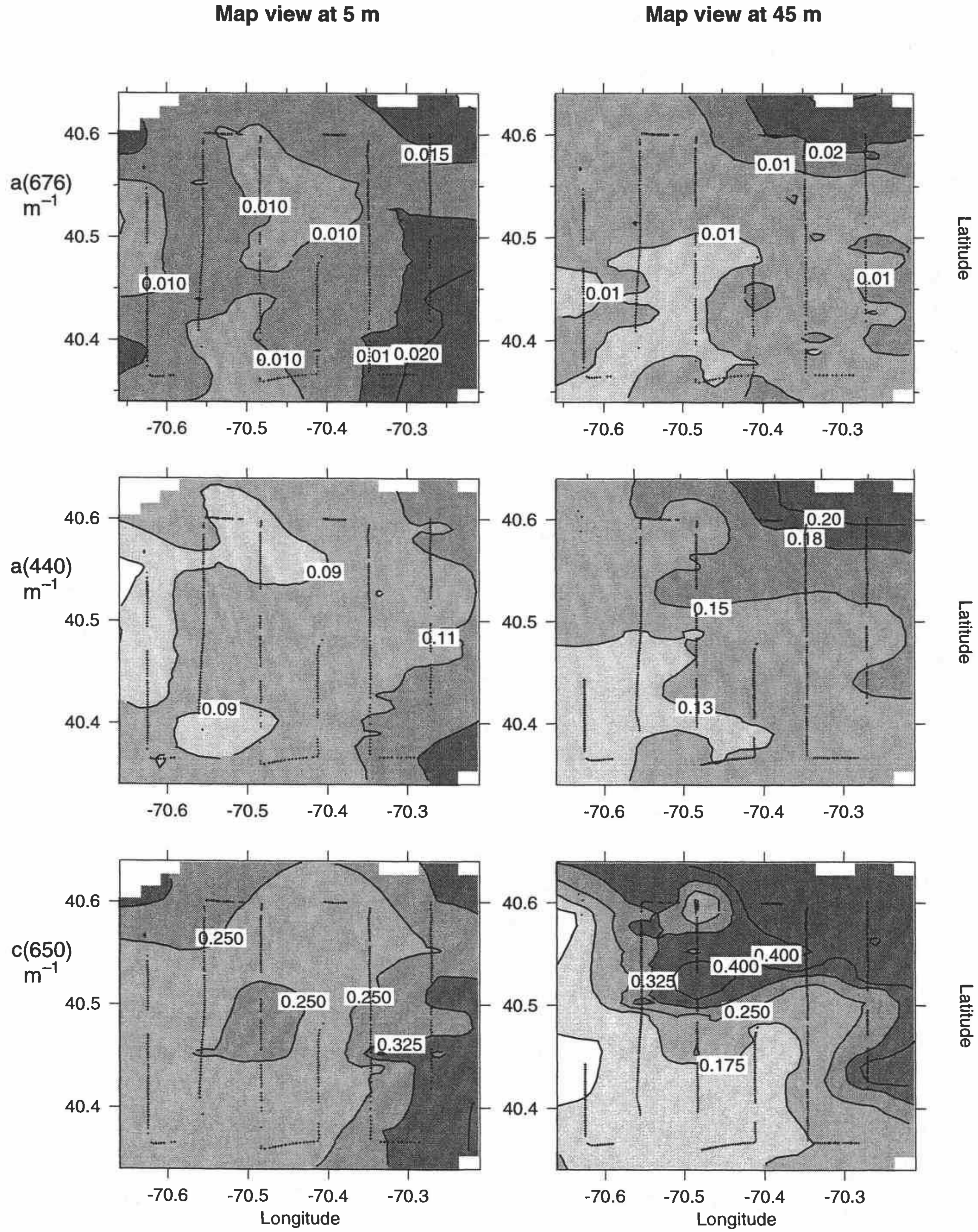

E9608 Smallbox 1

15-Aug-96 23:26 to 16-Aug-96 15:26

Map view at σ_t = 24.6 ± 0.025 kg/m³ **Map view at 10 m above the bottom**

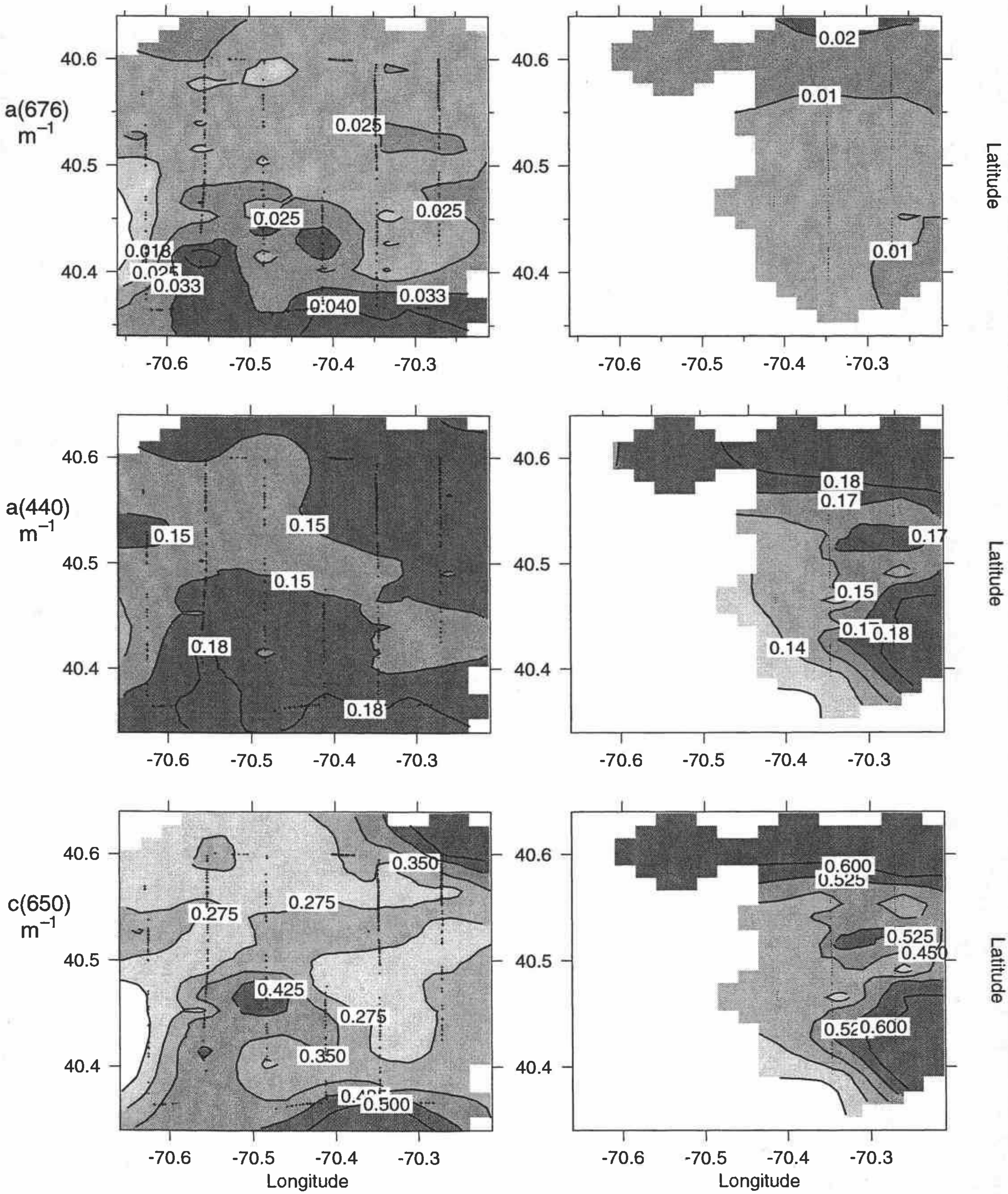

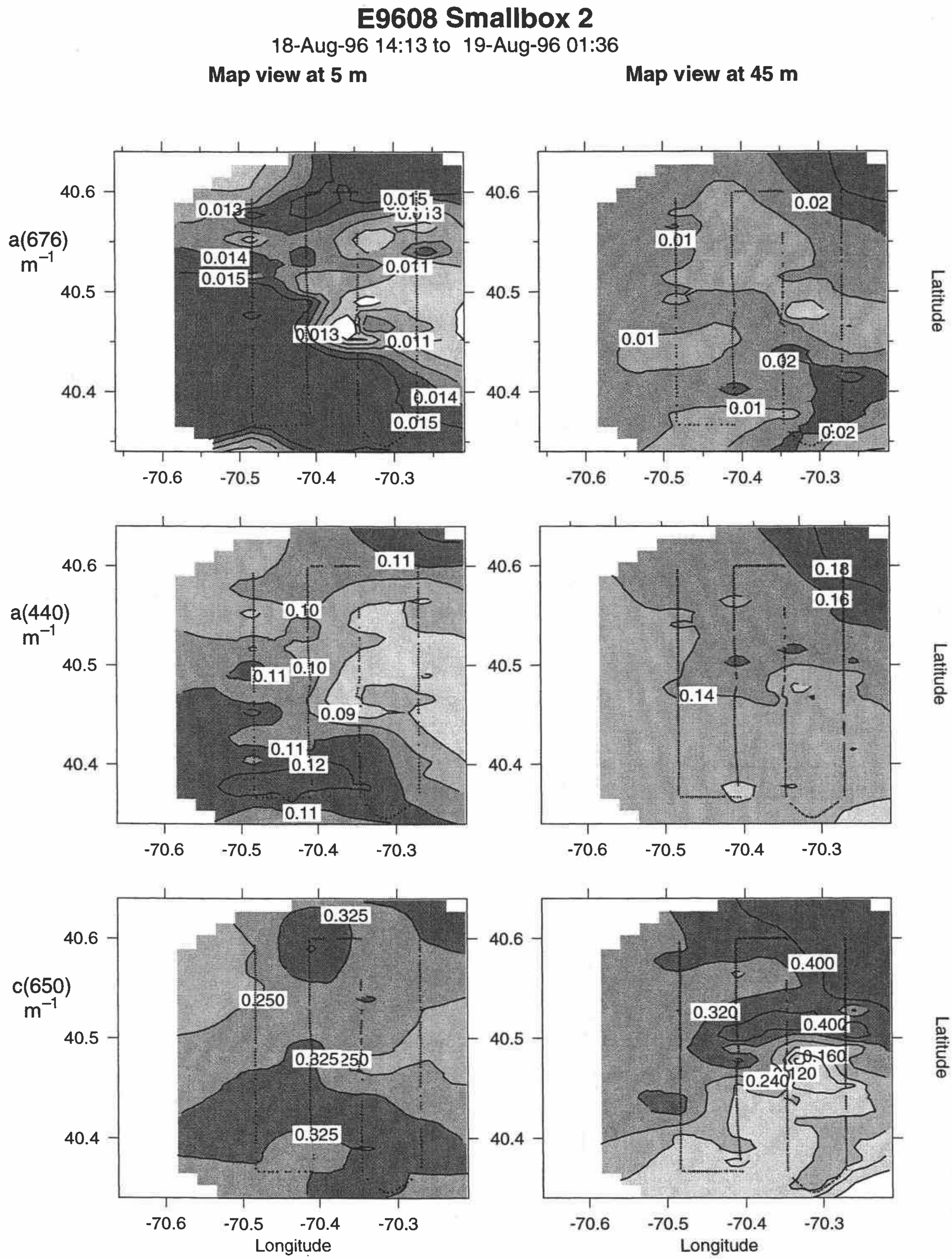
E9608 Smallbox 2
18-Aug-96 14:13 to 19-Aug-96 01:36
Map view at 5 m
Map view at 45 m
a(676) m⁻¹
a(440) m⁻¹
c(650) m⁻¹
Latitude
Longitude
40.6
40.5
40.4
-70.6
-70.5
-70.4
-70.3
0.013
0.015
0.014
0.011
0.01
0.02
0.11
0.10
0.09
0.12
0.18
0.16
0.14
0.325
0.250
0.400
0.320
0.160
0.240
120

E9608 Smallbox 2

18-Aug-96 14:13 to 19-Aug-96 01:36

Map view at $\sigma_t = 24.6 \pm 0.025$ kg/m^3 **Map view at 10 m above the bottom**

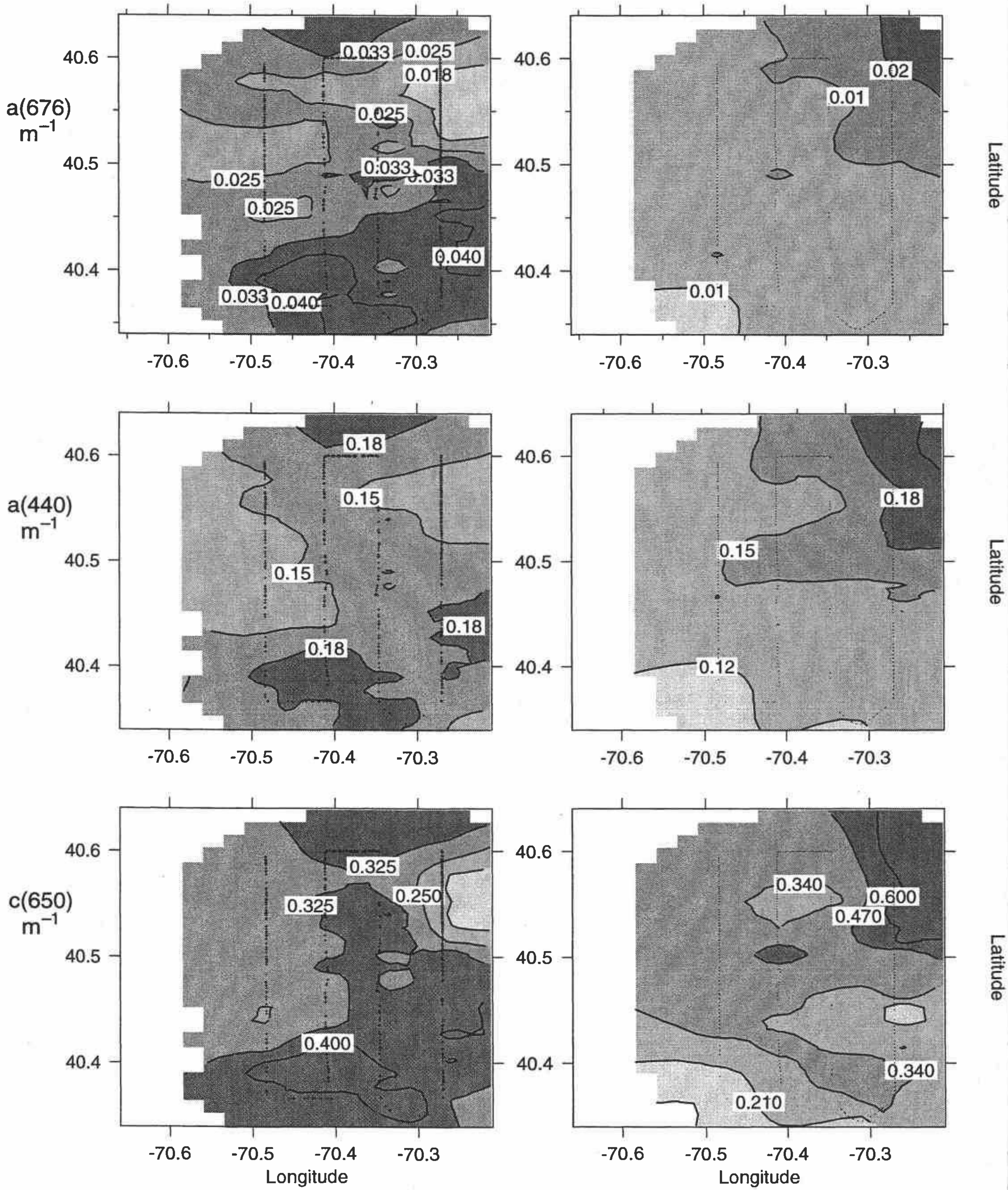

E9608 Smallbox 3

20-Aug-96 01:41 to 20-Aug-96 14:32

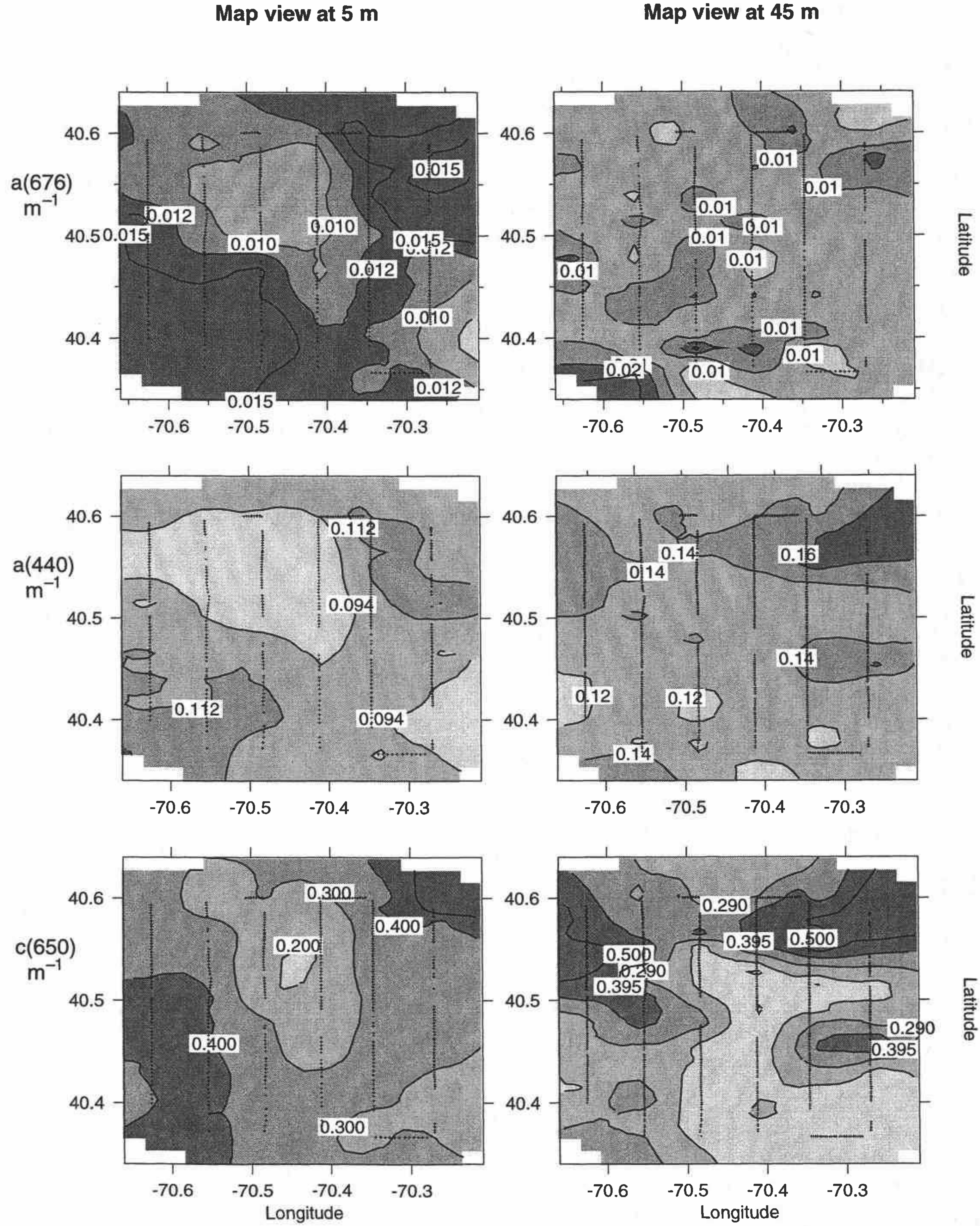

E9608 Smallbox 3

20-Aug-96 01:41 to 20-Aug-96 14:32

Map view at $\sigma_t = 24.6 \pm 0.025$ kg/m^3 **Map view at 10 m above the bottom**

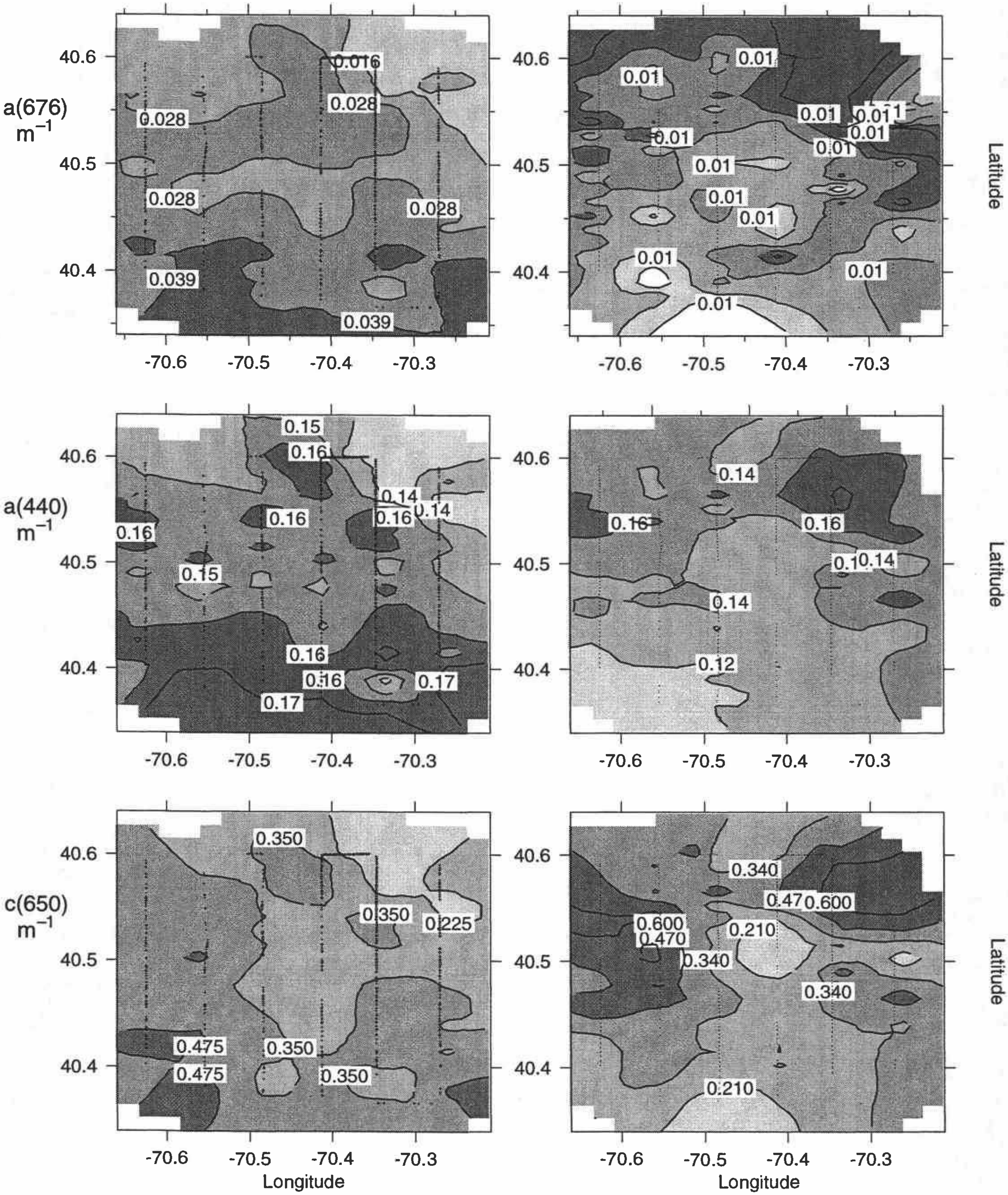

E9608 Smallbox 4

24-Aug-96 20:05 to 25-Aug-96 11:34

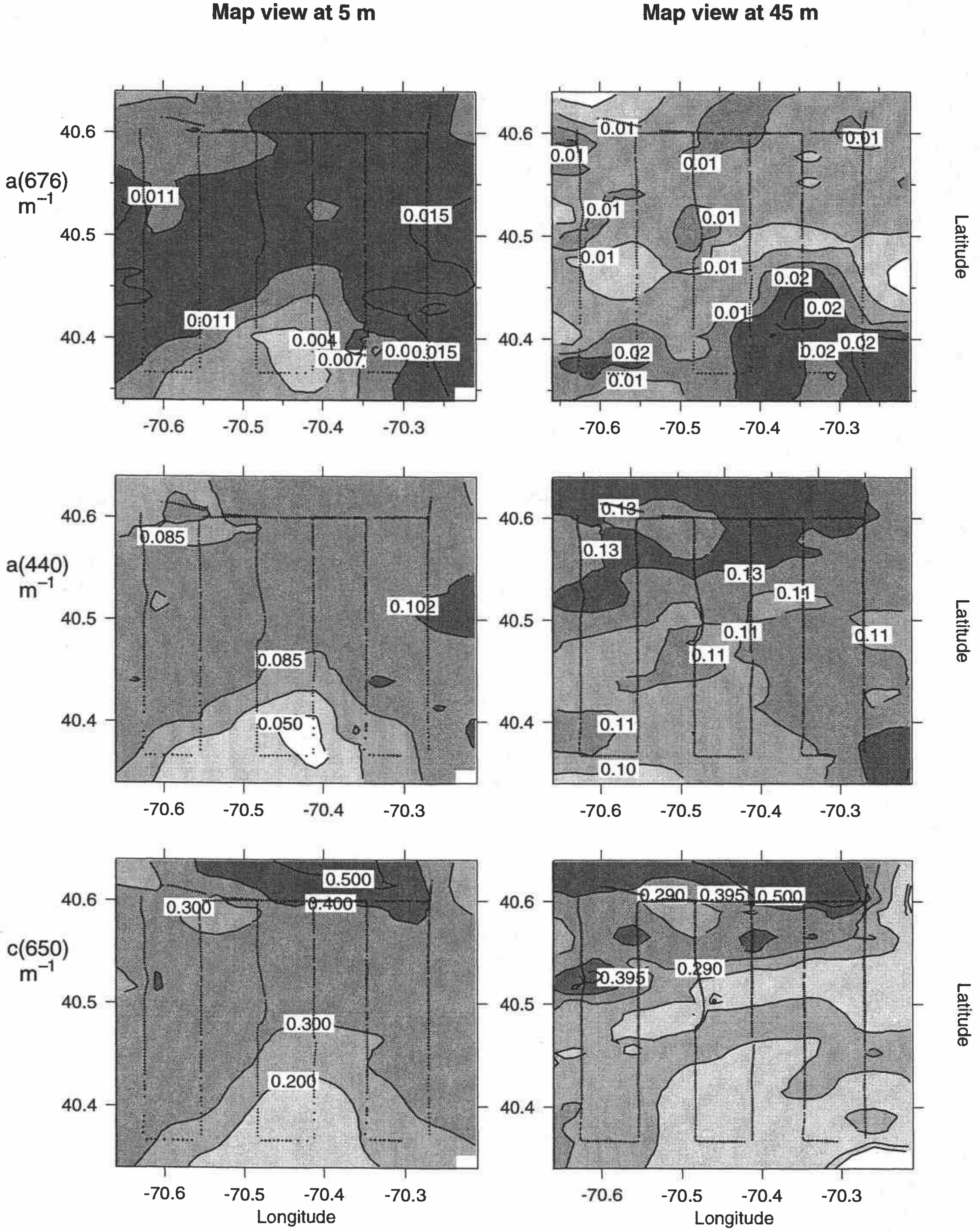

E9608 Smallbox 4

24-Aug-96 20:05 to 25-Aug-96 11:34

Map view at $\sigma_t = 24.6 \pm 0.025$ kg/m^3 | **Map view at 10 m above the bottom**

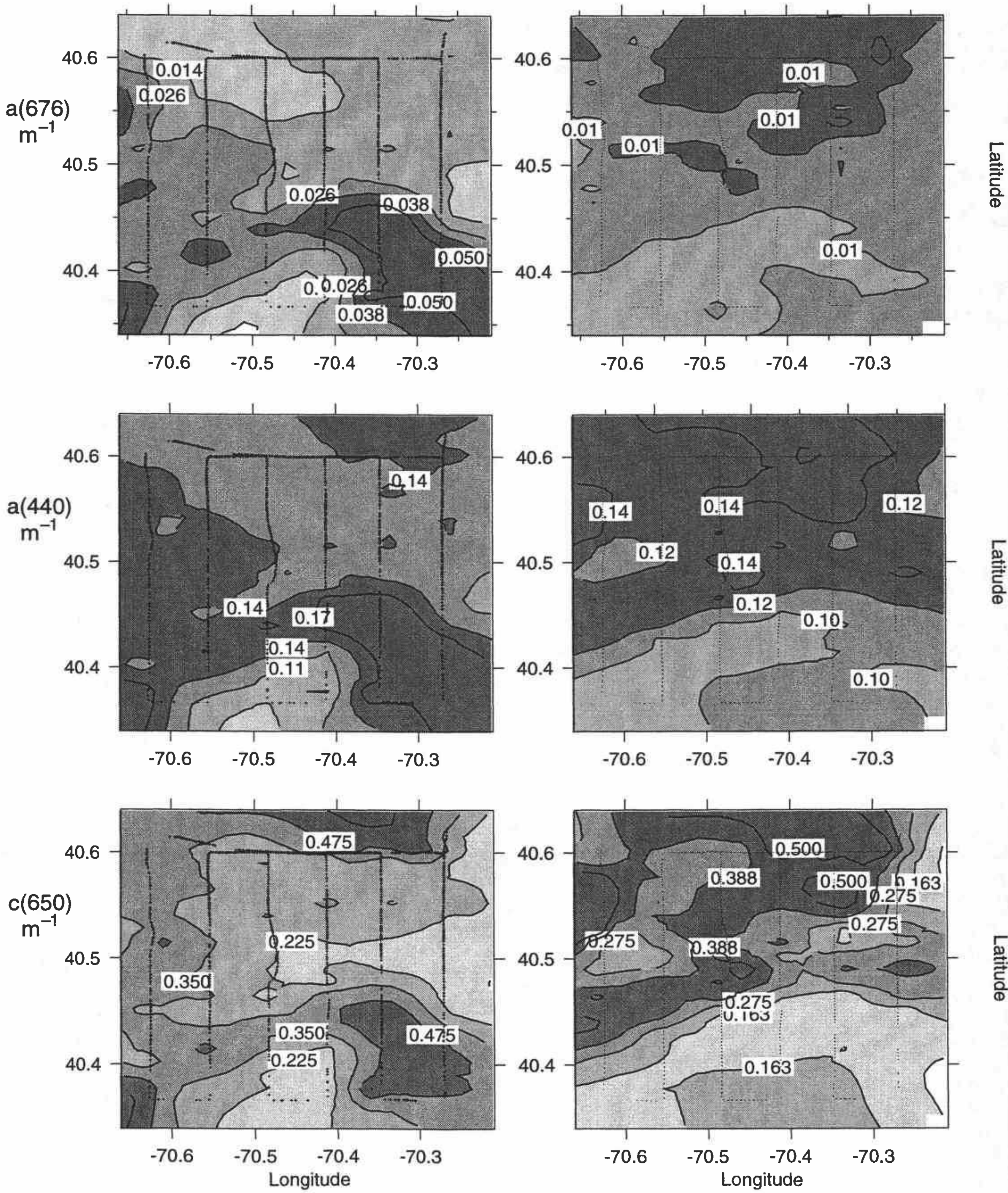

E9608 Smallbox 5

25-Aug-96 23:15 to 26-Apr-96 01:05

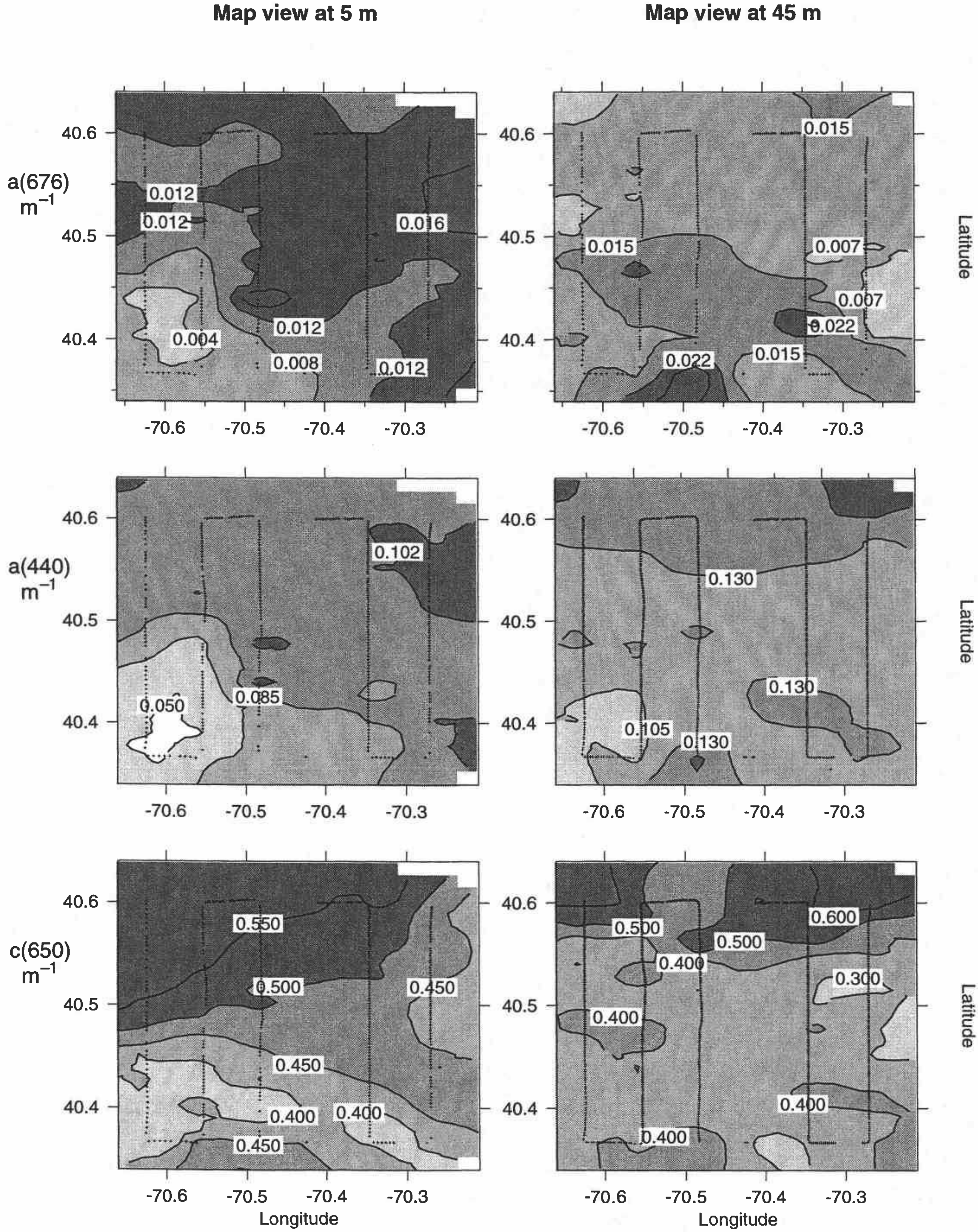

E9608 Smallbox 5

25-Aug-96 23:15 to 26-Aug-96 01:05

Map view at $\sigma_t = 24.6 \pm 0.025$ kg/m^3 **Map view at 10 m above the bottom**

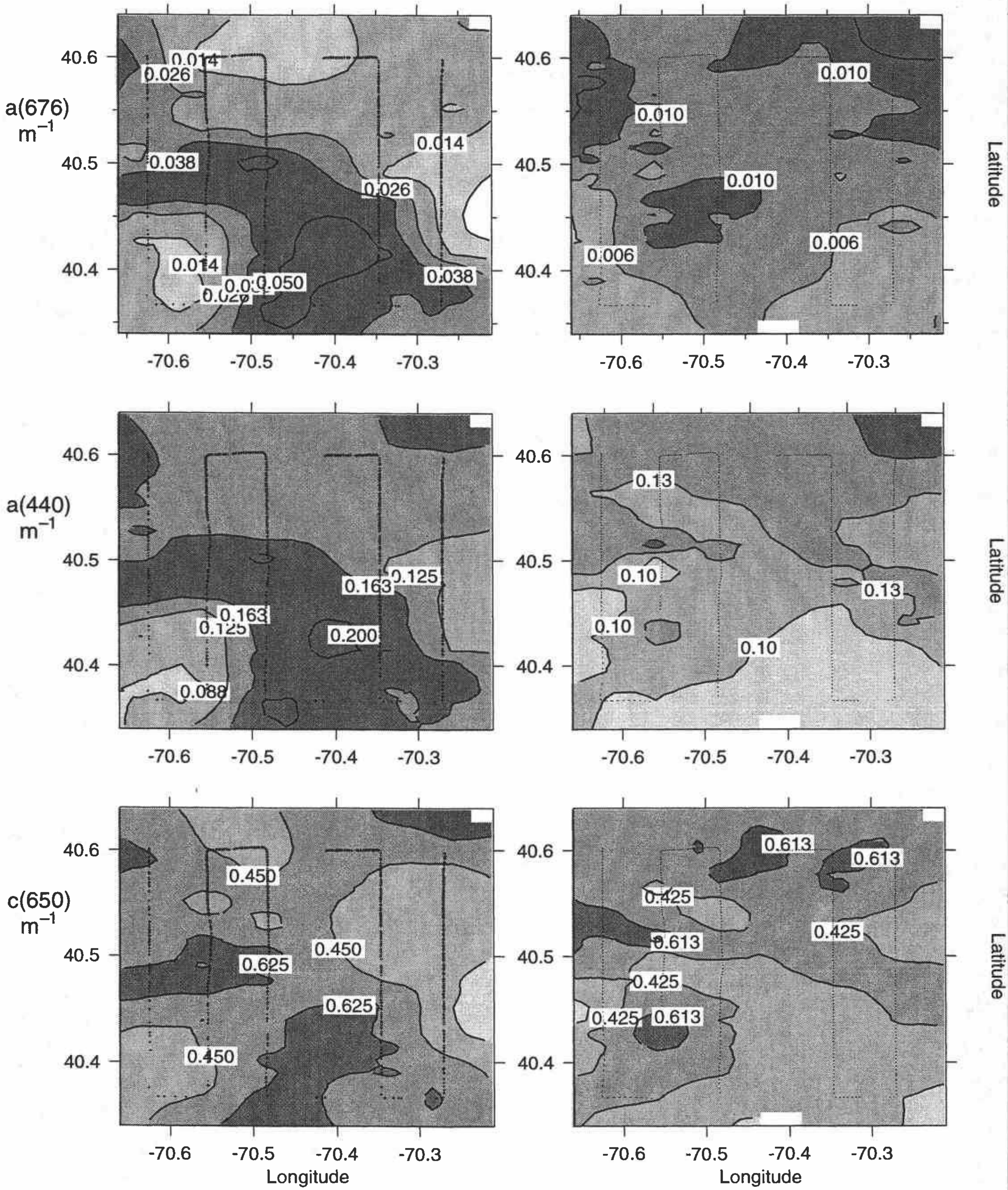

E9608 Smallbox 6

26-Aug-96 14:48 to 26-Aug-96 04:55

Map view at 5 m **Map view at 45 m**

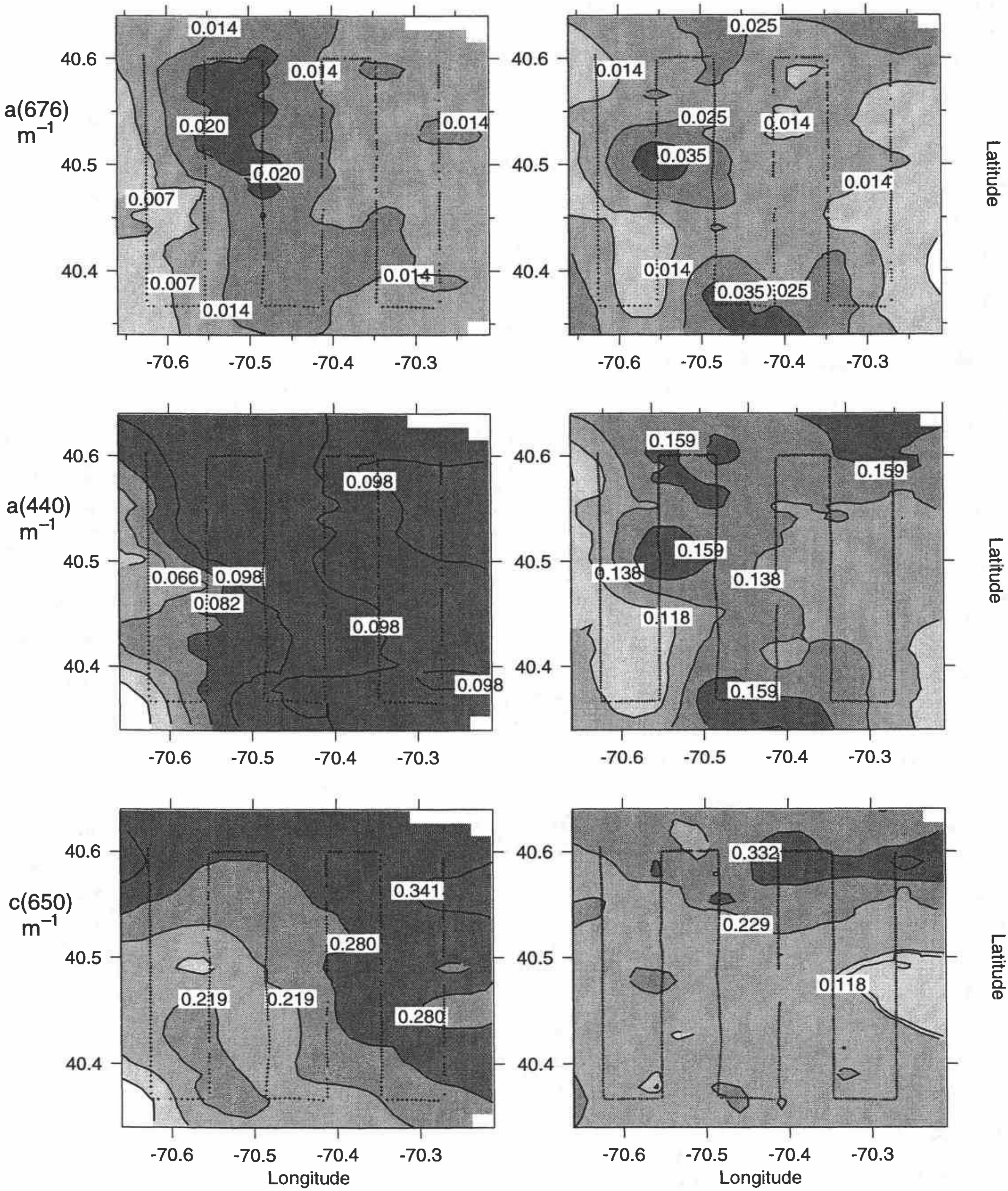

E9608 Smallbox 6

26-Aug-96 03:11 to 26-Aug-96 16:52

Map view at $\sigma_t = 24.6 \pm 0.025$ kg/m^3 **Map view at 10 m above the bottom**

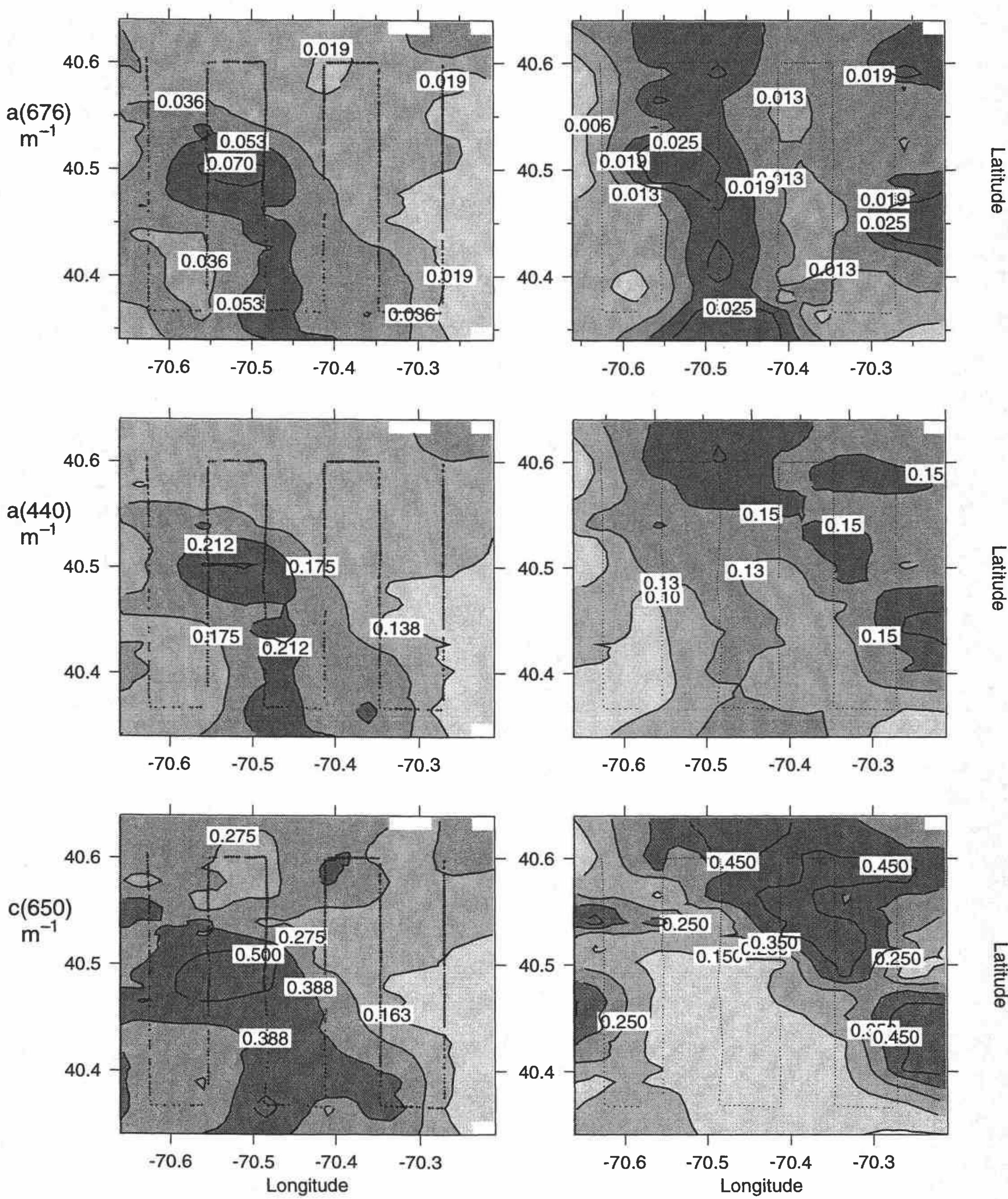

E9608 Smallbox 7

29-Aug-96 05:52 to 29-Aug-96 16:42

Map view at 5 m **Map view at 45 m**

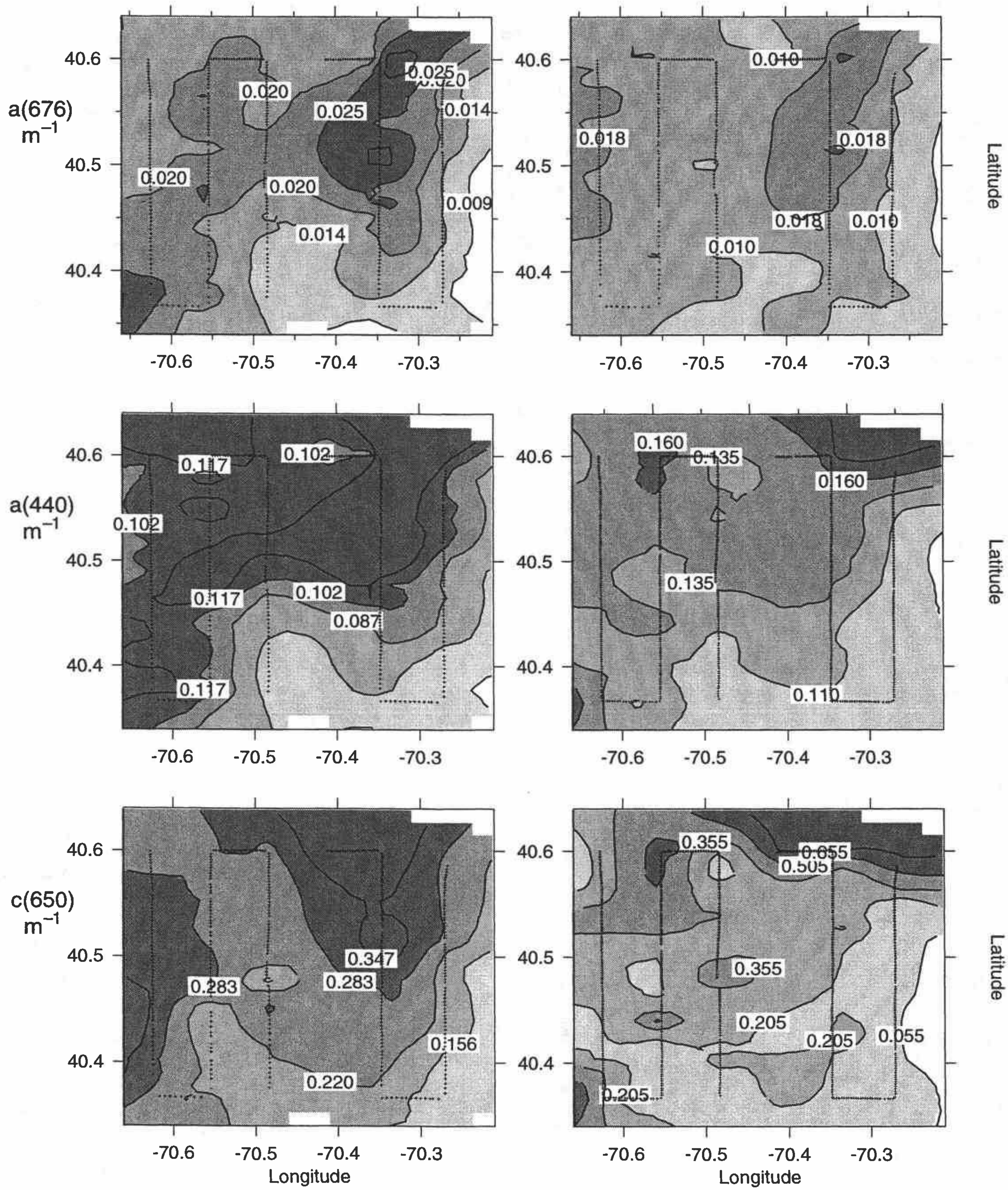

E9608 Smallbox 7

29-Aug-96 04:00 to 29-Aug-96 18:50

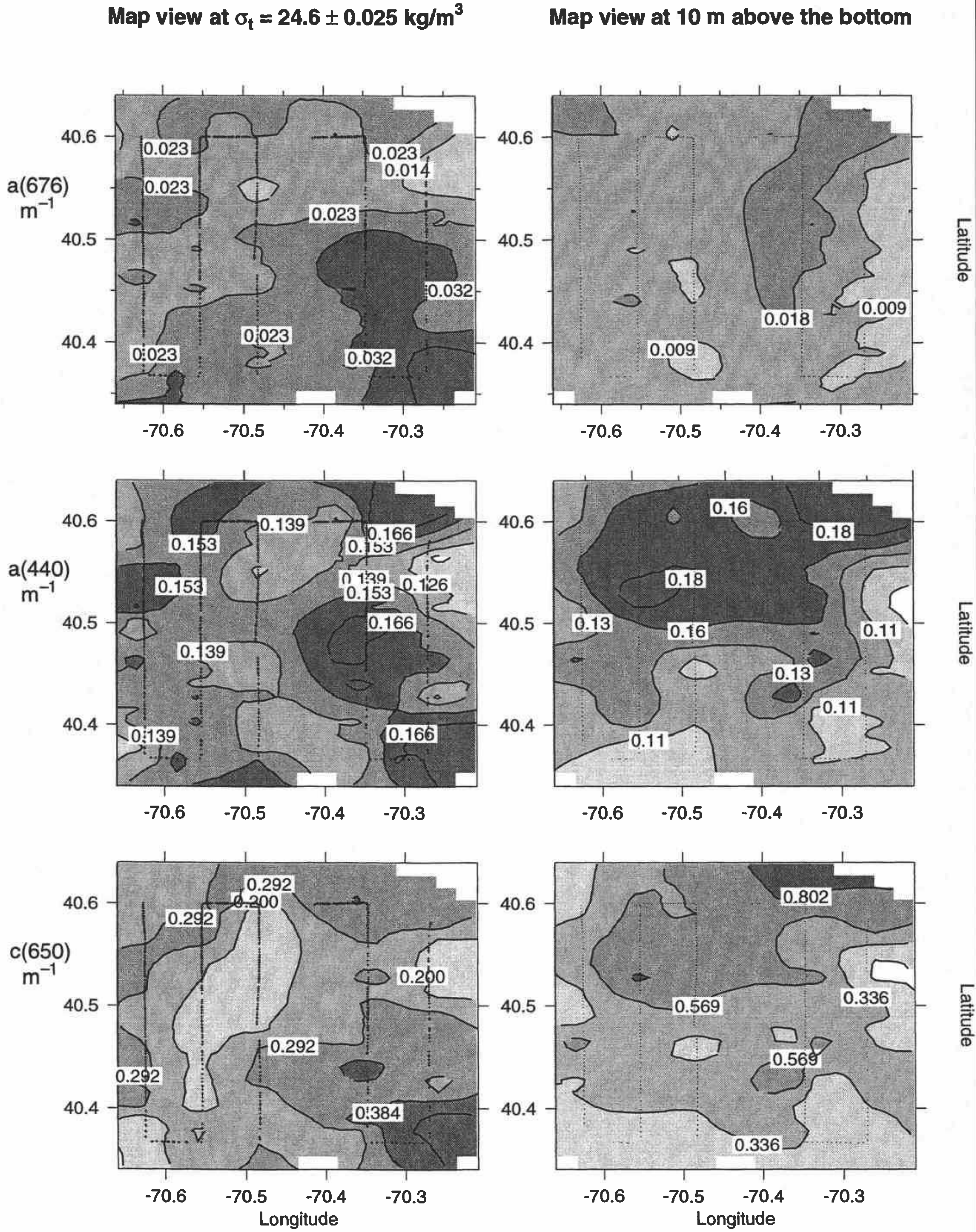

E9608 Smallbox 8

30-Aug-96 10:07 to 29-Aug-96 21:55

Map view at 5 m **Map view at 45 m**

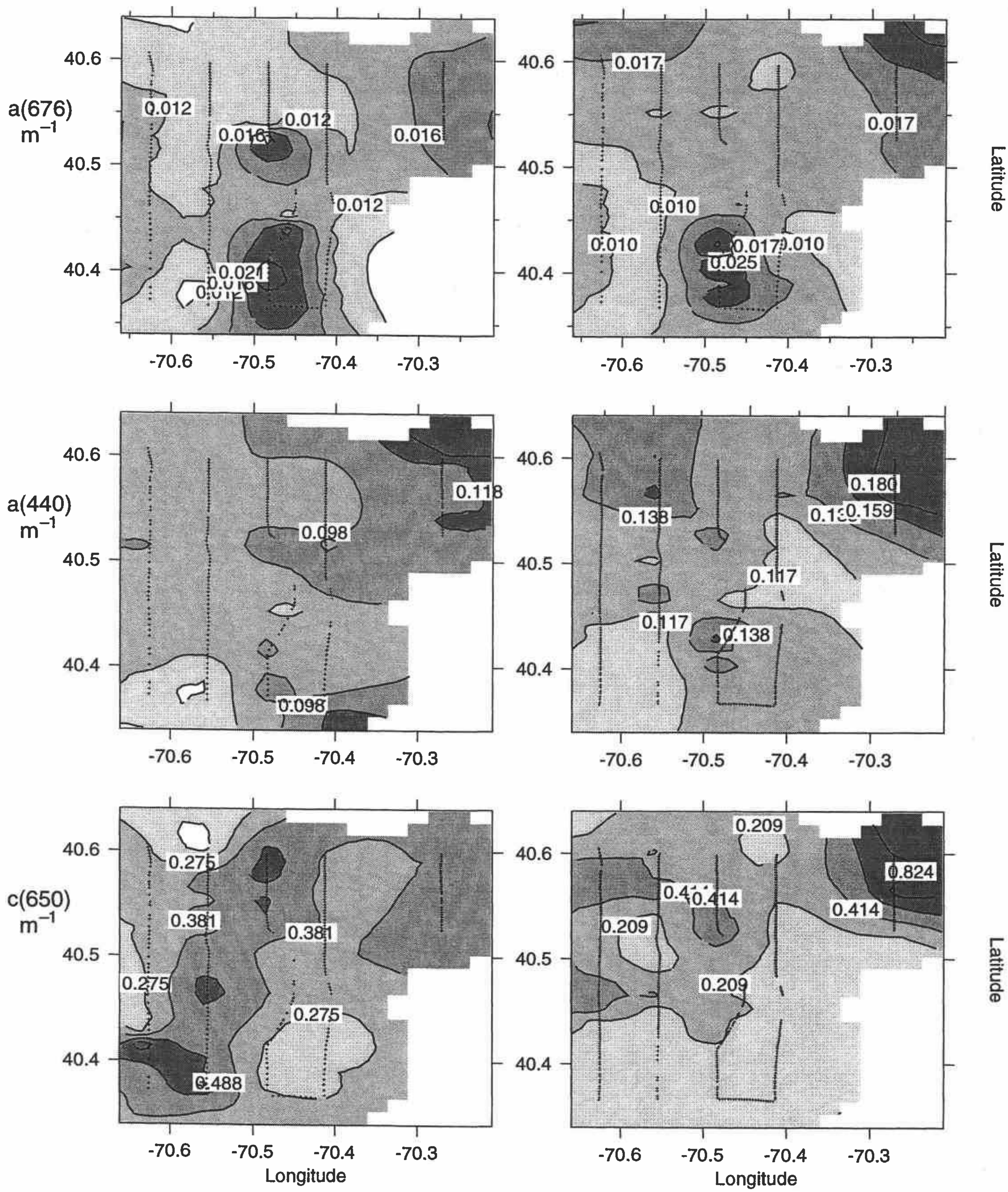

E9608 Smallbox 8

30-Aug-96 10:07 to 30-Aug-96 12:10

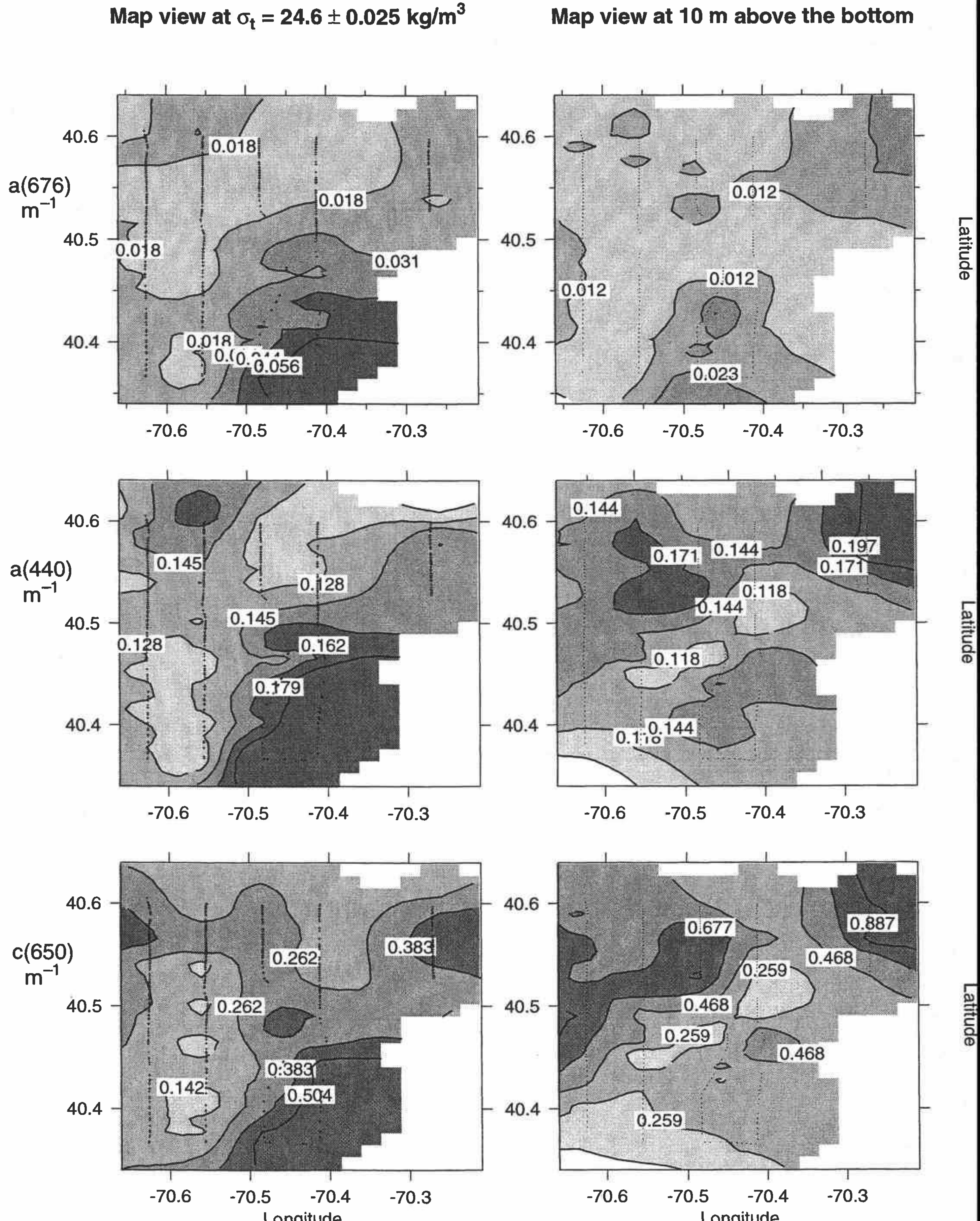

E9608 Smallbox 9

31-Aug-96 02:58 to 31-Aug-96 05:48

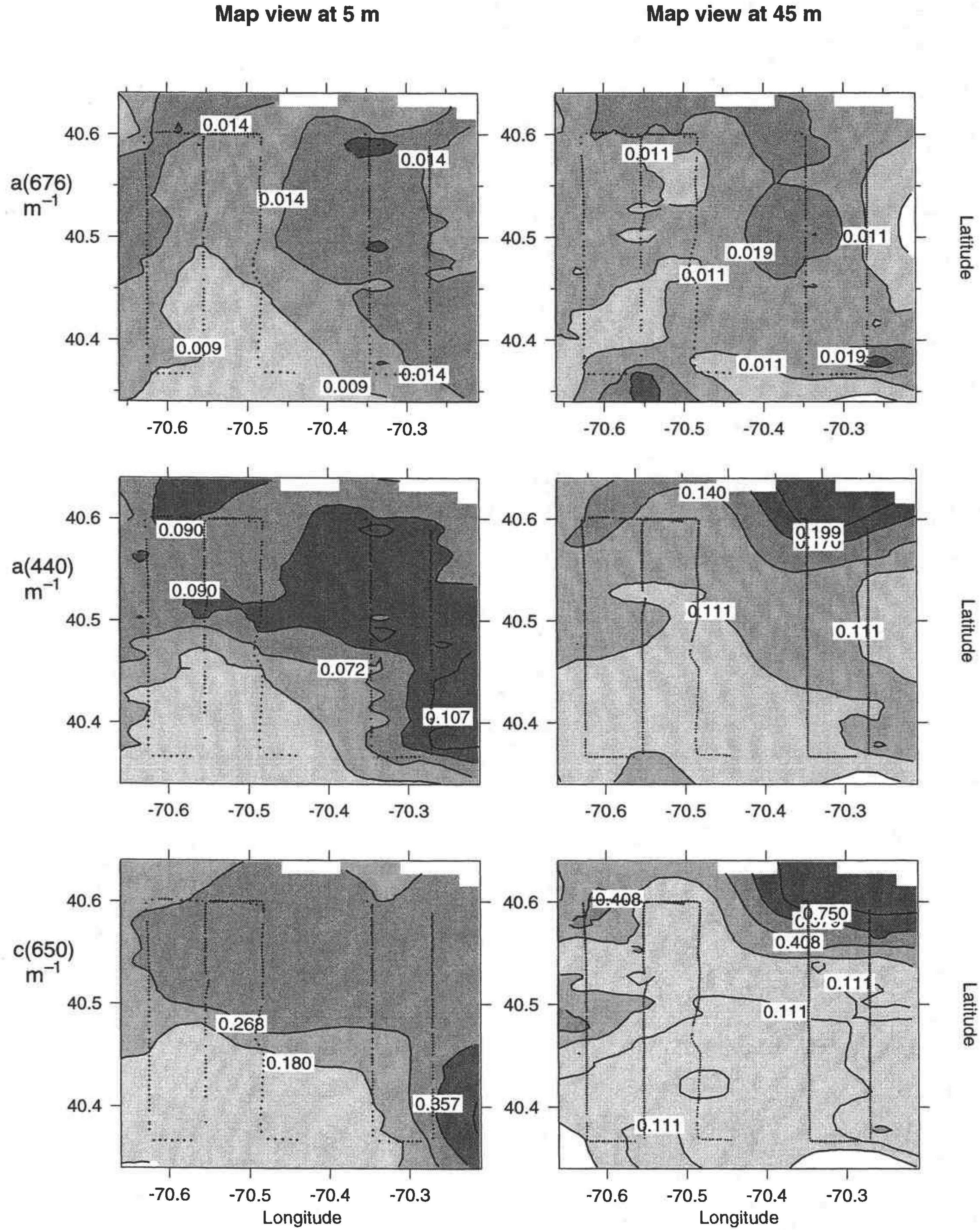

E9608 Smallbox 9

30-Aug-96 14:52 to 31-Aug-96 05:48

Map view at $\sigma_t = 24.6 \pm 0.025$ kg/m^3 | **Map view at 10 m above the bottom**

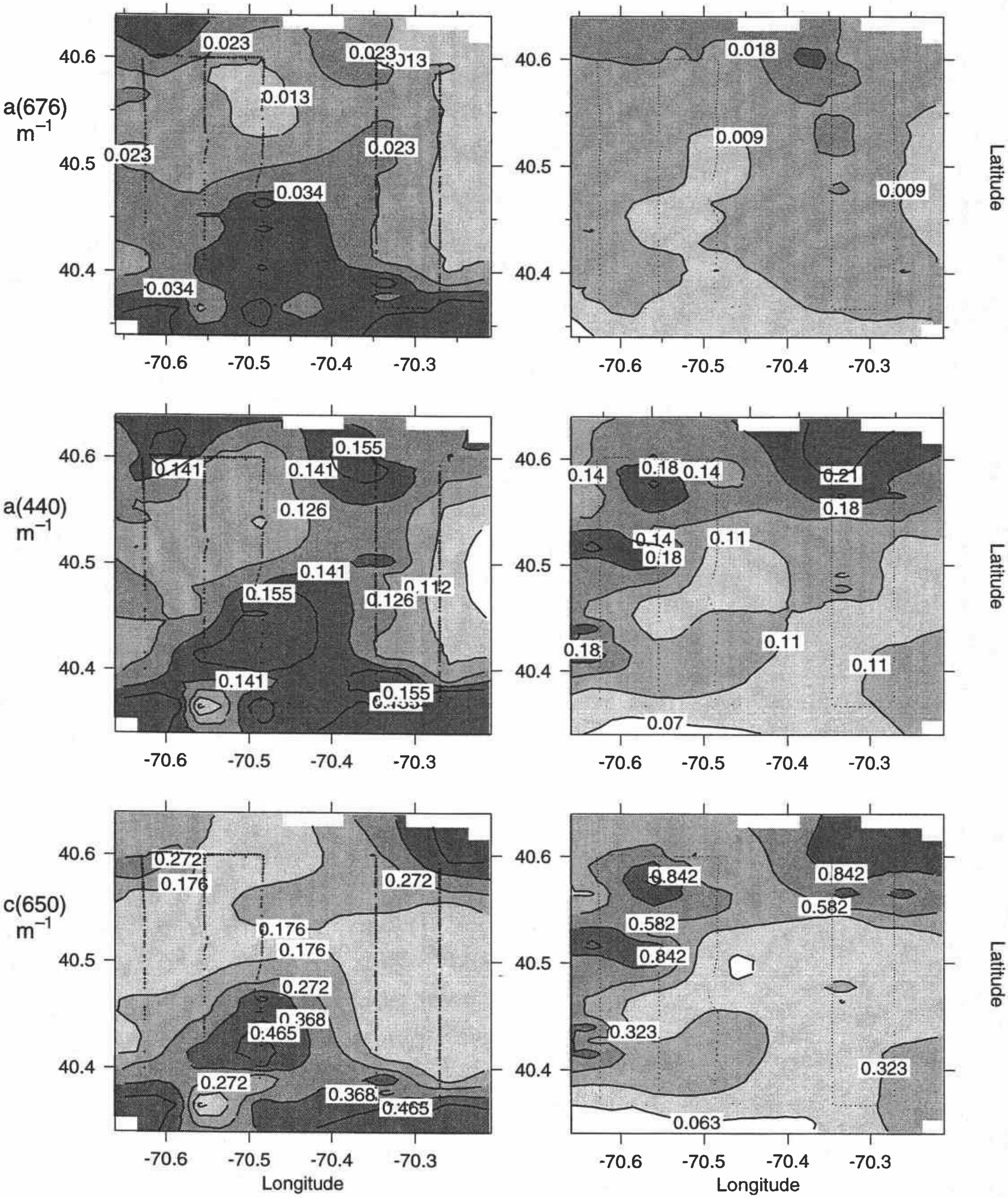

E9608 Bigbox Sections

E9608 Bigbox 1

Line B 70.6249°W

18-Aug-96 01:28 to 18-Aug-96 05:21

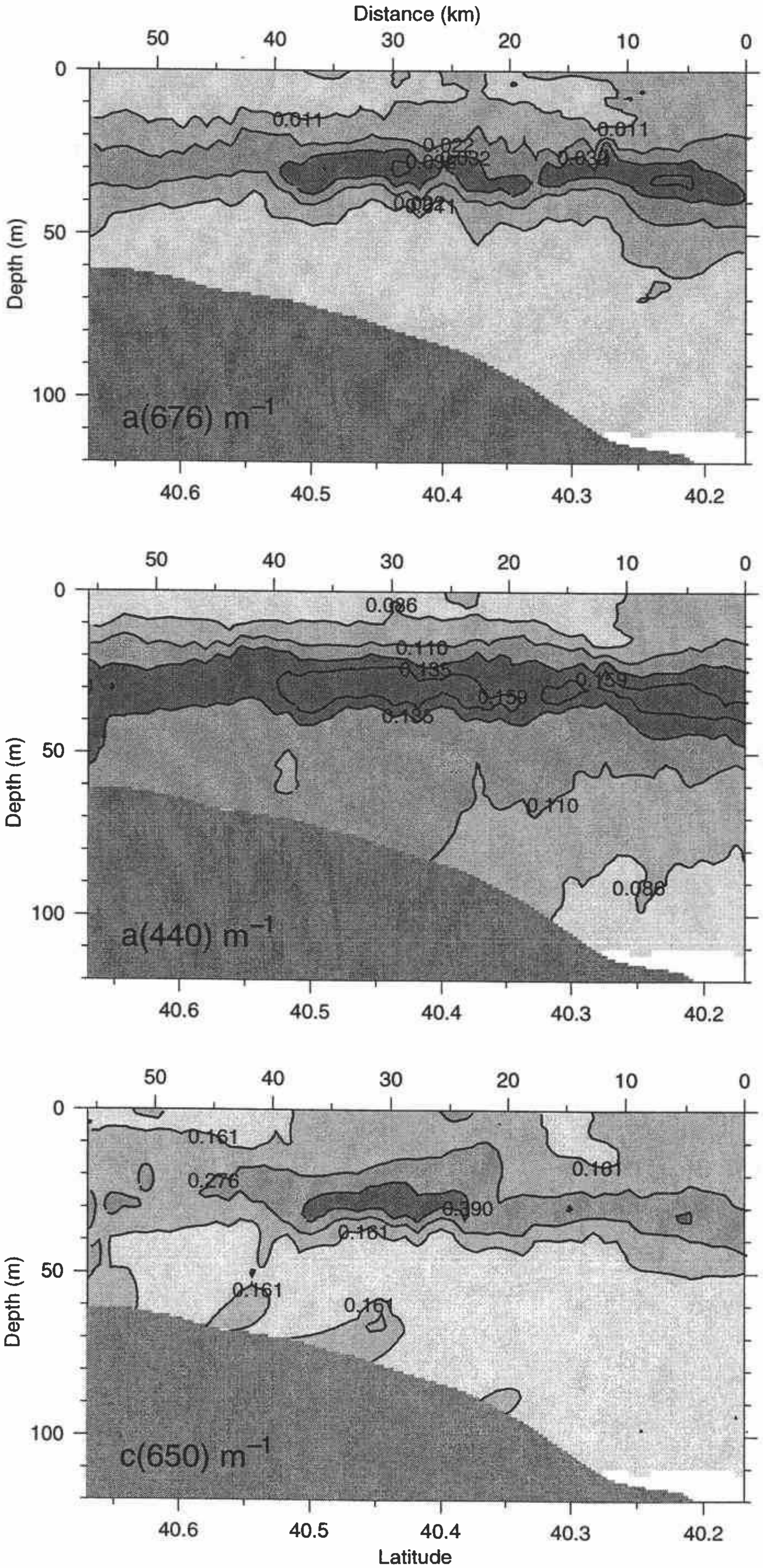

E9608 Bigbox 1

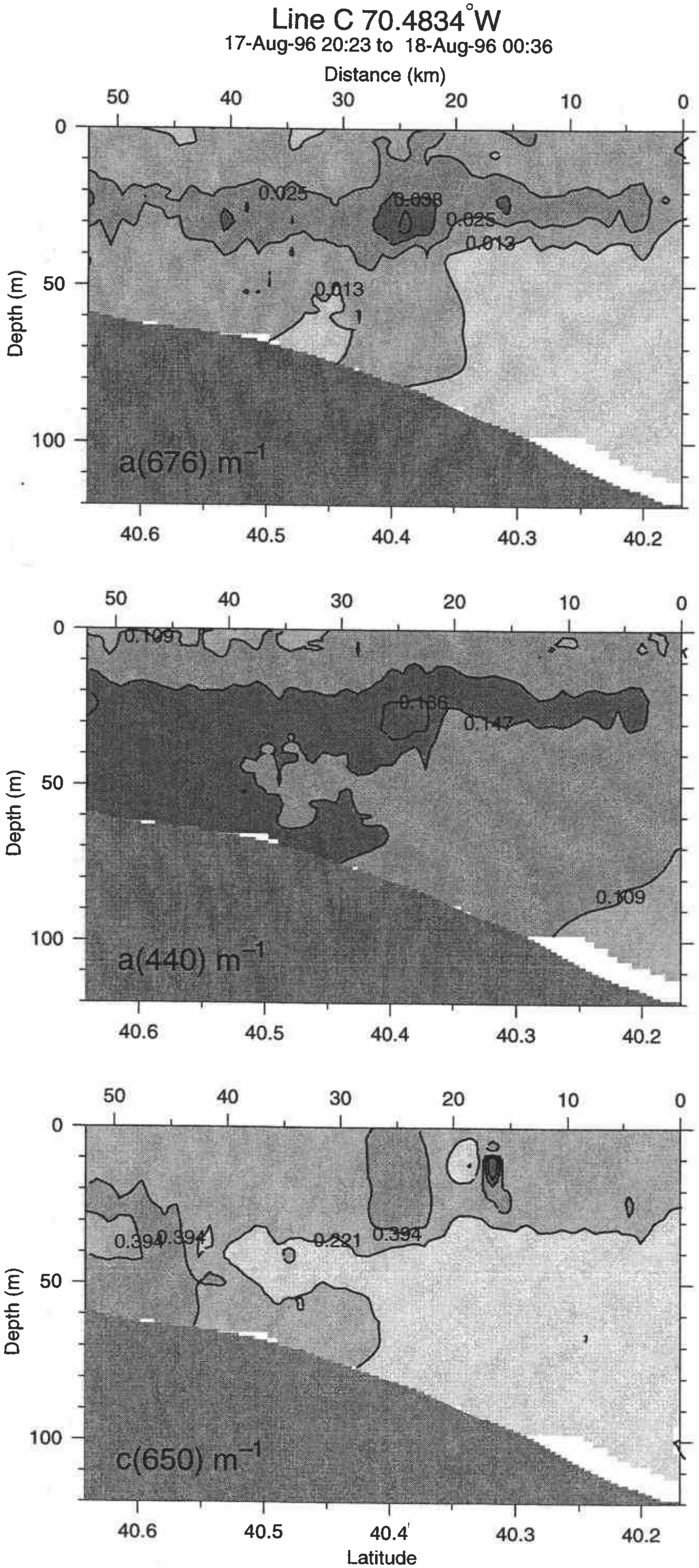

E9608 Bigbox 1

Line D 70.3466°W

17-Aug-96 13:43 to 17-Aug-96 19:24

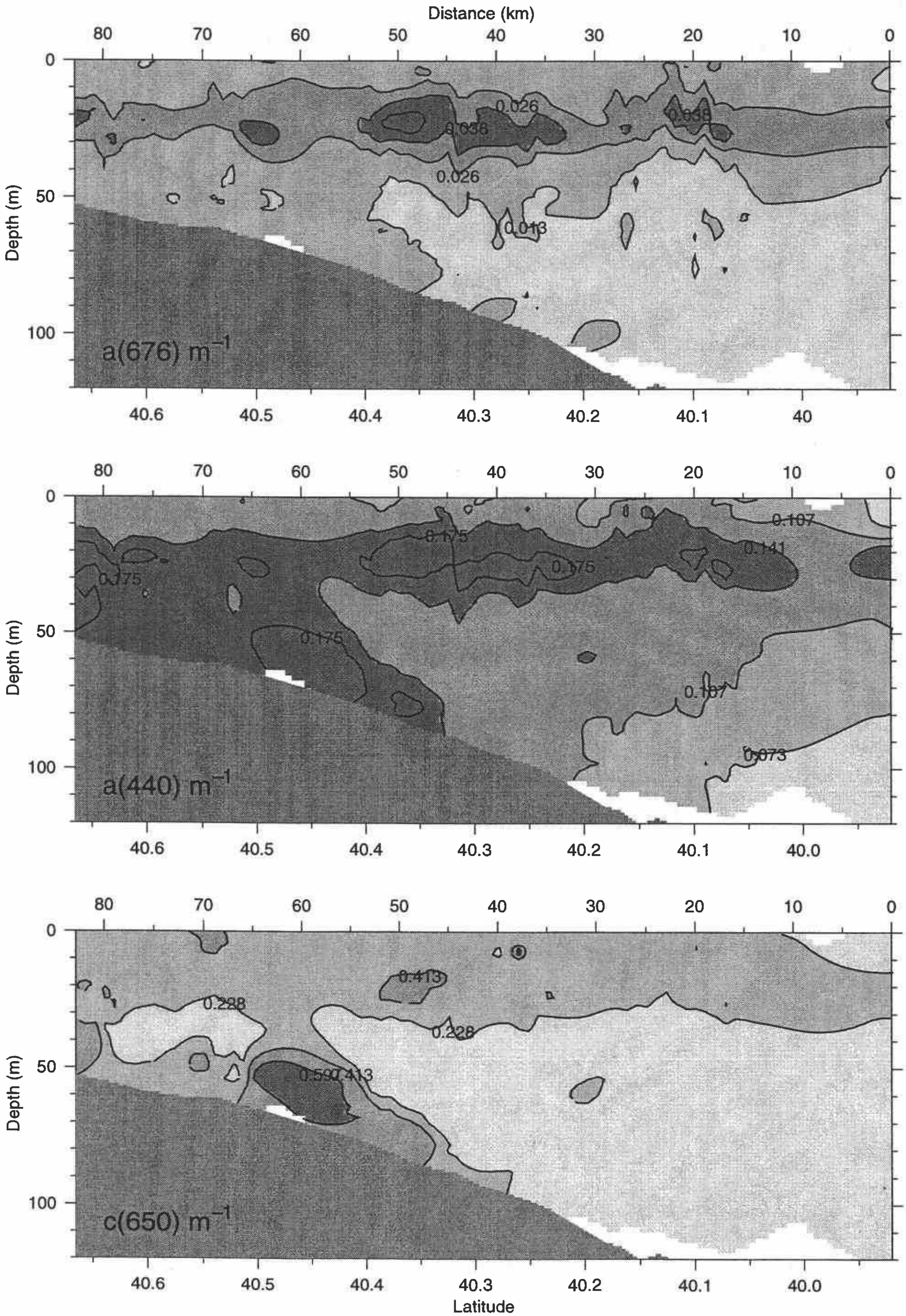

E9608 Bigbox 1

Line E 70.2002°W

17-Aug-96 07:00 to 17-Aug-96 12:39

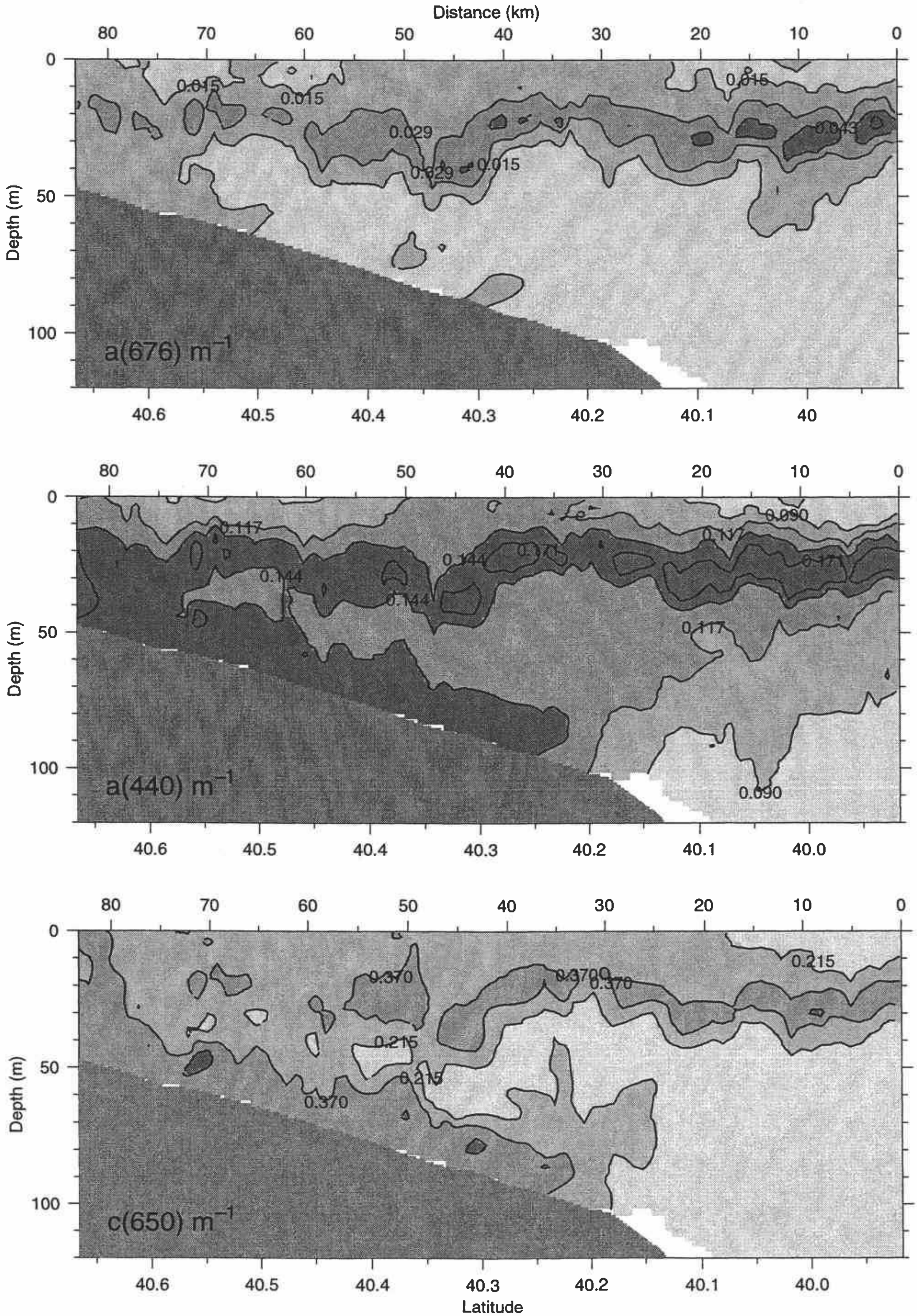

E9608 Bigbox 1

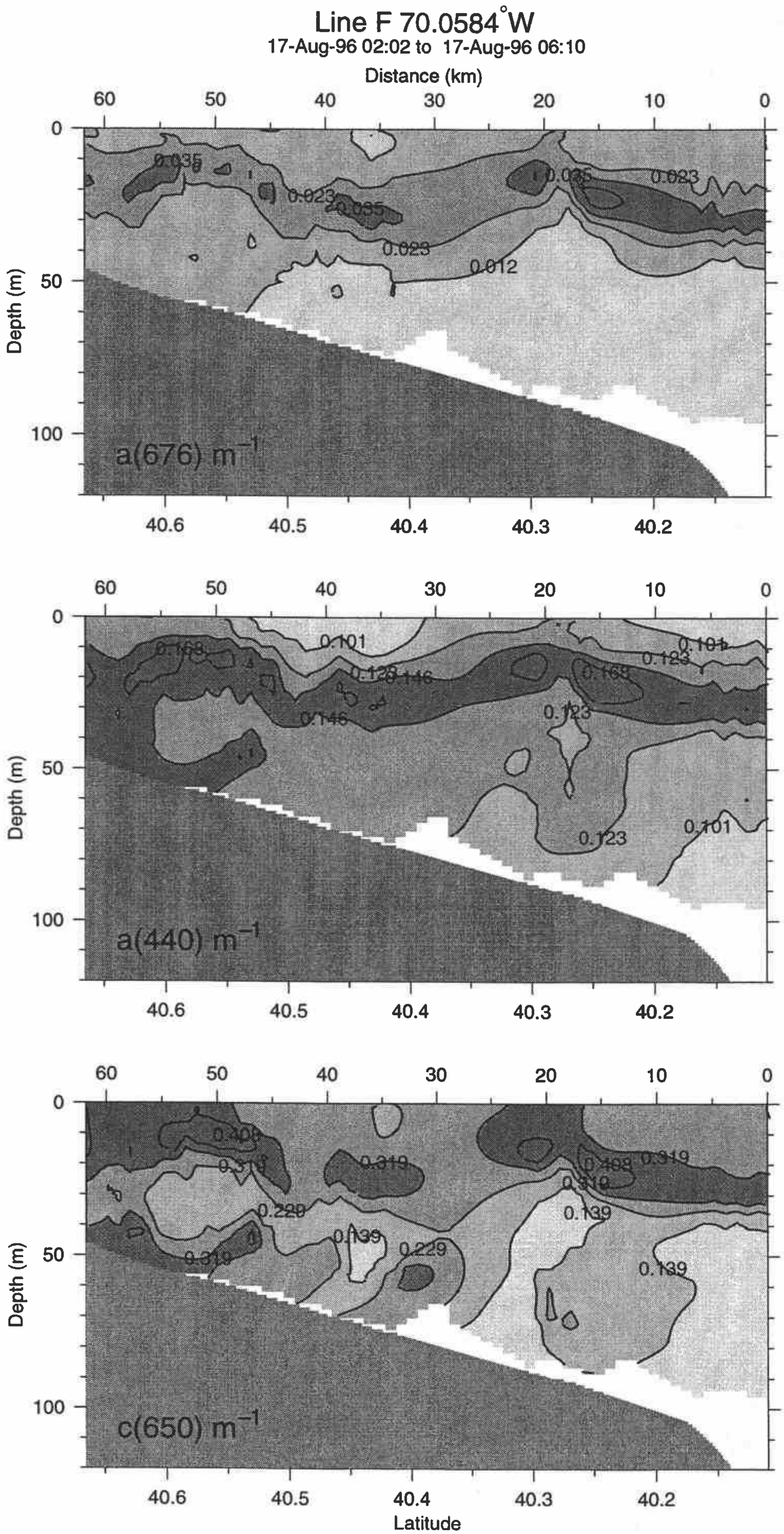

E9608 Bigbox 2

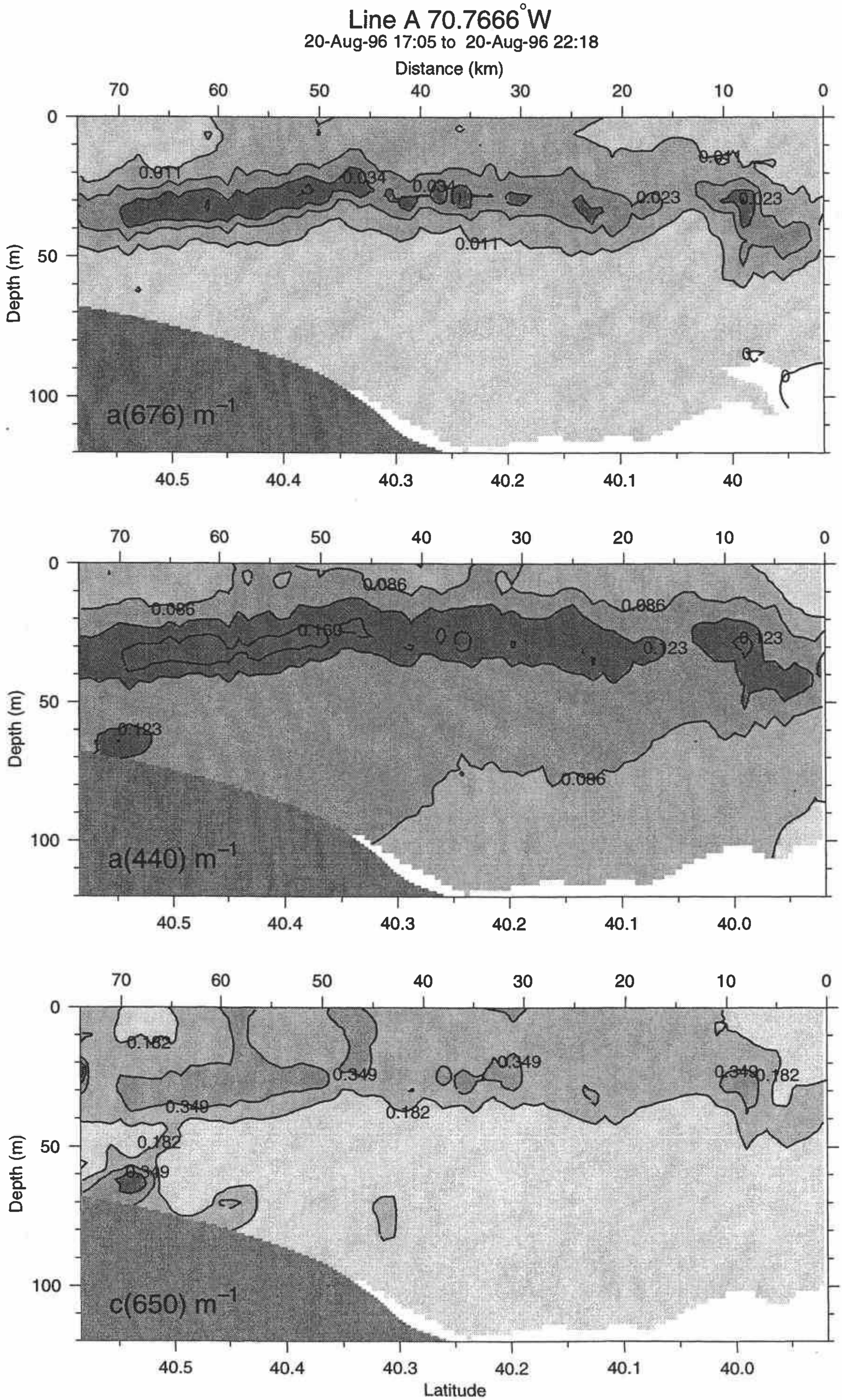

E9608 Bigbox 2

Line B 70.6250°W

20-Aug-96 23:10 to 21-Aug-96 04:52

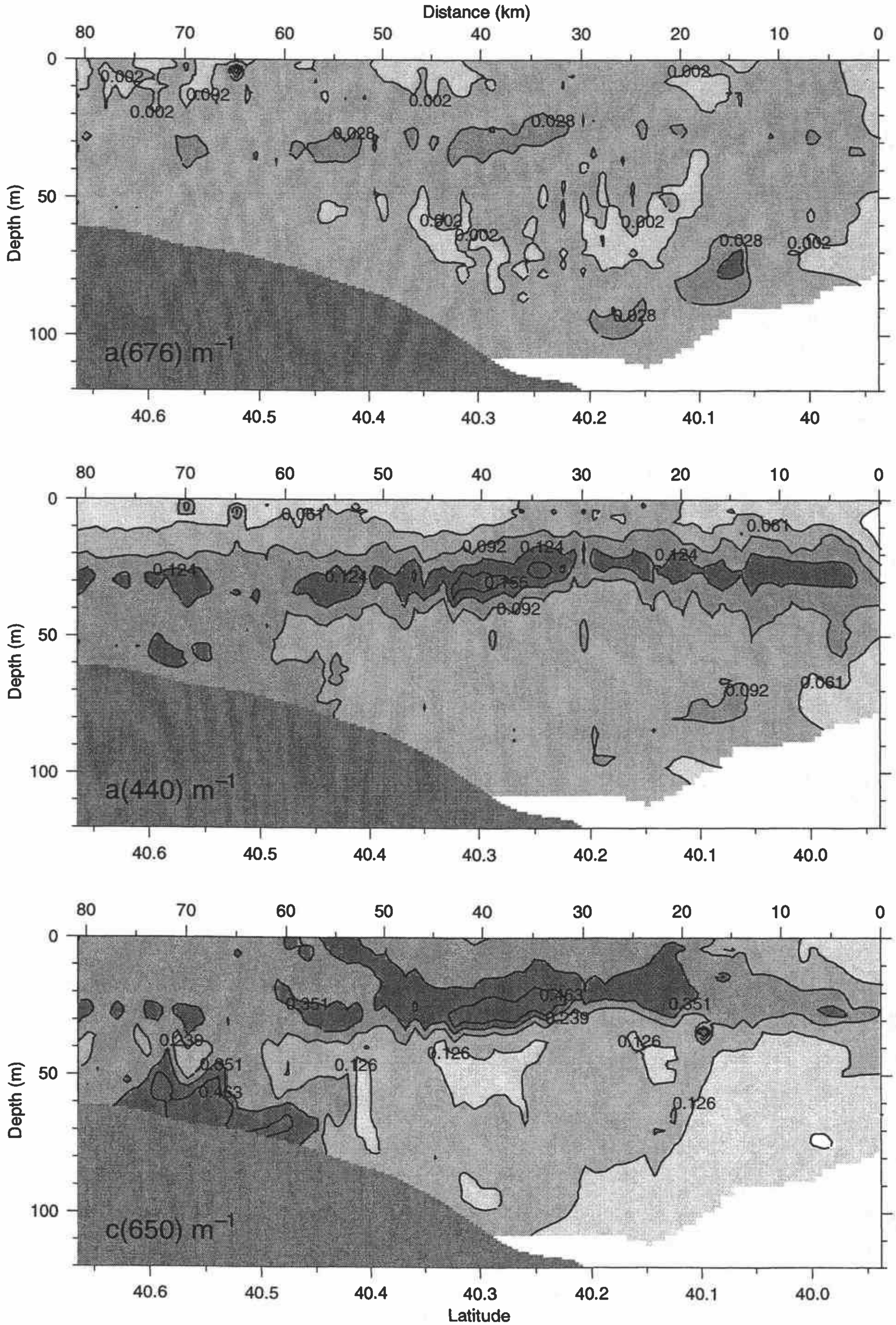

E9608 Bigbox 2

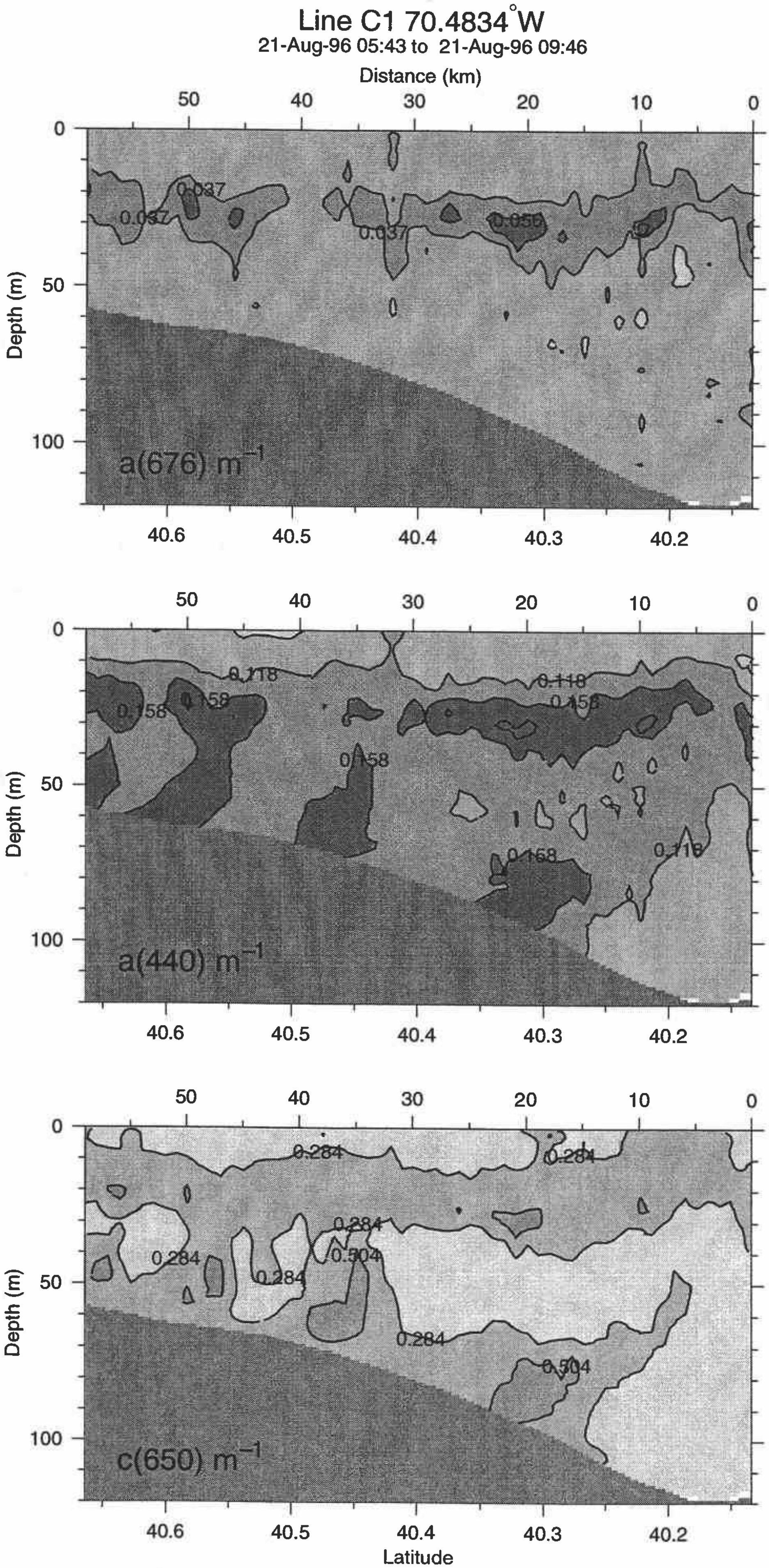

E9608 Bigbox 2

Line C2 70.4833°W

21-Aug-96 13:15 to 21-Aug-96 19:34

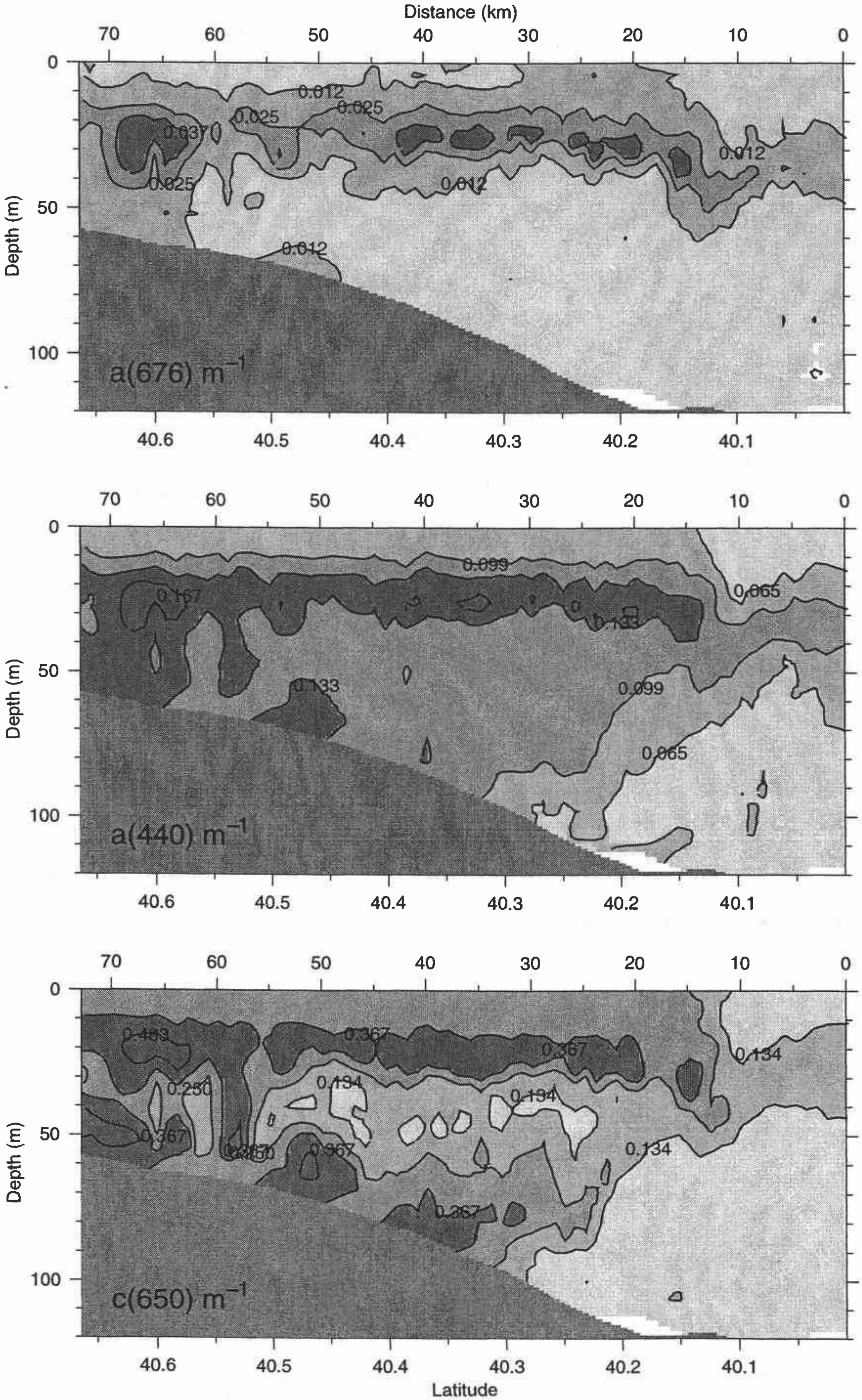

E9608 Bigbox 2

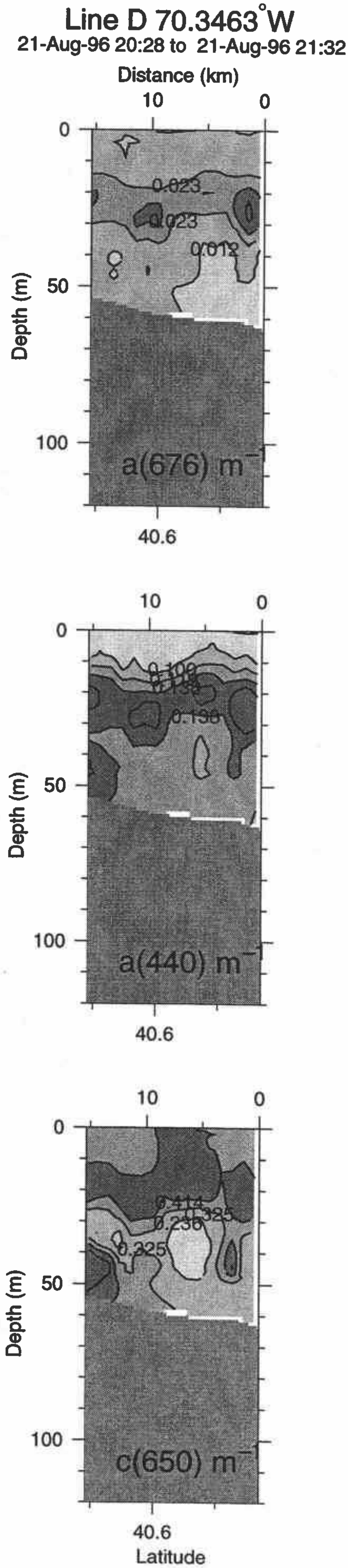

E9608 Bigbox 3

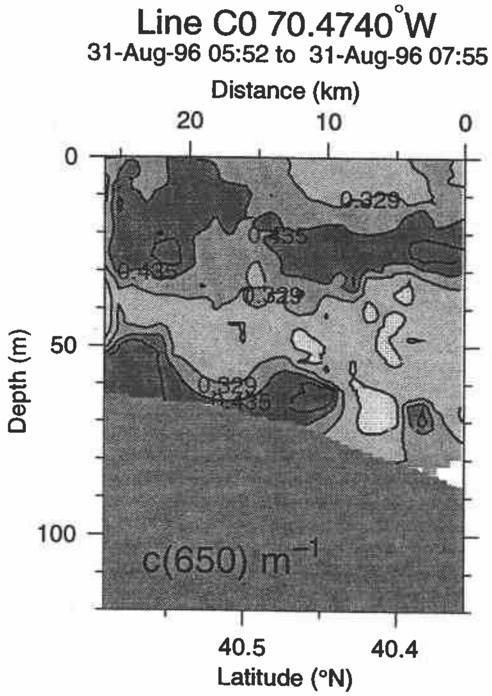

E9608 Bigbox 3

Line C1 70.4836°W

31-Aug-96 09:07 to 31-Aug-96 14:28

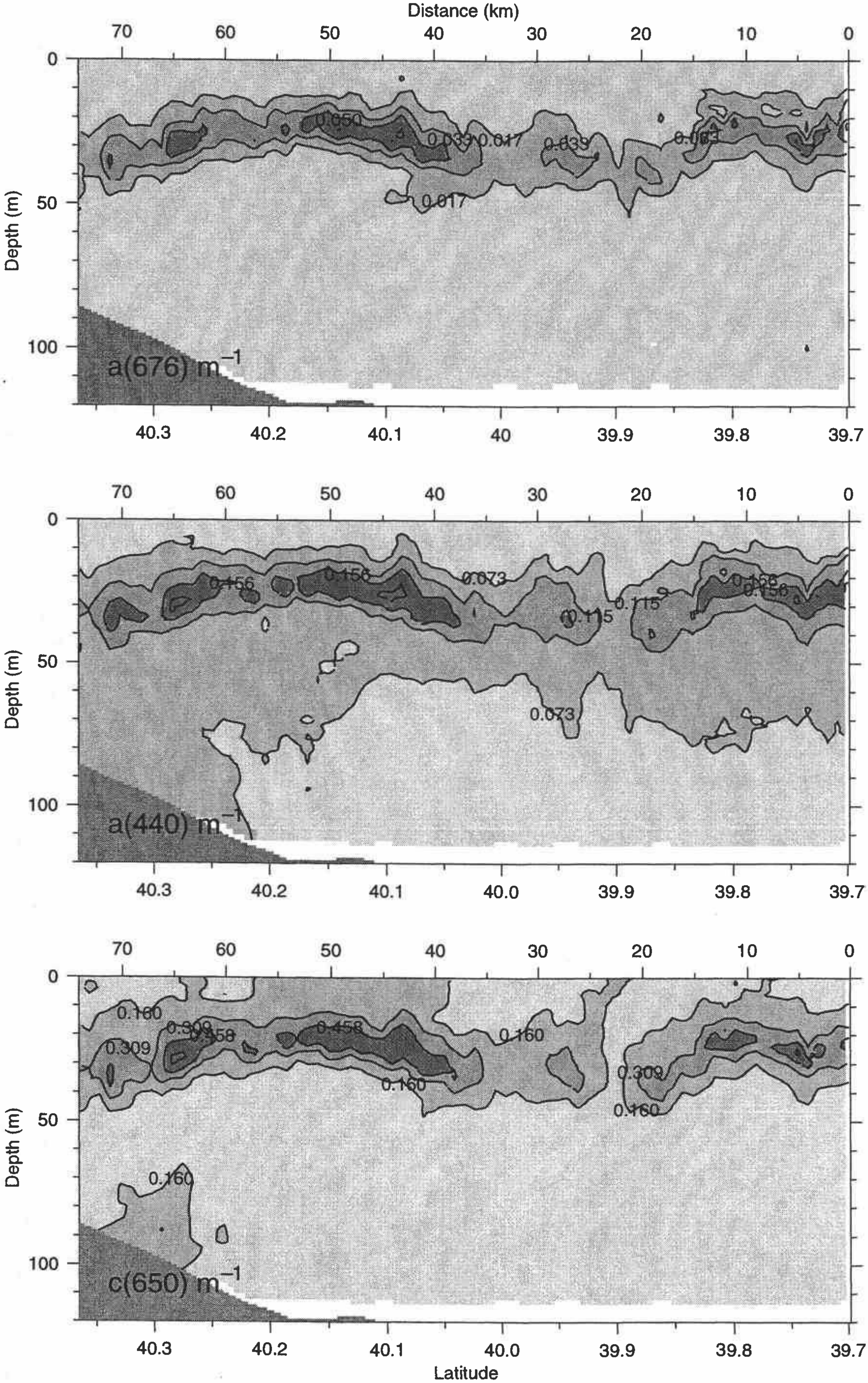

E9608 Bigbox 3

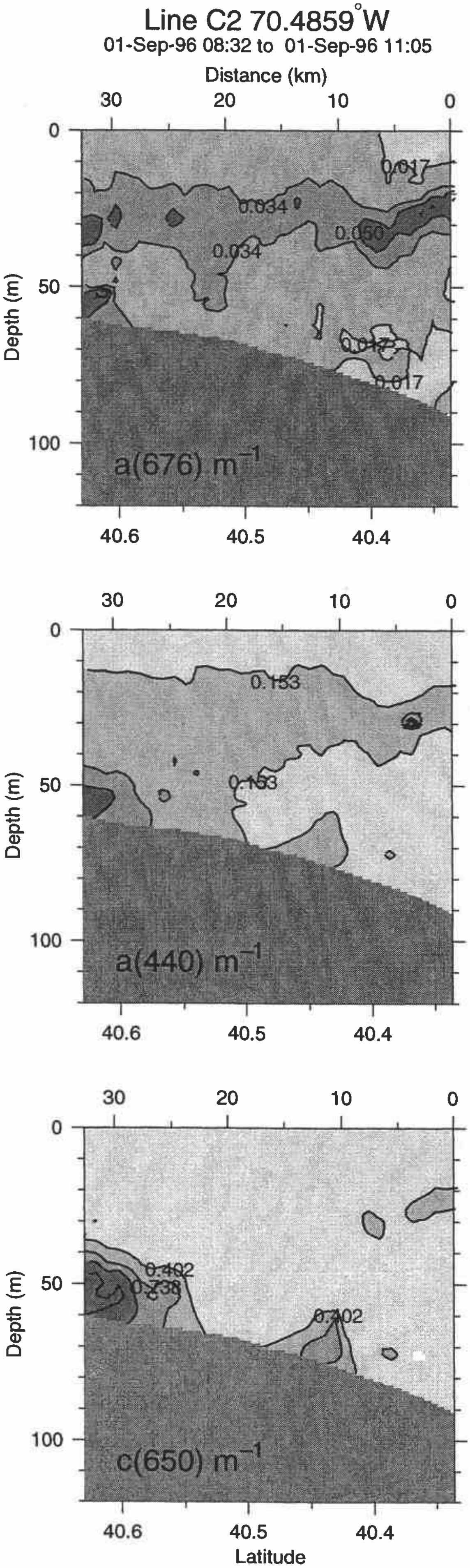

E9608 Bigbox 3

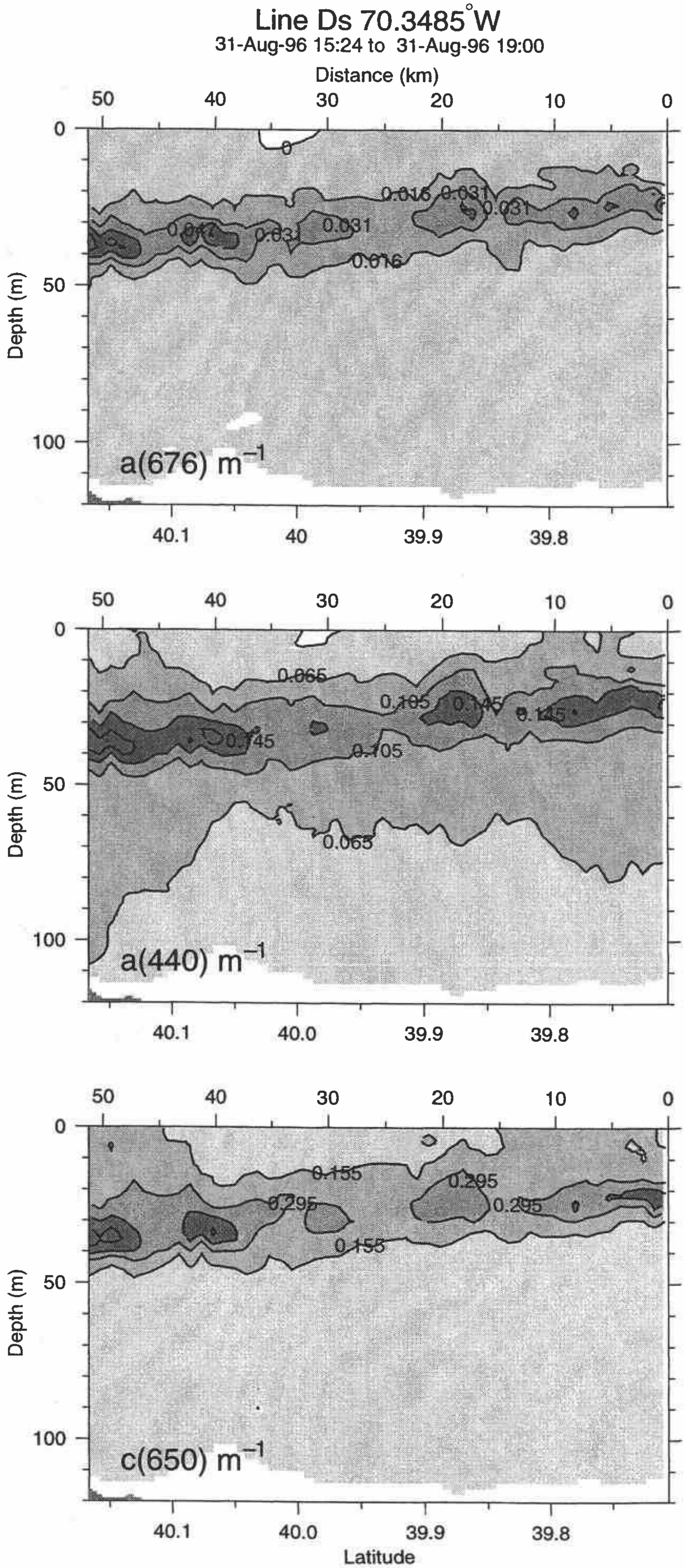

E9608 Bigbox 3

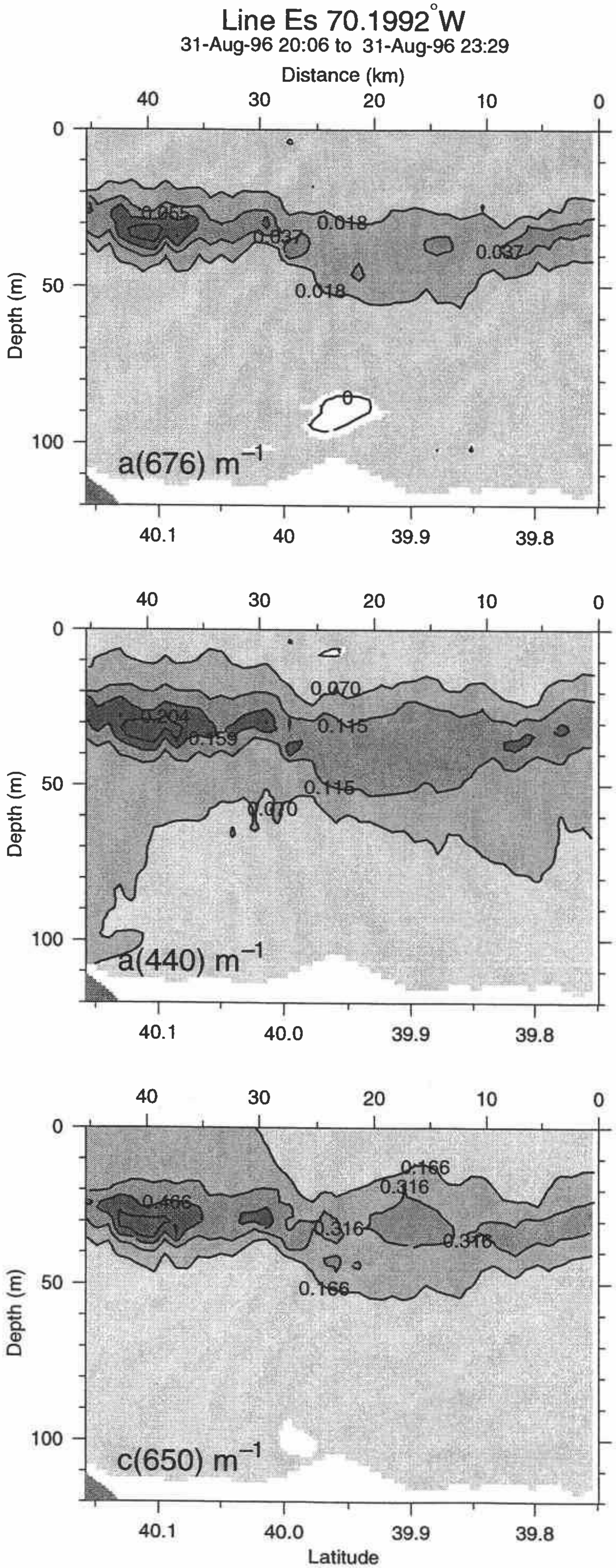

E9608 Bigbox 3

Line F 70.0597°W

01-Sep-96 00:22 to 01-Sep-96 04:45